

ERICE LECTURES ON INFLATIONARY REHEATING**D. Boyanovsky^(a), H.J. de Vega^(b) and R. Holman^(c)***(a) Department of Physics and Astronomy, University of Pittsburgh, Pittsburgh, PA. 15260, U.S.A.**(b) LPTHE, * Université Pierre et Marie Curie (Paris VI) et Denis Diderot (Paris VII), Tour 16, 1er. étage, 4, Place Jussieu 75252 Paris, Cedex 05, France**(c) Department of Physics, Carnegie Mellon University, Pittsburgh, PA. 15213, U. S. A.*

(November 1996)

Abstract

At the end of the inflationary stage of the early universe, profuse particle production leads to the reheating of the universe. Such explosive particle production is due to parametric amplification of quantum fluctuations for the unbroken symmetry case (appropriate for chaotic inflation), or spinodal instabilities in the broken symmetry phase (which is the case in new inflation). This mechanism is non-perturbative and depends on the details of the particle physics models involved. A consistent study of this mechanism requires a detailed analysis and numerical treatment with an approximation scheme that ensures energy (covariant) conservation and a consistent non-perturbative implementation.

We study the $O(N)$ symmetric vector model with a quartic self-interaction in the large N limit, Hartree and resummed one-loop approximations (with $N = 1$) to address the non-perturbative issues. The non-equilibrium equations of motions, their renormalization and the implementation of the approximations are studied in arbitrary spatially flat FRW cosmologies. A full description, analytically and numerically is provided in Minkowski space-time to illustrate the fundamental phenomena in a simpler setting.

We give analytic results for weak couplings and times short compared to the time at which the fluctuations become of the same order as the tree level terms, as well as numerical results including the full backreaction. In the case where the symmetry is unbroken, the analytical results agree spectacularly well with the numerical ones in their common domain of validity. In the broken symmetry case, interesting situations, corresponding to slow roll initial conditions from the unstable minimum at the origin, give rise to a new and unexpected phenomenon: the dynamical relaxation of the vacuum energy.

*Laboratoire Associé au CNRS UA280.

That is, particles are abundantly produced at the expense of the quantum vacuum energy while the zero mode comes back to almost its initial value. We obtain analytically and numerically the equation of state which in both cases can be written in terms of an effective polytropic index that interpolates between vacuum and radiation-like domination.

The self-consistent methods presented in these lectures are the only approaches, so far, that lead to reliable quantitative results on the reheating mechanism in the inflationary universe. These approaches take into account the non-linear interaction between the quantum modes and exactly conserve energy (covariantly). Simplified analysis that do not include the full backreaction and do not conserve energy, result in unbound particle production and lead to quantitatively erroneous results.

For spontaneously broken theories the issue of whether the symmetry may be restored or not by the quantum fluctuations is analyzed. The precise criterion for symmetry restoration is presented. The field dynamics is symmetric when the energy density in the initial state is larger than the top of the tree level potential. When the initial energy density is below the top of the tree level potential, the symmetry is broken.

Finally, we provide estimates of the reheating temperature as well as a discussion of the inconsistency of a kinetic approach to thermalization when a non-perturbatively large number of particles is created.

I. INTRODUCTION

Research activity on inflationary cosmologies has continued steadily since the concept of inflationary cosmology was first proposed in 1981 [1].

It was recognized that in order to merge an inflationary scenario with standard Big Bang cosmology a mechanism to reheat the universe was needed. Such a mechanism must be present in any inflationary model to raise the temperature of the Universe at the end of inflation, thus the problem of reheating acquired further importance deserving more careful investigation. The original version of reheating envisaged that during the last stages of inflation when the universe expansion slows down, the energy stored in the oscillations of the inflaton zero mode transforms into particles via single particle decay. Such particle production reheats the universe whose temperature was redshifted to almost zero during the inflationary expansion [2].

It was realized recently [4,6,7,19], that the elementary theory of reheating [2] does not describe accurately the quantum dynamics of the fields when the oscillations of the inflaton field (zero mode) have large amplitude.

Our programme on non-equilibrium dynamics in quantum field theory, started in 1992 [3], is naturally poised to provide a framework to study these problems. The larger goal of the program is to study the dynamics of non-equilibrium processes, such as phase transitions, from a fundamental field-theoretical description, by obtaining and solving the dynamical equations of motion for expectation values and correlation functions of the underlying four

dimensional quantum field theory for physically relevant problems: phase transitions and particle production out of equilibrium, symmetry breaking and dissipative processes.

The focus of our work is to describe the quantum field dynamics when the energy density is **large**. That is, a large number of particles per volume m^{-3} , where m is the typical mass scale in the theory. Usual S-matrix calculations apply in the opposite limit of low energy density and since they only provide information on *in* \rightarrow *out* matrix elements, are unsuitable for calculations of time dependent expectation values. Our methods were naturally applied to different physical problems like pion condensates [5,10,11], supercooled phase transitions [3,8,9], inflationary cosmology [4,8,9,15–17], the hadronization stage of the quark-gluon plasma [13] as well as trying to understand out of equilibrium particle production in strong electromagnetic fields and in heavy ion collisions [3,5,14].

When a large energy density is concentrated in one or few modes, for example the inflaton zero mode in inflationary cosmology, under time evolution this energy density will be transferred to other modes driving a large amplification of quantum fluctuations. This, in turn, gives rise to profuse particle production for bosonic fields, creating quanta in a highly non-equilibrium distribution, radically changing the standard picture of reheating the post-inflationary universe [2,12]. Fermionic fields are not very efficient for this mechanism of energy “cascading” because of Pauli blocking [10].

The detail of the processes giving rise to preheating can be different depending on the potential for the scalar field and couplings to other fields involved, as well as the initial conditions. For example, in new inflationary scenarios, where the expectation value of the zero mode of the inflaton field evolves down the flat portion of a potential admitting spontaneous symmetry breaking, particle production occurs due to the existence of unstable field modes whose amplitude is amplified until the zero mode leaves the instability region. These are the instabilities that give rise to spinodal decomposition and phase separation. In contrast, if we start with chaotic initial conditions, so that the field has large initial amplitude, particles are created from the parametric amplification of the quantum fluctuations due to the oscillations of the zero mode and the transfer of energy to higher modes.

In these lectures we analyze the details of this so-called **preheating** process both analytically as well as numerically. Preheating is a non-perturbative process, with typically $1/\lambda$ particles being produced, where λ is the self coupling of the field. Due to this fact, any attempts at analyzing the detailed dynamics of preheating must also be non-perturbative in nature. This leads us to consider the $O(N)$ vector model in the large N limit. This is a non-perturbative approximation that has many important features that justify its use: unlike the Hartree or mean-field approximation [8], it can be systematically improved in the $1/N$ expansion. It conserves energy, satisfies the Ward identities of the underlying symmetry, and again unlike the Hartree approximation it predicts the correct order of the transition in equilibrium.

This approximation has also been used in other non-equilibrium contexts [3,5,14].

Our main results can be summarized as follows [15].

We provide consistent non-perturbative analytic estimates of the non-equilibrium processes occurring during the preheating stage taking into account the **exact** evolution of the inflaton zero mode for large amplitudes when the quantum back-reaction due to the produced particles is negligible i.e. at early and intermediate times. We also compute the momentum distribution of the number of particles created, as well as the effective equa-

tion of state during this stage. Explicit expressions for the growth of quantum fluctuations, the preheating time scale, and the effective (time dependent) polytropic index defining the equation of state are given in sec. IV and V.

We go beyond the early/intermediate time regime and evolve the equations of motion numerically, taking into account back-reaction effects. (That is, the non-linear quantum field interaction). These results confirm the analytic estimates in their domain of validity and show how, when back-reaction effects are large enough to compete with tree level effects, dissipational effects arise in the zero mode. Energy conservation is guaranteed in the full backreaction problem, leading to the eventual shut-off of particle production. This is an important ingredient in the dynamics that determines the relevant time scales.

We also find a novel dynamical relaxation of the vacuum energy in this regime when the theory is in the broken phase. Namely, particles are produced at the expense of the quantum vacuum energy while the zero mode contributes very little. We find a radiation type equation of state for late times ($p \approx \frac{1}{3} \varepsilon$) despite the lack of local thermodynamic equilibrium.

Finally, we provide an estimate of the reheating temperature under clearly specified (and physically reasonable assumptions) in a class of models. We comment on when the kinetic approach to thermalization and equilibration is applicable.

There have been a number of papers (see refs. [6,7,19] - [20]) dedicated to the analysis of the preheating process where particle production and back-reaction are estimated in different approximations [38]. Our analysis differs from other works in many important aspects. We emphasize the need of a non-perturbative, self-consistent treatment that includes backreaction and guarantees energy conservation (covariant conservation in the expanding universe) and the conservation of all of the important symmetries. Although analytic simplified arguments may provide a qualitative picture of the phenomena involved, a quantitative statement requires a detailed numerical study in a consistent manner. Only a self-consistent, energy conserving scheme that includes backreaction effects can capture the corresponding time scales. Otherwise infinite particle production may result from uncontrolled approximations.

The layout of these lectures is as follows. Section II presents the model, the evolution equations, the renormalization of the equations of motion and introduces the relevant definitions of particle number, energy and pressure and the details of their renormalization. The unbroken and broken symmetry cases are presented in detail and the differences in their treatment are clearly explained.

In sections III through V we present a detailed analytic and numerical treatment of both the unbroken and broken symmetry phases emphasizing the description of particle production, energy, pressure and the equation of state. In the broken symmetry case, when the inflaton zero mode begins very close to the top of the potential, we find that there is a novel phenomenon of relaxation of the vacuum energy that explicitly accounts for profuse particle production through the spinodal instabilities and energy conservation. We discuss in section VI why the phenomenon of symmetry restoration at preheating, discussed by various authors [7,20,34,35] is **not** seen to occur in the cases treated by us in ref. [8,15] and relevant for new inflationary scenarios [38].

A precise criterion for symmetry restoration is given. The symmetry is broken or unbroken depending on the value of the initial energy density of the state. When the energy density in the initial state is larger than the top of the tree level potential then the sym-

metry is restored [38]. When it is smaller than the top of the tree level potential, then it is broken and Goldstone bosons appear [8,15]. In the first case, the amplitude of the zero mode is such that $V(\eta_0) > V(0)$ (all energy is initially on the zero mode). In this case the dynamics is very similar to the unbroken symmetry case, the amplitude of the zero mode will damp out, transferring energy to the quantum fluctuations via parametric amplification, but asymptotically oscillating around zero with a fairly large amplitude.

In section VII we briefly discuss the amplitude expansion (linearizing in the field amplitude) and compare with a full non-linear treatment in a model for reheating where the inflaton decays into a lighter scalar field [10].

In section VIII we provide estimates, under suitably specified assumptions, of the reheating temperature in the $O(N)$ model as well as other models in which the inflaton couples to lighter scalars. In this section we argue that thermalization cannot be studied with a kinetic approach because of the non-perturbatively large occupation number of long-wavelength modes.

Finally, we summarize our results and discuss future avenues of study in the conclusions.

II. NON EQUILIBRIUM SCALAR FIELD DYNAMICS AT LARGE ENERGY DENSITIES

Two essential parameters characterize the dynamics of quantum fields: the strength of the coupling λ and the energy density in units of the typical mass m . If initially most of the energy is stored in one (or few) modes, the energy density is controlled by the amplitude of the expectation value of such mode(s) $A \equiv \sqrt{\lambda} \Phi/m$. Usual field theory treatments consider the small amplitude limit $A \ll 1$ in which case the dynamics essentially reduces to the calculation of S -matrix elements. The S -matrix describes the interaction of typically few particles in infinite space-time. This is within the small amplitude limit even for high energies.

We shall be concerned here with the **non-perturbative** regime in $A = \sqrt{\lambda} \Phi/m \simeq \mathcal{O}(\infty)$. The crucial point is that non-linear effects appear in such regime even for very small λ .

The small amplitude limit is also instructive to study [8,11] as an initial condition problem. In such regime, the field evolution equations linearize and can be solved explicitly by Laplace transform. Moreover, their solution can be interpreted using the S -matrix language: contributions from particle poles, production thresholds for many-particle cuts, and so on.

We consider the $O(N)$ vector model with quartic interaction in a cosmological spacetime with metric

$$ds^2 = dt^2 - a^2(t) d\vec{x}^2,$$

Here, $a(t)$ is the scale factor and t is the cosmic time coordinate.

The action and Lagrangian density are given by,

$$S = \int d^4x \mathcal{L},$$

$$\mathcal{L} = a^3(t) \left[\frac{1}{2} \dot{\vec{\Phi}}^2(x) - \frac{1}{2} \frac{(\vec{\nabla} \vec{\Phi}(x))^2}{a^2(t)} - V(\vec{\Phi}(x)) \right],$$

$$V(\vec{\Phi}) = \frac{\lambda}{8N} \left(\vec{\Phi}^2 + \frac{2Nm^2(t)}{\lambda} \right)^2 - \frac{Nm^4(t)}{2\lambda} ; \quad m^2(t) \equiv m^2 + \xi \mathcal{R}(t) \quad . \quad (2.1)$$

Here, $\mathcal{R}(t)$ stands for the scalar curvature.

$$\mathcal{R}(t) = 6 \left(\frac{\ddot{a}(t)}{a(t)} + \frac{\dot{a}^2(t)}{a^2(t)} \right),$$

where we have included the coupling ξ of $\vec{\Phi}(x)^2$ to the scalar curvature since it will arise as a consequence of renormalization. The canonical momentum conjugate to $\vec{\Phi}(x)$ is,

$$\vec{\Pi}(x) = a^3(t) \dot{\vec{\Phi}}(x),$$

and the *time dependent* Hamiltonian is given by,

$$H(t) = \int d^3x \left\{ \frac{\vec{\Pi}^2(x)}{2a^3(t)} + \frac{a(t)}{2} (\nabla \vec{\Phi}(x))^2 + a^3(t) V(\vec{\Phi}) \right\}.$$

In general, the system is in a mixed state described by a density matrix $\hat{\rho}(\vec{\Phi}(\cdot), \Phi(\cdot), t)$ in the Fock space. Here $\vec{\Phi}(\cdot)$ and $\Phi(\cdot)$ label the row and columns of the density matrix. Its time evolution is defined by the quantum Liouville equation

$$i \frac{\partial \hat{\rho}}{\partial t} = [H(t), \hat{\rho}] \quad (2.2)$$

and we normalize it according to

$$\text{Tr} \hat{\rho} = 1 .$$

The expectation value of any physical magnitude \mathcal{A} is given as usual by

$$\langle \mathcal{A} \rangle = \text{Tr}[\hat{\rho} \mathcal{A}] .$$

The time evolution of all physical magnitudes is unitary as we see from eq. (2.2). This implies that Von Neuman's entropy

$$S \equiv \text{Tr}[\hat{\rho} \log \hat{\rho}] .$$

is conserved in time.

In the present lectures we will restrict ourselves to translationally invariant situations. Namely, the order parameter

$$\langle \vec{\Phi}(\vec{x}, t) \rangle$$

will be independent of the spatial coordinates \vec{x} .

There are two approximation schemes that have been used to study the non-equilibrium dynamics during phase transitions, each with its own advantages and disadvantages. The Hartree factorization [23,8,9,15,11,3,16] has the advantage that it can treat the dynamics of a scalar order parameter with discrete symmetry, while its disadvantage is that it is difficult to implement consistently beyond the lowest (mean field) level. The advantage of the large

N approximation [14,4,8,9,11,15,3,16,17] is that it allows a consistent expansion in a small parameter ($1/N$) and correctly treats continuous symmetries in the sense that it implements Goldstone's theorem. Moreover, the Hartree approximation becomes the resummed one-loop approximation for small values of λ . Therefore, it may be a reliable approximation for the typical values of λ in inflationary models. It should be noted that for spontaneous symmetry breaking, the large N limit always produces massless Goldstone bosons.

Both methods implement a resummation of a select set of diagrams to all orders and lead to a system of equations that is energy conserving in Minkowski space time, and as will be shown below, satisfies covariant conservation of the energy momentum tensor in FRW cosmologies. Furthermore, both methods are renormalizable and numerically implementable. Given that both methods have advantages and disadvantages and that choosing a particular scheme will undoubtedly lead to criticism and questions about their reliability, we use *both*, comparing the results to obtain universal features of the dynamics.

In this section we introduce the $O(N)$ vector model, obtain the non-equilibrium evolution equations both in the large N and Hartree approximations, the energy momentum tensor and analyze the issue of renormalization. We will then be poised to present the analytical and numerical solutions as well as the analysis of the physics in the later sections.

We choose the coupling λ fixed in the large N limit. The field $\vec{\Phi}$ is an $O(N)$ vector, $\vec{\Phi} = (\sigma, \vec{\pi})$ and $\vec{\pi}$ represents the $N - 1$ "pions". In what follows, we will consider two different cases of the potential (2.1) $V(\sigma, \vec{\pi})$, with ($m^2 < 0$) or without ($m^2 > 0$) symmetry breaking.

We can decompose the field σ into its zero mode and fluctuations $\chi(\vec{x}, t)$ about the zero mode:

$$\sigma(\vec{x}, t) = \sigma_0(t) + \chi(\vec{x}, t) .$$

The generating functional of real time non-equilibrium Green's functions can be written in terms of a path integral along a complex contour in time, corresponding to forward and backward time evolution and at finite temperature a branch down the imaginary time axis. This requires doubling the number of fields which now carry a label \pm corresponding to forward (+), and backward (-) time evolution. The reader is referred to the literature for more details [21,22]. This generating functional along the complex contour requires the Lagrangian density along the contour, which is given by [8]

$$\begin{aligned} & \mathcal{L}[\sigma_0 + \chi^+, \vec{\pi}^+] - \mathcal{L}[\sigma_0 + \chi^-, \vec{\pi}^-] = \left\{ \mathcal{L}[\sigma_0, \vec{\pi}^+] + \frac{\delta \mathcal{L}}{\delta \sigma_0} \chi^+ \right. \\ & + a^3(t) \left[\frac{1}{2} (\dot{\chi}^+)^2 - \frac{1}{2} \frac{(\vec{\nabla} \chi^+)^2}{a(t)^2} + \frac{1}{2} (\dot{\vec{\pi}}^+)^2 - \frac{1}{2} \frac{(\vec{\nabla} \vec{\pi}^+)^2}{a(t)^2} \right. \\ & \left. \left. - \left(\frac{1}{2!} V''(\sigma_0, \vec{\pi}^+) \chi^{+2} + \frac{1}{3!} V^{[3]}(\sigma_0, \vec{\pi}^+) (\chi^+)^3 + \frac{1}{4!} V^{[4]}(\sigma_0, \vec{\pi}^+) (\chi^+)^4 \right) \right] \right\} \\ & - \left\{ (\chi^+ \rightarrow \chi^-), (\vec{\pi}^+ \rightarrow \vec{\pi}^-) \right\} \end{aligned}$$

The tadpole condition $\langle \chi^\pm(\vec{x}, t) \rangle = 0$ will lead to the equations of motion as discussed in [8] and references therein.

A. The Large N limit

A consistent and elegant version of the large N limit for non-equilibrium problems can be obtained by introducing an auxiliary field (see for example [14]). This formulation has the advantage that it can incorporate the $O(1/N)$ corrections in a systematic fashion. Alternatively, the large N limit can be implemented via a Hartree-like factorization [8,15] in which i) there are no cross correlations between the pions and sigma field and ii) the two point correlation functions of the pion field are diagonal in the $O(N-1)$ space of the remaining unbroken symmetry group. To leading order in large N both methods are completely equivalent and for simplicity of presentation we chose the factorization method.

The factorization of the non-linear terms in the Lagrangian is (again for both \pm components):

$$\begin{aligned}\chi^4 &\rightarrow 6 \langle \chi^2 \rangle \chi^2 + \text{constant} \\ \chi^3 &\rightarrow 3 \langle \chi^2 \rangle \chi \\ (\vec{\pi} \cdot \vec{\pi})^2 &\rightarrow 2 \langle \vec{\pi}^2 \rangle \vec{\pi}^2 - \langle \vec{\pi}^2 \rangle^2 + \mathcal{O}(1/N) \\ \vec{\pi}^2 \chi^2 &\rightarrow \langle \vec{\pi}^2 \rangle \chi^2 + \vec{\pi}^2 \langle \chi^2 \rangle \\ \vec{\pi}^2 \chi &\rightarrow \langle \vec{\pi}^2 \rangle \chi\end{aligned}$$

To obtain a large N limit, we define

$$\vec{\pi}(\vec{x}, t) = \psi(\vec{x}, t) \overbrace{(1, 1, \dots, 1)}^{N-1} ; \quad \sigma_0(t) = \phi(t) \sqrt{N} \quad (2.3)$$

where the large N limit is implemented by the requirement that

$$\langle \psi^2 \rangle \approx \mathcal{O}(1), \quad \langle \chi^2 \rangle \approx \mathcal{O}(1), \quad \phi \approx \mathcal{O}(1).$$

The leading contribution is obtained by neglecting the $\mathcal{O}(1/N)$ terms in the formal large N limit.

$$\begin{aligned}\mathcal{L}[\sigma_0 + \chi^+, \vec{\pi}^+] - \mathcal{L}[\sigma_0 + \chi^-, \vec{\pi}^-] &= \left\{ \mathcal{L}[\sigma_0, \vec{\pi}^+] + \frac{\delta \mathcal{L}}{\delta \sigma_0} \chi^+ + a^3(t) \left[\frac{1}{2} (\dot{\chi}^+)^2 - \frac{1}{2} \frac{(\vec{\nabla} \chi^+)^2}{a(t)^2} \right. \right. \\ &+ \left. \left. \frac{1}{2} (\dot{\vec{\pi}}^+)^2 - \frac{1}{2} \frac{(\vec{\nabla} \vec{\pi}^+)^2}{a(t)^2} - \left(\frac{1}{2!} V''(\sigma_0, \vec{\pi}^+) \chi^{+2} + \frac{1}{3!} V^{[3]}(\sigma_0, \vec{\pi}^+) (\chi^+)^3 + \frac{1}{4!} V^{[4]}(\sigma_0, \vec{\pi}^+) (\chi^+)^4 \right) \right] \right\} \\ &- \left\{ (\chi^+ \rightarrow \chi^-), (\vec{\pi}^+ \rightarrow \vec{\pi}^-) \right\}\end{aligned}$$

The resulting Lagrangian density is quadratic, with a linear term in χ :

$$\begin{aligned}\mathcal{L}[\sigma_0 + \chi^+, \vec{\pi}^+] - \mathcal{L}[\sigma_0 + \chi^-, \vec{\pi}^-] &= \left\{ a^3(t) \left[\frac{1}{2} (\dot{\chi}^+)^2 - \frac{1}{2} \frac{(\vec{\nabla} \chi^+)^2}{a(t)^2} + \right. \right. \\ &\left. \left. \frac{1}{2} (\dot{\vec{\pi}}^+)^2 - \frac{1}{2} \frac{(\vec{\nabla} \vec{\pi}^+)^2}{a(t)^2} \right] - \chi^+ V'(t) \right. \\ &\left. - \frac{1}{2} \mathcal{M}_\chi^2(t) (\chi^+)^2 - \frac{1}{2} \mathcal{M}_{\vec{\pi}}^2(t) (\vec{\pi}^+)^2 \right\} - \left\{ (\chi^+ \rightarrow \chi^-), (\vec{\pi}^+ \rightarrow \vec{\pi}^-) \right\}\end{aligned} \quad (2.4)$$

where,

$$\begin{aligned}
V'(\phi(t), t) &= \sqrt{N}\phi(t) \left[m(t)^2 + \frac{\lambda}{2}\phi^2(t) + \frac{\lambda}{2}\langle\psi^2(t)\rangle \right] \\
\mathcal{M}_\pi^2(t) &= m(t)^2 + \frac{\lambda}{2}\phi^2(t) + \frac{\lambda}{2}\langle\psi^2(t)\rangle \\
\mathcal{M}_\chi^2(t) &= m(t)^2 + \frac{3\lambda}{2}\phi^2(t) + \frac{\lambda}{2}\langle\psi^2(t)\rangle.
\end{aligned}$$

where $m(t)^2$ is defined in eq.(2.1). Note that we have used spatial translational invariance as befits a spatially flat FRW cosmology, to write

$$\langle\psi^2(\vec{x}, t)\rangle \equiv \langle\psi^2(t)\rangle$$

When the initial state is in local thermodynamic equilibrium at temperature T_i , the finite temperature non-equilibrium Green's functions are obtained from the following ingredients

$$\begin{aligned}
G_k^>(t, t') &= \frac{i}{2} \{f_k(t)f_k^*(t')[1 + n_k] + n_k f_k(t')f_k^*(t)\} \\
G_k^<(t, t') &= \frac{i}{2} \{f_k(t')f_k^*(t)[1 + n_k] + n_k f_k(t)f_k^*(t')\}
\end{aligned}$$

where $n_k \equiv (e^{\frac{W_k}{T_i}} - 1)^{-1}$.

The Heisenberg field operator $\psi(\vec{x}, t)$ can be written as

$$\psi(\vec{x}, t) = \int \frac{d^3k}{(2\pi)^3} \frac{1}{\sqrt{2}} \left[a_{\vec{k}} f_k(t) e^{i\vec{k}\cdot\vec{x}} + a_{\vec{k}}^\dagger f_k^*(t) e^{-i\vec{k}\cdot\vec{x}} \right], \quad (2.5)$$

where a_k, a_k^\dagger are the canonical destruction and annihilation operators.

The evolution equations for the expectation value $\phi(t)$ and the mode functions $f_k(t)$ can be obtained by using the tadpole method [8] and are given by:

$$\ddot{\phi}(t) + 3H\dot{\phi}(t) + m(t)^2\phi(t) + \frac{\lambda}{2}\phi^3(t) + \frac{\lambda}{2}\phi(t)\langle\psi^2(t)\rangle_B = 0, \quad (2.6)$$

with the mode functions,

$$\left[\frac{d^2}{dt^2} + 3H\frac{d}{dt} + \omega_k^2(t) \right] f_k(t) = 0, \quad (2.7)$$

and the effective frequencies,

$$\omega_k^2(t) = \frac{k^2}{a^2(t)} + M^2(t),$$

where the effective mass takes the form,

$$M^2(t) = m(t)^2 + \frac{\lambda}{2}\phi^2(t) + \frac{\lambda}{2}\langle\psi^2(t)\rangle_B. \quad (2.8)$$

Here, the bare quantum fluctuations are given in terms of the mode functions by [14,4,8,3],

$$\langle \psi^2(t) \rangle_B = \int \frac{d^3k}{(2\pi)^3} \frac{|f_k(t)|^2}{2} \coth \left[\frac{W_k}{2T_i} \right]. \quad (2.9)$$

At this stage we must provide the initial conditions on the mode functions $f_k(t)$. As mentioned above our choice of initial conditions on the density matrix is that of local thermodynamic equilibrium for the instantaneous modes of the time dependent Hamiltonian at the initial time. Therefore we choose the initial conditions on the mode functions to represent positive energy particle states of the instantaneous Hamiltonian at $t = 0$, which is the initial time. Therefore our choice of boundary conditions at $t = 0$, is

$$f_k(0) = \frac{1}{\sqrt{W_k}}; \quad \dot{f}_k(0) = -i\sqrt{W_k}; \quad W_k = \sqrt{k^2 + M_0^2},$$

where the mass M_0 determines the frequencies $\omega_k(0)$ and will be obtained explicitly later. With these boundary conditions, the mode functions $f_k(0)$ correspond to positive frequency modes (particles) of the instantaneous quadratic Hamiltonian for oscillators of mass M_0 . The initial density matrix, at time $t = 0$ is thus chosen to be that of local thermodynamic equilibrium at the temperature T_i for these harmonic modes. The fluctuations $\chi(\vec{x}, t)$ obey an independent equation, that does not enter in the dynamics of the evolution of the expectation value or the $\vec{\pi}$ fields to this order and decouples in the leading order in the large N limit [8].

It is clear from the above equations that the Ward identities of Goldstone's theorem are fulfilled. Because $V'(\phi(t), t) = \sqrt{N}\phi(t)\mathcal{M}_{\vec{\pi}}^2(t)$, whenever $V'(\phi(t), t)$ vanishes for $\phi \neq 0$ then $\mathcal{M}_{\vec{\pi}} = 0$ and the "pions" are the Goldstone bosons. This observation will be important in the discussions of symmetry breaking in a later section.

Since in this approximation, the dynamics for the $\vec{\pi}$ and χ fields decouple, and the dynamics of χ does not influence that of ϕ , the mode functions or $\langle \psi^2 \rangle$, we will only concentrate on the solution for the $\vec{\pi}$ fields. We note however, that if the dynamics is such that the asymptotic value of $\phi \neq 0$ the masses for χ and the "pion" multiplet $\vec{\pi}$ are different, and the original $O(N)$ symmetry is broken down to the $O(N - 1)$ subgroup.

B. The Hartree and the One-loop Approximations

To implement the Hartree approximation, we set $N = 1$ and write,

$$\Phi(\vec{x}, t) = \phi(t) + \psi(\vec{x}, t),$$

with,

$$\phi(t) = \langle \Phi(\vec{x}, t) \rangle; \quad \langle \psi(\vec{x}, t) \rangle = 0,$$

where the expectation value is defined by the non-equilibrium density matrix specified below, and we have assumed spatial translational invariance, compatible with a spatially flat metric. The Hartree approximation is obtained after the factorization,

$$\psi^3(\vec{x}, t) \rightarrow 3 \langle \psi^2(\vec{x}, t) \rangle \psi(\vec{x}, t),$$

$$\psi^4(\vec{x}, t) \rightarrow 6 \langle \psi^2(\vec{x}, t) \rangle \psi^2(\vec{x}, t) - 3 \langle \psi^2(\vec{x}, t) \rangle^2,$$

where by translational invariance, the expectation values only depend on time. In this approximation, the Hamiltonian becomes quadratic at the expense of a self-consistent condition.

At this stage we must specify the non-equilibrium state in which we compute the expectation values above. In non-equilibrium field theory, the important ingredient is the time evolution of the density matrix $\rho(t)$ (see [22] and references therein). This density matrix obeys the quantum Liouville equation (2.2) whose solution only requires an initial condition $\rho(t_i)$ [22,24,4,8,9,11,15,3]. The choice of initial conditions for this density matrix is an issue that pervades any calculation in cosmology. Since we want to study the dynamics of the phase transition, it is natural to consider initial conditions that describe the *instantaneous* modes of the time dependent Hamiltonian as being initially in local thermodynamic equilibrium at some temperature $T_i > T_c$. Given this initial density matrix, we then evolve it in time using the time dependent Hamiltonian as in [4] or alternatively using the complex time path integral method as described in [22,24,14,8,9,11,15,3].

Following the steps of references [4,8,9,11,15,3] we find the equation of motion for the expectation value of the inflaton field to be,

$$\ddot{\phi}(t) + 3H\dot{\phi}(t) + M^2\phi(t) + \frac{\lambda}{2}\phi^3(t) + \frac{3\lambda}{2}\phi(t)\langle\psi^2(t)\rangle_B = 0. \quad (2.10)$$

The bare quantum fluctuations $\langle\psi^2(t)\rangle_B$ are obtained from the coincidence limit of the non-equilibrium Green's functions, which are obtained from the mode functions obeying,

$$\left[\frac{d^2}{dt^2} + 3H\frac{d}{dt} + \omega_k^2(t) \right] f_k(t) = 0, \quad (2.11)$$

with the effective frequencies,

$$\omega_k^2(t) = \frac{k^2}{a^2(t)} + M^2(t),$$

where

$$M^2(t) = m(t)^2 + \frac{3\lambda}{2}\phi^2(t) + \frac{3\lambda}{2}\langle\psi^2(t)\rangle. \quad (2.12)$$

Notice the only difference between Hartree and large N limits: a factor 3 in front of $\phi^2(t) + \langle\psi^2(t)\rangle$ in the effective mass squared for the mode functions as compared to the equation for the zero mode. In particular, when $\phi(t) = 0$ corresponding to a phase transition in absence of biased initial conditions, both descriptions yield the same results (up to a trivial rescaling of the coupling constant by a factor 3).

The equal time correlation function is given in terms of the mode functions as [4,3,14],

$$\langle\psi^2(t)\rangle = \int \frac{d^3k}{(2\pi)^3} \frac{|f_k(t)|^2}{2} \coth \left[\frac{W_k}{2T_i} \right]. \quad (2.13)$$

The initial conditions are chosen to reflect the same physical situation as in the large N case, that is, the instantaneous particle states of the Hamiltonian at $t = 0$ are in local thermodynamic equilibrium at some initial temperature higher than the critical value. Thus,

as in the large N case but with modified frequencies, the initial conditions at $t = 0$ are chosen to describe the instantaneous positive energy states,

$$f_k(0) = \frac{1}{\sqrt{W_k}} ; \dot{f}_k(0) = -i\sqrt{W_k} ; W_k = \sqrt{k^2 + M_0^2} . \quad (2.14)$$

We have maintained the same names for the mode functions and M_0 to avoid cluttering of notation; their meaning for each case should be clear from the context. Notice that the difference between the Hartree and large N case is rather minor. The most significant difference is that, in the equations for the zero modes, the Hartree case displays a factor 3 difference between the tree level non-linear term and the contribution from the fluctuation as compared to the corresponding terms in the large N case. The equations for the mode functions are the same upon a rescaling of the coupling constant by a factor 3.

A re-summed one-loop approximation is obtained by keeping only the leading quantum corrections. That is, the first non-trivial contribution in λ . Such approximation can be worked out by taking the expectation value of the evolution equations of the field operator $\bar{\Phi}$ to first order in λ . At this stage, we can straightforwardly obtain the resummed one-loop evolution equations from the Hartree equations for small λ . Just notice that $\langle\psi^2(t)\rangle$ is multiplied by λ in the zero mode equation (2.10). Therefore, to leading order in λ , we can neglect the term $\frac{3}{2}\lambda\langle\psi^2(t)\rangle$ in the mode equations (2.11). In summary, the resummed one-loop evolution equations take the form

$$\ddot{\phi}(t) + 3H\dot{\phi}(t) + M^2\phi(t) + \frac{\lambda}{2}\phi^3(t) + \frac{3\lambda}{2}\phi(t)\langle\psi^2(t)\rangle_B = 0 ,$$

$$\left[\frac{d^2}{dt^2} + 3H\frac{d}{dt} + \frac{k^2}{a^2(t)} + m(t)^2 + \frac{3\lambda}{2}\phi^2(t) \right] f_k(t) = 0 .$$

The bare one-loop quantum fluctuations $\langle\psi^2(t)\rangle_B$ are obtained by inserting the one-loop modes $f_k(t)$ into eq.(2.13).

It must be stressed, however, that a numerical implementation of the set of equations above, represents a *non-perturbative* treatment, in the sense that the (numerical) solution will incorporate arbitrary powers of λ . A naive perturbative expansion in λ is bound to break down due to secular terms whenever resonances are present as is the case in parametric amplification. A resummation of these secular terms as obtained via a numerical integration for example corresponds to a non-trivial resummation of the perturbative series.

These resummed one-loop equations are slightly simpler than the large N or Hartree equations. For small values of λ as in inflationary models (where $\lambda \sim 10^{-12}$) the resummed one-loop approximation provides reliable results [10].

C. Renormalization in Cosmological Spacetimes

We briefly review the most relevant features of the renormalization program in the large N limit that will be used frequently in our analysis. The Hartree case follows upon trivial changes. For more details the reader is referred to [14,8,15,3].

In this approximation, the Lagrangian is quadratic, and there are no counterterms. This implies that the equations for the mode functions must be finite. This requires that

$$m_B(t)^2 + \frac{\lambda_B}{2}\phi^2(t) + \xi_B \mathcal{R}(t) + \frac{\lambda_B}{2}\langle\psi^2(t)\rangle_B = m_R^2 + \frac{\lambda_R}{2}\phi^2(t) + \xi_R \mathcal{R}(t) + \frac{\lambda_R}{2}\langle\psi^2(t)\rangle_R ,$$

where the subscripts B , R refer to bare and renormalized quantities, respectively. Defining

$$\varphi_k(t) \equiv a(t)^{3/2} f_k(t) \quad , \quad \varphi_k(0) = \frac{1}{\sqrt{W_k}} \quad , \quad \dot{\varphi}_k(0) = -i\sqrt{W_k}$$

(with $a(0) = 1$).

The functions $\varphi_k(t)$ satisfy the Schrödinger-like differential equation

$$\left[\frac{d^2}{dt^2} - \frac{3}{2} \left(\frac{\ddot{a}}{a} + \frac{1}{2} \frac{\dot{a}^2}{a^2} \right) + \frac{\vec{k}^2}{a^2(t)} + M^2(t) \right] \varphi_k(t) = 0$$

In order to derive the large k behaviour, it is convenient to write the $\varphi_k(t)$ as linear combinations of WKB solutions of the form

$$\varphi_k(t) = A_k \exp \int_0^t R_k(t') dt' + B_k \exp \int_0^t R_k^*(t') dt'$$

with $R_k(t)$ obeying a Riccati equation [3] and the coefficients A_k , B_k are fixed by the initial conditions. After some algebra we find [4,16],

$$\begin{aligned} |f_k(t)|^2 &= \frac{1}{ka^2(t)} + \frac{1}{2k^3a^2(t)} \left[H^2(0) - B(t) \right] \\ &+ \frac{1}{8a(t)^2 k^5} \left\{ B(t)[3B(t) - 2H^2(0)] + a(t) \frac{d}{dt} [a(t)\dot{B}(t)] + D_0 \right\} + \mathcal{O}(1/k^7) \\ |\dot{f}_k(t)|^2 &= \frac{k}{a^4(t)} + \frac{1}{ka^2(t)} \left[H^2(t) + \frac{H^2(0)}{2a^2(t)} + \frac{1}{2} \left(M^2(t) - \frac{\mathcal{R}(t)}{6} \right) \right] \\ &+ \frac{1}{8a(t)^4 k^3} \left\{ -B(t)^2 - a(t)^2 \ddot{B}(t) + 3a(t)\dot{a}(t)\dot{B}(t) - 4\dot{a}^2(t)B(t) \right. \\ &\left. + 2H^2(0)[2\dot{a}^2(t) + B(t)] + D_0 \right\} + \mathcal{O}(1/k^5). \end{aligned} \tag{2.15}$$

where we defined $B(t)$ as

$$B(t) \equiv a^2(t) \left(M^2(t) - \frac{\mathcal{R}(t)}{6} \right) ,$$

in terms of the effective mass term for the large N limit given by (2.8) and the Hartree case, eq. (2.12). The constant D_0 depends on the initial conditions and is unimportant for our analysis.

Using this asymptotic forms, we obtain [8,15,3,4,16] the following renormalized quantities

$$m_B^2(t) + \frac{\lambda_B}{16\pi^2} \frac{\Lambda^2}{a^2(t)} + \frac{\lambda_B}{16\pi^2} \ln \left(\frac{\Lambda}{\kappa} \right) \frac{\dot{a}^2(t_o)}{a^2(t)} = m_R^2 \left[1 + \frac{\lambda_B}{16\pi^2} \ln \left(\frac{\Lambda}{\kappa} \right) \right]$$

$$\begin{aligned}
\lambda_B &= \frac{\lambda_R}{1 - \frac{\lambda_R}{16\pi^2} \ln\left(\frac{\Lambda}{\kappa}\right)} \\
\xi_B &= \xi_R + \frac{\lambda_B}{16\pi^2} \ln\left(\frac{\Lambda}{\kappa}\right) \left(\xi_R - \frac{1}{6}\right) \\
\langle\psi(t)^2\rangle_R &= \int \frac{d^3k}{(2\pi)^3} \left\{ \frac{|f_k(t)|^2}{2} \coth\left[\frac{W_k}{2T_i}\right] - \frac{1}{2k a^2(t)} \right. \\
&\quad \left. + \frac{\theta(k - \kappa)}{4k^3 a^2(t)} \left[-H^2(0) + a^2(t) \left(M^2(t) - \frac{\mathcal{R}(t)}{6} \right) \right] \right\} .
\end{aligned} \tag{2.16}$$

We have introduced the (arbitrary) renormalization scale κ . The conformal coupling $\xi = 1/6$ is a *fixed point* under renormalization [25]. In dimensional regularization the terms involving Λ^2 are absent and $\ln \Lambda$ is replaced by a simple pole at the physical dimension. Even in such a regularization scheme, however, a time dependent bare mass is needed. The presence of this new renormalization allows us to introduce a new renormalized mass term of the form

$$\frac{\varrho}{a^2(t)}$$

This counterterm may be interpreted as a squared mass red-shifted by the expansion of the universe. However, we shall set $\varrho = 0$ for simplicity.

At this point it is convenient to absorb a further *finite* renormalization in the definition of the mass and introduce the following quantities:

$$\begin{aligned}
M_R^2 &= m_R^2 + \frac{\lambda_R}{2} \langle\psi^2(0)\rangle_R \\
\tau &= |M_R|t \quad , \quad q = \frac{k}{|M_R|} \quad , \quad \Omega_q = \frac{W_k}{|M_R|} \quad , \quad \mathcal{T} = \frac{T_i}{|M_R|} \quad , \\
\eta^2(\tau) &= \frac{\lambda_R}{2|M_R|^2} \phi^2(t) \quad , \\
g\Sigma(\tau) &= \frac{\lambda_R}{2|M_R|^2} \left[\langle\psi^2(t)\rangle_R - \langle\psi^2(0)\rangle_R \right] \quad , \quad (\Sigma(0) = 0)
\end{aligned} \tag{2.17}$$

$$g = \frac{\lambda_R}{8\pi^2} \quad , \tag{2.18}$$

$$\varphi_q(\tau) \equiv \sqrt{|M_R|} f_k(t) \quad .$$

For simplicity in our numerical calculations later, we will chose the renormalization scale $\kappa = |M_R|$. The evolution equations are now written in terms of these dimensionless variables, in which dots now stand for derivatives with respect to τ .

III. THE RENORMALIZED EVOLUTION EQUATIONS AND THE ENERGY-MOMENTUM TENSOR

From now on we focus our analysis on the case of Minkowski space-time with the aim of understanding the fundamental phenomena in a simpler setting. The case of cosmological spacetimes is presented in refs. [16,17].

Let us summarize here the renormalized field equations in the Hartree and large N approximations that will be solved numerically and analytically in Minkowski spacetime.

A. Unbroken Symmetry

In this case $M_R^2 = |M_R|^2$, and in terms of the dimensionless variables introduced above we find the following equations of motion:

$$\ddot{\eta} + \eta + \eta^3 + g \eta(\tau) \Sigma(\tau) = 0 \quad (3.1)$$

$$\left[\frac{d^2}{d\tau^2} + q^2 + 1 + \eta(\tau)^2 + g \Sigma(\tau) \right] \varphi_q(\tau) = 0, \quad (3.2)$$

$$\varphi_q(0) = \frac{1}{\sqrt{\Omega_q}}, \quad \dot{\varphi}_q(0) = -i \sqrt{\Omega_q} \quad (3.3)$$

$$\eta(0) = \eta_0, \quad \dot{\eta}(0) = 0 \quad (3.4)$$

Hence, $\mathcal{M}^2(\tau) \equiv 1 + \eta(\tau)^2 + g \Sigma(\tau)$ plays the rôle of a (time dependent) renormalized effective mass squared.

As mentioned above, the choice of Ω_q determines the initial state. We will choose these such that at $t = 0$ the quantum fluctuations are in the ground state of the oscillators at the initial time. Recalling that by definition $g\Sigma(0) = 0$, we choose the dimensionless frequencies to be

$$\Omega_q = \sqrt{q^2 + 1 + \eta_0^2}. \quad (3.5)$$

The Wronskian of two solutions of (3.2) is given by

$$\mathcal{W}[\varphi_q, \bar{\varphi}_q] = 2i,$$

while $g\Sigma(\tau)$ is given by

$$g\Sigma(\tau) = g \int_0^\infty q^2 dq \left\{ |\varphi_q(\tau)|^2 \coth \left[\frac{\Omega_q}{2\mathcal{T}} \right] - \frac{1}{\Omega_q} + \frac{\theta(q-1)}{2q^3} [-\eta_0^2 + \eta^2(\tau) + g \Sigma(\tau)] \right\}. \quad (3.6)$$

B. Broken Symmetry

In the case of broken symmetry $M_R^2 = -|M_R^2|$ and the field equations in the $N = \infty$ limit become:

$$\ddot{\eta} - \eta + \eta^3 + g \eta(\tau) \Sigma(\tau) = 0 \quad (3.7)$$

$$\left[\frac{d^2}{d\tau^2} + q^2 - 1 + \eta(\tau)^2 + g \Sigma(\tau) \right] \varphi_q(\tau) = 0 \quad (3.8)$$

where $\Sigma(\tau)$ is given in terms of the mode functions $\varphi_q(\tau)$ by the same expression of the previous case, (3.6). Here, $\mathcal{M}^2(\tau) \equiv -1 + \eta(\tau)^2 + g \Sigma(\tau)$ plays the rôle of a (time dependent) renormalized effective mass squared.

The choice of boundary conditions is more subtle for broken symmetry. The situation of interest is when $0 < \eta_0^2 < 1$, corresponding to the situation where the expectation value rolls down the potential hill from the origin. The modes with $q^2 < 1 - \eta_0^2$ are unstable and thus do not represent simple harmonic oscillator quantum states. Therefore one *must* chose a different set of boundary conditions for these modes. Our choice will be that corresponding to the ground state of an *upright* harmonic oscillator. This particular initial condition corresponds to a quench type of situation in which the initial state is evolved in time in an inverted parabolic potential (for early times $t > 0$). Thus we shall use the following initial conditions for the mode functions:

$$\varphi_q(0) = \frac{1}{\sqrt{\Omega_q}} \quad , \quad \dot{\varphi}_q(0) = -i \sqrt{\Omega_q} \quad (3.9)$$

$$\begin{aligned} \Omega_q &= \sqrt{q^2 + 1 + \eta_0^2} \quad \text{for } q^2 < q_u^2 \equiv 1 - \eta_0^2 \\ \Omega_q &= \sqrt{q^2 - 1 + \eta_0^2} \quad \text{for } q^2 > q_u^2 \quad ; \quad 0 \leq \eta_0^2 < 1 . \end{aligned} \quad (3.10)$$

along with the initial conditions for the zero mode given by eq.(3.4).

C. Particle Number

Although the notion of particle number is ambiguous in a time dependent non-equilibrium situation, a suitable definition can be given with respect to some particular pointer state. We consider two particular definitions that are physically motivated and relevant as we will see later. The first is when we define particles with respect to the initial Fock vacuum state, while the second corresponds to defining particles with respect to the adiabatic vacuum state.

In the former case we write the spatial Fourier transform of the fluctuating field $\psi(\vec{x}, t)$ in (2.3) and (2.5) and its canonical momentum $\Pi(\vec{x}, t)$ as

$$\begin{aligned} \psi_k(t) &= \frac{1}{\sqrt{2}} \left[a_k f_k(t) + a_{-k}^\dagger f_k^*(t) \right] \\ \Pi_k(t) &= \frac{1}{\sqrt{2}} \left[a_k \dot{f}_k(t) + a_{-k}^\dagger \dot{f}_k^*(t) \right] \end{aligned}$$

with the *time independent* creation and annihilation operators, such that a_k annihilates the initial Fock vacuum state. Using the initial conditions on the mode functions, the Heisenberg field operators are written as

$$\begin{aligned} \psi_k(t) &= \mathcal{U}^{-1}(t) \psi_k(0) \mathcal{U}(t) = \frac{1}{\sqrt{2W_k}} \left[\tilde{a}_k(t) + \tilde{a}_{-k}^\dagger(t) \right] \\ \Pi_k(t) &= \mathcal{U}^{-1}(t) \Pi_k(0) \mathcal{U}(t) = -i \sqrt{\frac{W_k}{2}} \left[\tilde{a}_k(t) - \tilde{a}_{-k}^\dagger(t) \right] \\ \tilde{a}_k(t) &= \mathcal{U}^{-1}(t) a_k \mathcal{U}(t) \end{aligned}$$

with $\mathcal{U}(t)$ the time evolution operator with the boundary condition $\mathcal{U}(0) = 1$. The Heisenberg operators $\tilde{a}_k(t)$, $\tilde{a}_k^\dagger(t)$ are related to a_k, a_k^\dagger by a Bogoliubov (canonical) transformation (see reference [8] for details).

The particle number with respect to the initial Fock vacuum state is defined in term of the dimensionless variables introduced above as

$$\begin{aligned} N_q(\tau) &= \langle \tilde{a}_k^\dagger(t) \tilde{a}_k(t) \rangle \\ &= \frac{1}{2} N_q(0) \left[\Omega_q |\varphi_q(\tau)|^2 + \frac{|\dot{\varphi}_q(\tau)|^2}{\Omega_q} + 2 \right] + \frac{1}{4} \left[\Omega_q |\varphi_q(\tau)|^2 + \frac{|\dot{\varphi}_q(\tau)|^2}{\Omega_q} \right] - \frac{1}{2}. \end{aligned} \quad (3.11)$$

The initial occupation number $N_q(0)$ exhibits a thermal distribution

$$N_q(0) = \frac{1}{e^{\Omega_q/\mathcal{T}} - 1},$$

according to the initial temperature \mathcal{T} . The particle number is expressed in eq.(3.11) as the sum of two contributions: the first term is the spontaneous production (proportional to the initial thermal occupation) and the second is the induced production (independent of it).

It is the definition (3.11) of particle number that will be used for the numerical study.

In order to define the particle number with respect to the adiabatic vacuum state we note that the mode equations (3.2,3.8) are those of harmonic oscillators with time dependent squared frequencies

$$\omega_q^2(\tau) = q^2 \pm 1 + \eta^2(\tau) + g\Sigma(\tau)$$

with $+$ for the unbroken symmetry case and $-$ for the broken symmetry case, respectively. When the frequencies are real, the adiabatic modes can be introduced in the following manner:

$$\begin{aligned} \psi_k(t) &= \frac{1}{\sqrt{2\omega_k(t)}} \left[\alpha_k(t) e^{-i \int_0^t \omega_k(t') dt'} + \alpha_{-k}^\dagger(t) e^{i \int_0^t \omega_k(t') dt'} \right] \\ \Pi_k(t) &= -i \sqrt{\frac{\omega_k(t)}{2}} \left[\alpha_k(t) e^{-i \int_0^t \omega_k(t') dt'} - \alpha_{-k}^\dagger(t) e^{i \int_0^t \omega_k(t') dt'} \right] \end{aligned}$$

where now $\alpha_k(t)$ is a canonical operator that destroys the adiabatic vacuum state, and is related to a_k, a_k^\dagger by a Bogoliubov transformation. This expansion diagonalizes the instantaneous Hamiltonian in terms of the canonical operators $\alpha(t), \alpha^\dagger(t)$. The adiabatic particle number is

$$\begin{aligned} N_q^{ad}(\tau) &= \langle \alpha_k^\dagger(t) \alpha_k(t) \rangle \\ &= \frac{1}{2} N_q(0) \left[\omega_q(\tau) |\varphi_q(\tau)|^2 + \frac{|\dot{\varphi}_q(\tau)|^2}{\omega_q(\tau)} + 2 \right] + \frac{1}{4} \left[\omega_q(\tau) |\varphi_q(\tau)|^2 + \frac{|\dot{\varphi}_q(\tau)|^2}{\omega_q(\tau)} \right] - \frac{1}{2}. \end{aligned} \quad (3.12)$$

As mentioned above, the adiabatic particle number can *only* be defined when the frequencies $\omega_q(\tau)$ are real. Thus, in the broken symmetry state they can only be defined for wave-vectors larger than the maximum unstable wave-vector, $k > k_u = |M_R| \sqrt{1 - \eta_0^2}$. These adiabatic modes and the corresponding adiabatic particle number have been used previously within the non-equilibrium context [14] and will be very useful in the analysis of the energy below. Both definitions coincide at $\tau = 0$ because $\omega_q(0) = \Omega_q$. Notice that $N_q^{ad}(0) = N_q(0) = 0$ if we choose zero initial temperature. (We considered a non-zero initial temperature in refs. [8,3]).

D. Energy and Pressure

The energy-momentum tensor for this theory in Minkowski spacetime is given by

$$T^{\mu\nu} = \partial^\mu \vec{\phi} \cdot \partial^\nu \vec{\phi} - g^{\mu\nu} \left[\frac{1}{2} \partial_\alpha \vec{\phi} \cdot \partial^\alpha \vec{\phi} - V(\vec{\phi} \cdot \vec{\phi}) \right] \quad (3.13)$$

Since we consider translationally as well as rotationally invariant states, the expectation value of $T^{\mu\nu}$ takes the fluid form

Since we consider translationally and rotationally invariant states, the expectation value of the energy-momentum tensor takes the fluid form $p = \langle P \rangle / N\mathcal{V}$

$$E = \frac{1}{N\mathcal{V}} \langle T^{00}(x) \rangle = \frac{1}{N\mathcal{V}} \langle \frac{1}{2} \dot{\vec{\phi}}^2 + \frac{1}{2} (\nabla \vec{\phi})^2 + V(\phi) \rangle$$

$$N\mathcal{V} p(\tau) = \langle T^{11}(x) \rangle = \langle T^{22}(x) \rangle = \langle T^{33}(x) \rangle = \langle \frac{1}{3} (\nabla \vec{\phi})^2 + \dot{\vec{\phi}}^2 - T^{00}(x) \rangle ,$$

with all off-diagonal components vanishing.

Hence,

$$p(\tau) + E = \frac{1}{N\mathcal{V}} \langle \frac{1}{2} (\nabla \vec{\phi})^2 + \dot{\vec{\phi}}^2 \rangle$$

takes a particularly simple form.

Using the large N factorization (2.3-2.3) we find the energy density operator for zero initial temperature ($\mathcal{T} = 0$) to be,

$$\frac{E}{N\mathcal{V}} = \frac{1}{2} \dot{\phi}^2(t) + \frac{1}{2} m^2 \phi^2(t) + \frac{\lambda}{8} \phi^4(t) + \frac{1}{2} \int \frac{d^3k}{(2\pi)^3} \left[\dot{\psi}_k(t) \dot{\psi}_{-k}(t) + \omega_k^2(t) \psi_k(t) \psi_{-k}(t) \right]$$

$$- \frac{\lambda}{8} \langle \psi^2(t) \rangle^2 + \text{linear terms in } \psi + \mathcal{O}(1/N)$$

$$\omega_k^2(t) = k^2 + m^2 + \frac{\lambda}{2} \phi^2(t) + \frac{\lambda}{2} \langle \psi^2(t) \rangle .$$

Analogous expressions can be derived for the energy in the Hartree approximation.

The generalization to non-zero initial temperature is straightforward.

Taking the expectation value in the initial state and the infinite volume limit ($\mathcal{V} \rightarrow \infty$) and recalling that the tadpole condition requires that the expectation value of ψ vanishes, we find the expectation value of the bare energy to be

$$E_{bare} = \frac{2|M_R|^4}{\lambda_R} \left\{ \frac{1}{2} \left[\dot{\eta}^2 + \eta(\tau)^2 + \frac{1}{2} \eta(\tau)^4 \right] + \frac{g}{2} \int q^2 dq \left[|\dot{\varphi}_q(\tau)|^2 \right. \right.$$

$$\left. \left. + (q^2 + 1 + \eta(\tau)^2) |\varphi_q(\tau)|^2 \right] \right\} + \frac{\lambda}{8} \langle \psi^2(t) \rangle_B^2 , \quad (3.14)$$

where $\langle \psi^2(t) \rangle_B$ is given by eq.(2.9). It is easy to see that $\dot{E}_{bare} = 0$ using the bare equations of motion (2.6-2.7). It is important to account for the last term when taking the time derivative because this term cancels a similar term in the time derivative of $\eta^2(\tau)$.

We want to emphasize that the full evolution of the zero mode plus the back-reaction with quantum fluctuations conserves energy (covariantly in expanding cosmologies). Such

is obviously *not* the case in treatments of reheating in the literature in which back-reaction effects on the zero mode are not taken into account in a self-consistent way. Without energy conservation, the quantum fluctuations grow without bound. In cosmological scenarios energy is not conserved but its time dependence is not arbitrary; in a fixed space-time background metric it is determined by the covariant conservation of the energy momentum tensor. There again only a full account of the quantum back-reaction will maintain covariant conservation of the energy momentum tensor.

We find for the sum of bare energy plus pressure,

$$p(\tau)_{bare} + E_{bare} = \frac{2|M_R|^4}{\lambda_R} \left\{ \dot{\eta}^2 + g \int q^2 dq \left[|\dot{\varphi}_q(\tau)|^2 + \frac{1}{3} q^2 |\varphi_q(\tau)|^2 \right] \right\}. \quad (3.15)$$

It is clear that the integrals in eq. (3.14) and (3.15) are divergent.

In the previous section we have learned how to renormalize $\langle \psi^2(t) \rangle_B$, the renormalized quantum fluctuations are denoted by $\Sigma(\tau)$ [see eqs. (2.17) and (3.6)].

In order to renormalize E_{bare} and $p(\tau)_{bare}$ we need to use the large q behaviour of the mode functions $\varphi_q(\tau)$ (2.15). In Minkowski spacetime this large q behaviour reduces to

$$\begin{aligned} |\varphi_q(\tau)|^2 &\stackrel{q \rightarrow \infty}{\cong} \frac{1}{q} - \frac{\mathcal{M}^2(\tau)}{2q^3} + \frac{1}{8q^5} \left[3\mathcal{M}^4(\tau) + \frac{d^2}{d\tau^2} \mathcal{M}^2(\tau) \right] + O(q^{-7}), \\ |\dot{\varphi}_q(\tau)|^2 &\stackrel{q \rightarrow \infty}{\cong} q + \frac{\mathcal{M}^2(\tau)}{2q} - \frac{1}{8q^5} \left[\mathcal{M}^4(\tau) + \frac{d^2}{d\tau^2} \mathcal{M}^2(\tau) \right] + O(q^{-5}). \end{aligned} \quad (3.16)$$

where $\mathcal{M}^2(\tau) = \pm 1 + \eta(\tau)^2 + g \Sigma(\tau)$ is the renormalized effective mass squared.

We then subtract these asymptotic behaviours inside the integrand of eqs. (3.14) and (3.15) in order to make the integral finite. We find the following expression for the renormalized energy setting $\Lambda = \infty$:

$$\begin{aligned} E_{ren} &= \frac{2|M_R|^4}{\lambda_R} \left\{ \frac{1}{2} \left[\dot{\eta}^2 + \eta(\tau)^2 + \frac{1}{2} \eta(\tau)^4 \right] + \frac{g}{2} \int_0^\infty q^2 dq \left[|\dot{\varphi}_q(\tau)|^2 \right. \right. \\ &\quad \left. \left. + q^2 |\varphi_q(\tau)|^2 - 2q - \frac{\theta(q-1)}{4q^3} \mathcal{M}^4(\tau) \right] \right. \\ &\quad \left. + \frac{g}{2} \Sigma(\tau) \left[1 + \eta(\tau)^2 + \frac{g}{2} \Sigma(\tau) \right] \right\}, \end{aligned}$$

It is easy to see that E_{ren} is **finite**. Moreover, it is **conserved**. That is, we find that $\dot{E}_{ren} = 0$ using eqs.(2.6) and (2.7).

We find that aside from the time independent divergence that is present in the energy the pressure needs an extra subtraction

$$\frac{1}{6q^3} \frac{d^2}{d\tau^2} \vec{\Phi}^2(x)$$

compared with the energy. Such a term corresponds to an additive renormalization of the energy-momentum tensor of the form

$$\delta T^{\mu\nu} = A (\eta^{\mu\nu} \partial^2 - \partial^\mu \partial^\nu) \vec{\Phi}^2(x)$$

with A a (divergent) constant [26]. Performing the integrals with a spatial ultraviolet cutoff, and in terms of the renormalization scale κ introduced before, we find

$$A = -\frac{g}{12} \ln\left[\frac{\Lambda}{\kappa}\right]$$

In terms of dimensionless quantities and after subtracting a time independent quartic divergence, we finally find setting $\Lambda = \infty$, for the renormalized energy plus pressure

$$p(\tau)_{ren} + E_{ren} = \frac{2|M_R|^4}{\lambda_R} \left\{ \dot{\eta}^2 + g \int_0^\infty q^2 dq \left(|\dot{\varphi}_q(\tau)|^2 + \frac{1}{3} q^2 |\varphi_q(\tau)|^2 - \frac{4}{3} q - \frac{\mathcal{M}^2(\tau)}{3q} + \frac{\theta(q-K)}{12q^3} \frac{d^2}{d\tau^2} [\mathcal{M}^2(\tau)] \right) \right\} .$$

In order to obtain a better insight on this quantum conserved energy it is convenient to write eq.(3.14) as

$$E_{bare} = \frac{2|M_R|^4}{\lambda_R} \left\{ \frac{1}{2} \left[\dot{\eta}^2 + \eta(\tau)^2 + \frac{1}{2} \eta(\tau)^4 \right] + \frac{g}{2} \int q^2 dq \left[|\dot{\varphi}_q(\tau)|^2 + \omega_q(\tau)^2 |\varphi_q(\tau)|^2 \right] \right\} - \frac{\lambda}{8} \langle \psi^2(t) \rangle_B^2 ,$$

Then, we get using eq.(3.12),

$$\begin{aligned} \frac{1}{2} \int_0^\Lambda q^2 dq \left[|\dot{\varphi}_q(\tau)|^2 + \omega_q^2(\tau) |\varphi_q(\tau)|^2 \right] &= \varepsilon_U + 2 \int_{q_u}^\Lambda q^2 dq \omega_q(\tau) \left(N_q^{ad}(\tau) + \frac{1}{2} \right) , \\ \varepsilon_U &= \frac{1}{2} \int_0^{q_u} q^2 dq \left[|\dot{\varphi}_q(\tau)|^2 + \omega_q^2(\tau) |\varphi_q(\tau)|^2 \right] \end{aligned} \quad (3.17)$$

where Λ is a spatial upper momentum cutoff, taken to infinity after renormalization. In the broken symmetry case, ε_U is the contribution to the energy-momentum tensor from the unstable modes with negative squared frequencies, $q_u^2 = |M_R|^2 [1 - \eta_0^2]$ and $N_q^{ad}(\tau)$ is the adiabatic particle number given by eq.(3.12). For the unbroken symmetry case $\varepsilon_U = 0$ and $q_u = 0$.

This representation is particularly useful in dealing with renormalization of the energy. Since the energy is conserved, a subtraction at $\tau = 0$ suffices to render it finite in terms of the renormalized coupling and mass. Using energy conservation and the renormalization conditions in the large N limit, we find that the integral

$$\int_{q_u}^\infty q^2 dq \omega_q(\tau) N_q^{ad}(\tau)$$

is finite. This can also be seen from the asymptotic behaviors (3.16). We get from eqs. (3.12) and (3.16),

$$N_q^{ad}(\tau) \stackrel{q \rightarrow \infty}{\simeq} O\left(\frac{1}{q^6}\right) .$$

All ultraviolet divergences are contained in the last term of eq.(3.17). That is,

$$\int_{q_u}^{\Lambda} q^2 dq \omega_q(\tau) = \frac{\Lambda^4}{4} + \frac{\Lambda^2 \mathcal{M}^2}{4} - \frac{\mathcal{M}^4}{8} \log(2\Lambda) + \frac{1}{32} \mathcal{M}^4 \quad (3.18)$$

$$- \frac{1}{8} \left[q_u \sqrt{q_u^2 + \mathcal{M}^2} (\mathcal{M}^2 + 2q_u^2) - \mathcal{M}^4 \log \left(q_u + \sqrt{q_u^2 + \mathcal{M}^2} \right) \right] .$$

In terms of dimensionless quantities, the renormalized energy density is, after taking $\Lambda \rightarrow \infty$:

$$E_{ren} = \frac{2|M_R|^4}{\lambda_R} \left\{ \frac{\dot{\eta}^2}{2} + \frac{1}{2} (\pm 1 + \eta^2) \mathcal{M}^2(\tau) - \frac{\mathcal{M}^4(\tau) + 1}{4} + g \left[\varepsilon_F(\tau) + \frac{1}{2} J^\pm(\eta_0) \mathcal{M}^2(\tau) \right. \right.$$

$$- \frac{q_u}{4} (q_u^2 + \mathcal{M}^2(\tau)) \left(q_u + \sqrt{q_u^2 + \mathcal{M}^2(\tau)} \right) + \frac{q_u}{8} \mathcal{M}^2(\tau) \sqrt{q_u^2 + \mathcal{M}^2(\tau)}$$

$$\left. \left. + \frac{\mathcal{M}^4(\tau)}{32} + \frac{\mathcal{M}^4(\tau)}{8} \ln \left[q_u + \sqrt{q_u^2 + \mathcal{M}^2(\tau)} \right] + \mathcal{C}^\pm(\eta_0) \right] \right\} , \quad (3.19)$$

where,

$$\varepsilon_F(\tau) = \frac{1}{2} \int_0^{q_u} q^2 dq \left[|\dot{\varphi}_q|^2 + \omega_q^2(\tau) |\varphi_q|^2 \right] + 2 \int_{q_u}^{\infty} q^2 dq \omega_q(\tau) N_q^{ad}(\tau) \quad (3.20)$$

$$\mathcal{M}^2(\tau) = \pm 1 + \eta^2(\tau) + g\Sigma(\tau) \quad , \quad \omega_q^2(\tau) = q^2 + \mathcal{M}^2(\tau) , \quad (3.21)$$

Here the lower sign and $q_u = \sqrt{1 - \eta_0^2}$ apply to the broken symmetry case while the upper sign and $q_u = 0$ correspond to the unbroken symmetry case. The constant $J^\pm(\eta_0)$ is defined as,

$$J^\pm(\eta_0) \equiv \int_0^\infty q^2 dq \left[\frac{1}{q} - \frac{1}{\Omega_q} - \frac{\eta_0^2 \pm 1}{2q^3} \theta(q - 1) \right] . \quad (3.22)$$

The constant $\mathcal{C}^\pm(\eta_0)$ is chosen such that E_{ren} coincides with the classical energy for the zero mode at $\tau = 0$. The quantity $\mathcal{M}(\tau)$ is identified as the effective (dimensionless) mass for the ‘‘pions’’.

In the unbroken symmetry case (upper sign) we find

$$J^+(\eta_0) = -\frac{1 + \eta_0^2}{4} \left[1 + \log \left(\frac{1 + \eta_0^2}{4} \right) \right]$$

and

$$\mathcal{C}^+(\eta_0) = -\frac{3}{4} (1 + \eta_0^2) J^+(\eta_0) .$$

We find using the renormalized eqs. (3.1), (3.2), (3.6), (3.7) and (3.8), that the renormalized energy E_{ren} is indeed **conserved** both for unbroken and for broken symmetry.

Let us now make contact with the effective potential which is a quantity defined for **time independent** expectation value of the field. That is, for constant η .

We recognize in eq. (3.19) that the sum of terms *without* ε_F for $q_u = 0$ coincide with the effective potential in this approximation. These arise from the ‘zero point’ energy of the oscillators in (3.17). That is, for $\eta(\tau) = \eta_0$,

$$V_{eff}(\eta_0) = \frac{2|M_R|^4}{\lambda_R} \left\{ \frac{\mathcal{M}^4 - 1}{4} + g \left[\frac{1}{2} J^\pm(\eta_0) \mathcal{M}^2 + \frac{\mathcal{M}^4}{32} + \frac{\mathcal{M}^4}{8} \ln \mathcal{M} + \mathcal{C}^\pm(\eta_0) \right] \right\}, \quad (3.23)$$

Notice that $\mathcal{M}^2(\tau) = \mathcal{M}^2 = \pm 1 + \eta_0^2$ for a time independent order parameter $\eta(\tau) = \eta_0$ as it follows from eq.(3.6).

In the broken symmetry case the term ε_F describes the dynamics of the spinodal instabilities [3] since the mode functions will grow in time. Ignoring these instabilities and setting $q_u = 0$ as is done in a calculation of the effective potential results in an imaginary part. In the unbroken symmetry ($q_u = 0$) case the sum of terms without ε_F give the effective potential in the large N limit. The term ε_F **cannot** be obtained in a purely static calculation. Such term describes the profuse particle production via parametric amplification, the mode functions in the unstable bands give a contribution to this term that eventually becomes non-perturbatively large and comparable to the tree level terms as will be described in detail below. Clearly both in the broken and unbroken symmetry cases the effective potential misses *all* of the interesting dynamics, that is the exponential growth of quantum fluctuations and the ensuing particle production, either associated with unstable bands in the unbroken symmetry case or spinodal instabilities in the broken symmetry phase.

The expression for the renormalized energy density given by (3.19-3.21) differs from the effective potential in several fundamental aspects: i) it is always real as opposed to the effective potential that becomes complex in the spinodal region, ii) it accounts for particle production and time dependent phenomena.

At this stage we can recognize why the effective potential is an irrelevant quantity to study the dynamics.

The effective potential is a useless tool to study the dynamics precisely because it misses the profuse particle production associated with these dynamical, non-equilibrium and non-perturbative processes.

IV. THE UNBROKEN SYMMETRY CASE

The full resolution of the large N or Hartree equations needs a numerical treatment [8,9,15]. However an analytic treatment can be performed for early times while the non-linear effects are still small.

A. Analytic Results for large N

In this section we turn to the analytic treatment of equations (3.1), (3.2) and (3.6) in the unbroken symmetry case. Our approximations will only be valid in the weak coupling regime and for times small enough so that the quantum fluctuations, i.e. $g\Sigma(\tau)$ are not large compared to the “tree level” quantities. We will see that this encompasses the times in which most of the interesting physics occurs.

Since $\Sigma(0) = 0$, the back-reaction term $g\Sigma(\tau)$ is expected to be small for small g during an interval say $0 \leq \tau < \tau_1$. This time τ_1 , to be determined below, determines the relevant time scale for preheating and will be called the preheating time.

During the interval of time in which the back-reaction term $g\Sigma(\tau)$ can be neglected eq.(3.1) reduces to

$$\ddot{\eta} + \eta + \eta^3 = 0 .$$

The solution of this equation with the initial conditions (3.4) can be written in terms of elliptic functions with the result:

$$\begin{aligned} \eta(\tau) &= \eta_0 \operatorname{cn} \left(\tau \sqrt{1 + \eta_0^2}, k \right) \\ k &= \frac{\eta_0}{\sqrt{2(1 + \eta_0^2)}} , \end{aligned} \quad (4.1)$$

where cn stands for the Jacobi cosine. Notice that $\eta(\tau)$ has period $4\omega \equiv 4K(k)/\sqrt{1 + \eta_0^2}$, where $K(k)$ is the complete elliptic integral of first kind. In addition we note that since

$$\eta(\tau + 2\omega) = -\eta(\tau) ,$$

if we neglect the back-reaction in the mode equations, the ‘potential’ $(-1 - \eta^2(\tau))$ is periodic with period 2ω . Inserting this form for $\eta(\tau)$ in eq.(3.2) and neglecting $g\Sigma(\tau)$ yields

$$\left[\frac{d^2}{d\tau^2} + q^2 + 1 + \eta_0^2 - \eta_0^2 \operatorname{sn}^2 \left(\tau \sqrt{1 + \eta_0^2}, k \right) \right] \varphi_q(\tau) = 0 . \quad (4.2)$$

This is the Lamé equation for a particular value of the coefficients that make it solvable in terms of Jacobi functions [27]. We summarize here the results for the mode functions. The derivations are given in ref. [15].

Since the coefficients of eq.(4.2) are periodic with period 2ω , the mode functions can be chosen to be quasi-periodic (Floquet type) with quasi-period 2ω .

$$U_q(\tau + 2\omega) = e^{iF(q)} U_q(\tau) , \quad (4.3)$$

where the Floquet indices $F(q)$ are independent of τ . In the allowed zones, $F(q)$ is a real number and the functions are bounded with a constant maximum amplitude. In the forbidden zones $F(q)$ has a non-zero imaginary part and the amplitude of the solutions either grows or decreases exponentially.

Obviously, the Floquet modes $U_q(\tau)$ cannot obey in general the initial conditions given by (3.3) and the proper mode functions with these initial conditions will be obtained as linear combinations of the Floquet solutions. We normalize the Floquet solutions as

$$U_q(0) = 1 .$$

We choose $U_q(\tau)$ and $U_q(-\tau)$ as an independent set of solutions of the second order differential equation (4.2). It follows from eq.(4.3) that $U_q(-\tau)$ has $-F(q)$ as its Floquet index.

We can now express the modes $\varphi_q(\tau)$ with the proper boundary conditions [see eq.(3.3)] as the following linear combinations of $U_q(\tau)$ and $U_q(-\tau)$

$$\varphi_q(\tau) = \frac{1}{2\sqrt{\Omega_q}} \left[\left(1 - \frac{2i\Omega_q}{\mathcal{W}_q} \right) U_q(-\tau) + \left(1 + \frac{2i\Omega_q}{\mathcal{W}_q} \right) U_q(\tau) \right] , \quad (4.4)$$

where \mathcal{W}_q is the Wronskian of the two Floquet solutions

$$\mathcal{W}_q \equiv W[U_q(\tau), U_q(-\tau)] = -2\dot{U}_q(0) .$$

Eq.(4.2) corresponds to a Schrödinger-like equation with a one-zone potential [28]. We find *two* allowed bands and *two* forbidden bands. The allowed bands correspond to

$$-1 - \frac{\eta_0^2}{2} \leq q^2 \leq 0 \quad \text{and} \quad \frac{\eta_0^2}{2} \leq q^2 \leq +\infty ,$$

and the forbidden bands to

$$-\infty \leq q^2 \leq -1 - \frac{\eta_0^2}{2} \quad \text{and} \quad 0 \leq q^2 \leq \frac{\eta_0^2}{2} .$$

The last forbidden band is for *positive* q^2 and hence will contribute to the exponential growth of the fluctuation function $\Sigma(\tau)$.

The mode functions can be written explicitly in terms of Jacobi ϑ -functions for each band. We find for the forbidden band,

$$U_q(\tau) = e^{-\tau} \sqrt{1+\eta_0^2} Z(2K(k)v) \frac{\vartheta_4(0) \vartheta_1(v + \frac{\tau}{2\omega})}{\vartheta_1(v) \vartheta_4(\frac{\tau}{2\omega})} , \quad (4.5)$$

where v is a function of q in the forbidden band $0 \leq q \leq \frac{\eta_0}{\sqrt{2}}$ defined by

$$q = \frac{\eta_0}{\sqrt{2}} \text{cn}(2K(k)v, k) , \quad 0 \leq v \leq \frac{1}{2} . \quad (4.6)$$

and $Z(u)$ is the Jacobi zeta function [29]. It can be expanded in series as follows

$$2K(k) Z(2K(k)v) = 4\pi \sum_{n=1}^{\infty} \frac{\hat{q}^n}{1 - \hat{q}^{2n}} \sin(2n\pi v) \quad (4.7)$$

where $\hat{q} \equiv e^{-\pi K'(k)/K(k)}$. The Jacobi ϑ -functions can be expanded in series as follows [30]

$$\begin{aligned} \vartheta_1(v|\hat{q}) &= 2 \sum_{n=1}^{\infty} (-1)^{n+1} \hat{q}^{(n-1/2)^2} \sin(2n-1)\pi v , \\ \vartheta_4(v|\hat{q}) &= 1 + 2 \sum_{n=1}^{\infty} (-1)^n \hat{q}^{n^2} \cos(2n\pi v) . \end{aligned}$$

We explicitly see in eq.(4.5) that $U_q(\tau)$ factorizes into a real exponential with an exponent linear in τ and an antiperiodic function of τ with period 2ω . Recall that

$$\vartheta_1(x+1) = -\vartheta_1(x) \quad , \quad \vartheta_4(x+1) = +\vartheta_4(x) . \quad (4.8)$$

We see that the solution $U_q(\tau)$ decreases with τ . The other independent solution $U_q(-\tau)$ grows with τ .

The Floquet indices can be read comparing eq.(4.3), (4.5) and (4.8),

$$F(q) = 2i K(k) Z(2K(k)v) \pm \pi .$$

$U_q(\tau)$ turns out to be a real function in the forbidden band. It has real zeroes at

$$\tau = 2\omega(n - v) \quad , \quad n \in \mathcal{Z} .$$

and complex poles at

$$\tau = 2\omega n_1 + (2n_2 + 1)\omega' \quad , \quad n_1, n_2 \in \mathcal{Z} . \quad (4.9)$$

where ω' is the complex period of the Jacobi functions. Notice that the pole positions are q -independent, and that $U_q(\tau)$ becomes an antiperiodic function on the borders of this forbidden band, $q = 0$ and $q = \frac{\eta_0}{\sqrt{2}}$. We find using eq.(4.5) and ref. [29],

$$U_q(\tau)|_{q=0} = \text{cn}(\tau\sqrt{1 + \eta_0^2}, k)$$

$$\lim_{q \rightarrow \frac{\eta_0}{\sqrt{2}}} [vU_q(\tau)] = \frac{1}{\pi\vartheta_3^2(0)} \text{sn}(\tau\sqrt{1 + \eta_0^2}, k) ,$$

respectively.

The functions $U_q(\tau)$ transform under complex conjugation in the forbidden band as

$$[U_q(\tau)]^* = U_q(\tau) . \quad (4.10)$$

For the allowed band $\frac{\eta_0}{\sqrt{2}} \leq q \leq \infty$, we find for the mode functions

$$U_q(\tau) = e^{-\frac{\tau}{2\omega} \frac{\vartheta_1'}{\vartheta_1}(i \frac{K'(k)}{K(k)} v)} \frac{\vartheta_4(0) \vartheta_4(i \frac{K'(k)}{K(k)} v + \frac{\tau}{2\omega})}{\vartheta_4(i \frac{K'(k)}{K(k)} v) \vartheta_4(\frac{\tau}{2\omega})} , \quad (4.11)$$

where

$$q = \sqrt{\eta_0^2 + 1} \frac{\text{dn}}{\text{sn}}(2 K'(k) v, k') ,$$

$$0 \leq v \leq \frac{1}{2} \quad , \quad \infty \geq q \geq \frac{\eta_0}{\sqrt{2}}$$

We see that $U_q(\tau)$ in this allowed band factorizes into a phase proportional to τ and a complex periodic function with period 2ω . This function $U_q(\tau)$ has *no real zeroes* in τ except when q is at the lower border $q = \frac{\eta_0}{\sqrt{2}}$. Its poles in τ are q -independent and they are the same as those in the forbidden band [see eq.(4.9)].

The Floquet indices can be read off by comparing eq.(4.3), (4.8) and (4.11)

$$F(q) = i \frac{\vartheta_1'}{\vartheta_1} \left(i \frac{K'(k)}{K(k)} v \right) .$$

These indices are real in the allowed band.

The functions $U_q(\tau)$ transform under complex conjugation in the allowed band as

$$[U_q(\tau)]^* = U_q(-\tau) . \quad (4.12)$$

Obviously these modes will give contributions to the fluctuation $\Sigma(\tau)$ which are always bounded in time and at long times will be subdominant with respect to the contributions of the modes in the forbidden band that grow exponentially.

The form of these functions is rather complicated, and it is useful to find convenient approximations of them for calculational convenience.

The expansion of the ϑ -functions in powers of $\hat{q} = e^{-\pi K'(k)/K(k)}$ converges quite rapidly in our case. Since $0 \leq k \leq 1/\sqrt{2}$ [see eq.(4.1)], we have

$$0 \leq \hat{q} \leq e^{-\pi} = 0.0432139 \dots$$

\hat{q} can be computed with high precision from the series [30]

$$\hat{q} = \lambda + 2\lambda^5 + 15\lambda^9 + 150\lambda^{13} + 1707\lambda^{17} + \dots,$$

where (not to be confused with the coupling constant)

$$\lambda \equiv \frac{1}{2} \frac{1 - \sqrt{k'}}{1 + \sqrt{k'}}.$$

We find from eq.(4.1)

$$\lambda = \frac{1}{2} \frac{(1 + \eta_0^2)^{1/4} - (1 + \eta_0^2/2)^{1/4}}{(1 + \eta_0^2)^{1/4} + (1 + \eta_0^2/2)^{1/4}}.$$

The quantity λ can be computed and is a small number: for $0 \leq \eta_0 \leq \infty$, we find $0 \leq \lambda \leq 0.0432136 \dots$. Therefore, to very good approximation, with an error smaller than $\sim 10^{-7}$, we may use:

$$\hat{q} = \frac{1}{2} \frac{(1 + \eta_0^2)^{1/4} - (1 + \eta_0^2/2)^{1/4}}{(1 + \eta_0^2)^{1/4} + (1 + \eta_0^2/2)^{1/4}}. \quad (4.13)$$

We find in the forbidden band from eq.(4.5) and [29]

$$U_q(\tau) = e^{-4\tau} \sqrt{1 + \eta_0^2} \hat{q} \sin(2\pi v) \left[1 + 2\hat{q} (\cos 2\pi v - 2) + O(\hat{q}^2) \right] \frac{1 - 2\hat{q}}{1 - 2\hat{q} \cos(\frac{\pi\tau}{\omega})} \frac{\sin \pi(v + \frac{\tau}{2\omega})}{\sin \pi v} \left[1 + O(\hat{q}^2) \right], \quad (4.14)$$

where now we can relate v to q in the simpler form

$$q = \frac{\eta_0}{\sqrt{2}} \cos \pi v \left[1 - 4\hat{q} \sin^2 \pi v + 4\hat{q}^2 \sin^2 \pi v (1 + 4 \cos^2 \pi v) + O(\hat{q}^3) \right],$$

which makes it more convenient to write $q(v)$ in the integrals, and

$$\frac{\pi}{2\omega} = \sqrt{1 + \eta_0^2} \left[1 - 4\hat{q} + 12\hat{q}^2 + O(\hat{q}^4) \right], \quad (4.15)$$

where $0 \leq v \leq \frac{1}{2}$.

The Floquet indices can now be written in a very compact form amenable for analytical estimates

$$F(q) = 4i\pi \hat{q} \sin(2\pi v) \left[1 + 2\hat{q} \cos 2\pi v + O(\hat{q}^2) \right] + \pi.$$

In this approximation the zero mode (4.1) becomes

$$\eta(\tau) = \eta_0 \cos\left(\frac{\pi\tau}{2\omega}\right) \left[1 - 4\hat{q} \sin^2\left(\frac{\pi\tau}{2\omega}\right) + O(\hat{q}^2)\right]. \quad (4.16)$$

This expression is very illuminating, because we find that a Mathieu equation approximation, based on the first term of eq.(4.16) to the evolution of the mode functions is *never* a good approximation. The reason for this is that the second and higher order terms are of the same order as the secular terms in the solution which after resummation lead to the identification of the unstable bands. In fact, whereas the Mathieu equation has *infinitely many* forbidden bands, the exact equation has only *one* forbidden band. Even for small \hat{q} , the Mathieu equation is not a good approximation to the Lamé equation [38].

From eq.(4.11) analogous formulae can be obtained for the allowed band

$$U_q(\tau) = e^{-\frac{i\pi\tau}{2\omega} \coth\left[\frac{\pi K'(k)}{K(k)} v\right]} \frac{1 - 2\hat{q}}{1 - 2\hat{q} \cos\left(\frac{\pi\tau}{\omega}\right)} \frac{1 - 2\hat{q} \cos\left[\frac{\pi\tau}{\omega} - 2iv \log \hat{q}\right]}{1 - 2\hat{q} \cosh(2v \log \hat{q})} \left[1 + O(\hat{q}^2)\right],$$

where

$$q = \frac{\sqrt{\eta_0}}{2^{3/2} \sinh\left(\frac{\pi K'(k)}{K(k)} v\right)} \left(\frac{\eta_0^2 + 2}{\hat{q}}\right)^{1/4} \left\{1 + 2\hat{q} \cosh(2v \log \hat{q}) + O(\hat{q}^2)\right\}.$$

Here,

$$0 \leq v \leq \frac{1}{2}, \quad \infty \geq q \geq \frac{\eta_0}{\sqrt{2}}.$$

Note that eq.(4.15) holds in all bands.

We can now estimate the size and growth of the quantum fluctuations, at least for relatively short times and weak couplings. For small times $0 \leq \tau < \tau_1$ (to be determined consistently later) and small coupling $g \ll 1$, we can safely neglect the back-reaction term $g\Sigma(\tau)$ in eq.(3.2) and express the modes $\varphi_q(\tau)$ in terms of the functions $U_q(\tau)$ and $U_q(-\tau)$ for this however, we need the Wronskian, which in the forbidden band is found to be given by:

$$\mathcal{W}_q = -\frac{1}{\omega} \frac{d}{dv} \log \frac{\vartheta_1(v)}{\vartheta_4(v)} = -2\sqrt{1 + \eta_0^2} \frac{\text{cn dn}}{\text{sn}}(2vK(k), k).$$

In terms of the variable q^2 this becomes, after using eq.(4.6):

$$\mathcal{W}_q = -2q \sqrt{\frac{\frac{\eta_0^2}{2} + 1 + q^2}{\frac{\eta_0^2}{2} - q^2}}.$$

This Wronskian is regular and non-zero except at the four borders of the bands.

We find from eq.(4.4) that $|\varphi_q(\tau)|^2$ is given by

$$|\varphi_q(\tau)|^2 = \frac{1}{4\Omega_q} \left\{ [U_q(\tau) + U_q(-\tau)]^2 + \frac{4\Omega_q^2}{\mathcal{W}_q^2} [U_q(\tau) - U_q(-\tau)]^2 \right\} \quad (4.17)$$

where we took into account eqs. (4.10 and (4.12). Notice that both terms in the rhs of eq.(4.17) are real and positive for real q . For very weak coupling and after renormalization, the contribution to $g\Sigma(\tau)$ from the stable bands will always be perturbatively small, while the contribution from the modes in the unstable band will grow in time exponentially, eventually yielding a non-perturbatively large contribution. Thus these are the only important modes for the fluctuations and the back-reaction. An estimate of the preheating time scale can be obtained by looking for the time when $g\Sigma(\tau)$ is of the same order of the classical contributions to the equations of motion. In order to obtain an estimate for the latter, we consider the average over a period of the classical zero mode:

$$1 + \langle \eta^2(\tau) \rangle = (1 + \eta_0^2) \left[\frac{2E(k)}{K(k)} - 1 \right]$$

which yields for small and large initial amplitudes the following results

$$\begin{aligned} \langle \eta^2(\tau) \rangle &\stackrel{\eta_0 \rightarrow 0}{=} \frac{\eta_0^2}{2} \\ \langle \eta^2(\tau) \rangle &\stackrel{\eta_0 \rightarrow \infty}{=} 0.4569 \dots \eta_0^2 . \end{aligned}$$

Therefore the average over a period of $\eta^2(\tau)$ is to a very good approximation $\eta_0^2/2$ for all initial amplitudes. This result provides an estimate for the preheating time scale τ_1 ; this occurs when $g\Sigma(\tau_1) \approx (1 + \eta_0^2/2)$. Furthermore, at long times (but before $g\Sigma \approx (1 + \eta_0^2/2)$) we need only keep the exponentially growing modes and $g\Sigma(\tau)$ can be approximated by

$$g\Sigma_{est}(\tau) = \frac{g}{4} \int_0^{\frac{\eta_0}{\sqrt{2}}} q^2 dq \frac{1}{\Omega_q} \left[1 + \frac{4\Omega_q^2}{\mathcal{W}_q^2} \right] |U_q(-\tau)|^2 .$$

Moreover, choosing τ such that the oscillatory factors in $U_q(-\tau)$ attain the value 1 (the envelope), and using eq.(4.5) we finally obtain:

$$\Sigma_{est-env}(\tau) = \frac{1}{4} \int_0^{\frac{\eta_0}{\sqrt{2}}} q^2 dq \frac{1}{\Omega_q} \left[1 + \frac{4\Omega_q^2}{\mathcal{W}_q^2} \right] e^{2\tau \sqrt{1+\eta_0^2} Z(2K(k)v, k)} \quad (4.18)$$

where v depends on the integration variable through eq.(4.6).

The Jacobi Z function can be accurately represented using eq.(4.7)

$$Z(2K(k)v, k) = 4\hat{q} \sin 2\pi v [1 - 2\hat{q}(2 - \cos 2\pi v)] + O(\hat{q}^3) .$$

where we recall that $\hat{q} < 0.0433$.

The integral (4.18) will be dominated by the point q that maximizes the coefficient of τ in the exponent. This happens at $q = q_1$, $v = v_1$, where

$$q_1 = \frac{1}{2} \eta_0 (1 - \hat{q}) + O(\hat{q}^2) \quad (4.19)$$

$$Z(2K(k)v_1, k) = 4\hat{q} (1 - 4\hat{q}) + O(\hat{q}^3)$$

We can compute the integral (4.18) by saddle point approximation to find:

$$\begin{aligned}
\Sigma_{est-env}(\tau) &= \frac{q_1^2 \left[1 + \frac{4\Omega_{q_1}^2}{\mathcal{W}_{q_1}^2} \right]}{2 \Omega_{q_1}} e^{8\tau \sqrt{1+\eta_0^2} \hat{q} (1-4\hat{q})} \\
&\quad \int_{-\infty}^{+\infty} dq e^{-64\tau (q-q_1)^2 \hat{q} \sqrt{1+\eta_0^2} \eta_0^{-2} (1-6\hat{q})} [1 + O(\hat{q})] \\
&= \frac{\eta_0^3 \sqrt{\pi} \left[1 + \frac{4\Omega_{q_1}^2}{\mathcal{W}_{q_1}^2} \right] (1 + \hat{q})}{64 (1 + \eta_0^2)^{1/4} \sqrt{\tau \hat{q}} \Omega_{q_1}} e^{8\tau \sqrt{1+\eta_0^2} \hat{q} (1-4\hat{q})} \left[1 + O\left(\frac{1}{\tau}\right) \right].
\end{aligned}$$

We can relate \hat{q} to η_0 using eq.(4.13), and we have used the small \hat{q} expansion

$$\begin{aligned}
\frac{d^2 Z}{dv^2} (2K(k) v_1, k) &= -16\pi^2 \hat{q} (1 - 4\hat{q}) + O(\hat{q}^3) \\
\frac{dq}{dv} \Big|_{v_1} &= -\frac{\eta_0 \pi}{2} (1 + \hat{q}) + O(\hat{q}^2).
\end{aligned}$$

In summary, during the preheating time where parametric resonance is important, $\Sigma_{est-env}(\tau)$ can be represented to a very good approximation by the formula

$$\Sigma_{est-env}(\tau) = \frac{1}{N \sqrt{\tau}} e^{B\tau}, \quad (4.20)$$

where B and N are functions of η_0 given by

$$\begin{aligned}
B &= 8 \sqrt{1 + \eta_0^2} \hat{q} (1 - 4\hat{q}) + O(\hat{q}^3), \\
N &= \frac{64}{\pi^{1/2}} \frac{(1 + \eta_0^2)^{1/4} \sqrt{\hat{q}} \Omega_{q_1} (1 - \hat{q})}{\eta_0^3 \left[1 + \frac{4\Omega_{q_1}^2}{\mathcal{W}_{q_1}^2} \right]} \\
&= \frac{4}{\sqrt{\pi}} \sqrt{\hat{q}} \frac{(4 + 3\eta_0^2) \sqrt{4 + 5\eta_0^2}}{\eta_0^3 (1 + \eta_0^2)^{3/4}} [1 + O(\hat{q})]. \quad (4.21)
\end{aligned}$$

and eq.(4.13) gives \hat{q} as a function of η_0 . This is one of the main results of ref. [15].

We display in Table I below some relevant values of \hat{q} , B and N as functions of η_0 .

We notice that the limiting values of B and N for $\eta_0 \rightarrow \infty$ yield a very good approximation even for $\eta_0 \sim 1$. Namely,

$$\Sigma(\tau) \approx \sqrt{\frac{\eta_0^3}{\tau}} \frac{e^{B_\infty \eta_0 \tau}}{N_\infty}. \quad (4.22)$$

with the asymptotic values given by

$$\begin{aligned}
B_\infty &= 8e^{-\pi}(1 - 4e^{-\pi})[1 + O(\eta_0^{-2})] = 0.285953 \dots [1 + O(\eta_0^{-2})] \\
N_\infty &= \frac{12}{\sqrt{\pi}} \sqrt{5} e^{-\pi/2} [1 + O(\eta_0^{-2})] = 3.147 \dots [1 + O(\eta_0^{-2})]. \quad (4.23)
\end{aligned}$$

These rather simple expressions (4.20-4.23) allow us to perform analytic estimates with great accuracy and constitute one of our main analytic results. The accuracy of this result will be discussed below in connection with the full numerical analysis including back-reaction.

Using this estimate for the back-reaction term, we can now estimate the value of the preheating time scale τ_1 at which the back-reaction becomes comparable to the classical terms in the differential equations. Such a time is defined by $g\Sigma(\tau_1) \sim (1 + \eta_0^2/2)$. From the results presented above, we find

$$\tau_1 \approx \frac{1}{B} \log \frac{N(1 + \eta_0^2/2)}{g\sqrt{B}}. \quad (4.24)$$

The time interval from $\tau = 0$ to $\tau \sim \tau_1$ is when most of the particle production takes place. After $\tau \sim \tau_1$ the quantum fluctuation become large enough to shut-off the growth of the modes and particle production essentially stops. We will compare these results to our numerical analysis below.

We can now use our analytic results to study the different contributions to the energy and pressure coming from the zero mode and the quantum fluctuations and begin by analyzing the contribution to the energy ϵ_0 and pressure p_0 from the zero mode $\eta(\tau)$.

The dimensionless energy and pressure, (normalized by the factor $2M_R^4/\lambda_R$) are given by the following expressions,

$$\begin{aligned} \epsilon_0(\tau) &= \frac{1}{2} \left[\dot{\eta}^2 + \eta(\tau)^2 + \frac{1}{2}\eta(\tau)^4 \right], \\ p_0(\tau) &= \frac{1}{2} \left[\dot{\eta}^2 - \eta(\tau)^2 - \frac{1}{2}\eta(\tau)^4 \right]. \end{aligned}$$

When the back-reaction term $g\Sigma(\tau)$ can be neglected, we can use eq.(4.1) as a good approximation to $\eta(\tau)$. In this approximation

$$\begin{aligned} \epsilon_0 &= \frac{1}{2}\eta_0^2 \left[1 + \frac{1}{2}\eta_0^2 \right], \\ p_0(\tau) + \epsilon_0 &= \eta_0^2 (1 + \eta_0^2) \operatorname{sn}^2 \operatorname{dn}^2 \left(\tau \sqrt{1 + \eta_0^2}, k \right). \end{aligned} \quad (4.25)$$

The zero mode energy is conserved and the pressure oscillates between plus and minus ϵ_0 with period 2ω .

Averaging $p_0(\tau)$ over one period yields

$$\langle p_0 \rangle \equiv \frac{1}{2\omega} \int_0^{2\omega} d\tau p_0(\tau). \quad (4.26)$$

Inserting eq.(4.25) into eq.(4.26) yields [33]

$$\langle p_0 \rangle = -\frac{1}{6}\eta_0^2 \left[1 - \frac{1}{2}\eta_0^2 \right] + \frac{2}{3} (1 + \eta_0^2) \left[1 - \frac{E(k)}{K(k)} \right] \quad (4.27)$$

where k is given by eq.(4.1).

$\langle p_0 \rangle$ vanishes for small η_0 faster than ϵ_0 ,

$$\langle p_0 \rangle \stackrel{\eta_0 \rightarrow 0}{\equiv} \frac{1}{24}\eta_0^4 + O(\eta_0^6),$$

so that the zero mode contribution to the equation of state is that of dust for small η_0 . For large η_0 we find from eq. (4.27),

$$\langle p_0 \rangle^{\eta_0 \rightarrow \infty} \equiv \frac{1}{12} \eta_0^4 + \eta_0^2 \left[\frac{1}{2} - \frac{2}{3} \frac{E(1/\sqrt{2})}{K(1/\sqrt{2})} \right] + O(1)$$

where $\frac{1}{2} - \frac{2}{3} \frac{E(1/\sqrt{2})}{K(1/\sqrt{2})} = 0.01437 \dots$. The equation of state approaches that of radiation for $\eta_0 \rightarrow \infty$:

$$\langle p_0 \rangle^{\eta_0 \rightarrow \infty} \equiv \epsilon_0 \left[\frac{1}{3} - \frac{0.6092 \dots}{\eta_0^2} + O(\eta_0^{-4}) \right].$$

Thus we see that for small amplitudes the zero mode stress-energy, averaged over an oscillation period, behaves as dust while for large amplitudes, the behavior is that of a radiation fluid. The ratio $\langle p_0 \rangle / \epsilon_0$ for zero mode vs. ϵ_0 is shown in figure 1.

The contribution from the $k \neq 0$ modes originates in the quantum fluctuations during the the stage of parametric amplification.

Since we have fluid behaviour, we can define an effective (time-dependent) polytropic index $\gamma(\tau)$ as

$$\gamma(\tau) \equiv \frac{p(\tau)}{\epsilon} + 1.$$

where renormalized quantities are understood throughout. Within a cosmological setting whenever $\gamma(\tau)$ reaches a constant value such equation of state implies a scale factor $R(\tau) = R_0 \tau^{\frac{2}{3\gamma}}$.

In the case being studied here, that of Minkowski space, ϵ is time-independent and hence equal to the initial energy density (divided by N and restoring pre-factors) which after a suitable choice of the constant \mathcal{C} is given by:

$$\epsilon = \frac{2|M_R|^4}{\lambda_R} \left\{ \frac{1}{2} \eta_0^2 \left[1 + \frac{1}{2} \eta_0^2 \right] \right\}.$$

As argued before, for weak coupling the important contribution to the quantum fluctuations come from the modes in unstable bands, since these grow exponentially in time and give rise to a non-perturbatively large contribution. Thus we concentrate only on these modes in calculating the pressure.

The contribution of the forbidden band to the renormalized $p(\tau) + \epsilon$ can be written as

$$[p(\tau) + \epsilon]_{unst} = \frac{2|M_R|^4}{\lambda_R} \left\{ g \int_0^{\eta_0/\sqrt{2}} q^2 dq \left[|\dot{\varphi}_q(\tau)|^2 + \frac{1}{3} q^2 |\varphi_q(\tau)|^2 \right] \right\}.$$

After renormalization, the terms that we have neglected in this approximation are perturbatively small (of order g) whereas the terms inside the bracket eventually become of order 1 (comparable to the tree-level contribution). We now only keep the exponentially growing pieces in the mode functions $\varphi_q(\tau)$ and $\dot{\varphi}_q(\tau)$ since these will dominate the contribution to the pressure. This is simplified considerably by writing to leading order in \hat{q}

$$\dot{\varphi}_q(\tau) = \varphi_q(\tau) \left\{ \sqrt{1 + \eta_0^2} \cot \left[\pi \left(v - \frac{\tau}{2\omega} \right) \right] + O(\hat{q}) \right\}.$$

Averaging over a period of oscillation yields

$$[p(\tau) + \varepsilon]_{unst} = \frac{2|M_R|^4}{\lambda_R} \left\{ \frac{g}{4} \int_0^{\frac{\eta_0}{\sqrt{2}}} \frac{q^2 dq}{(4\pi)^2} \frac{1}{2\Omega_q \sin^2 \pi v} \left[1 + \frac{4\Omega_q^2}{\mathcal{W}_q^2} \right] e^{2\tau \sqrt{1+\eta_0^2} Z(2K(k)v,k)} \left[1 + \eta_0^2 + \frac{1}{3} q^2 \right] \right\}. \quad (4.28)$$

This integral is similar to the one in eq.(4.18) and we find that they are proportional in the saddle point approximation. In fact,

$$[p(\tau) + \varepsilon]_{unst} = \frac{2|M_R|^4}{\lambda_R} \left[g\Sigma_{est-env}(\tau) \left(1 + \frac{13}{12} \eta_0^2 \right) \right].$$

where $\Sigma_{est-env}(\tau)$ is given by eq.(4.20).

The effective polytropic index $\gamma(\tau)$ is:

$$\gamma(\tau) = g\Sigma_{est-env}(\tau) \frac{12 + 13\eta_0^2}{3\eta_0^2(\eta_0^2 + 2)}.$$

When $g\Sigma_{est-env}(\tau_1) \sim 1 + \eta_0^2/2$, i.e. at the end of the preheating phase, $\gamma(\tau)$ is given by

$$\gamma_{eff} \propto \frac{12 + 13\eta_0^2}{6\eta_0^2}$$

We note here that for very large η_0 the effective polytropic index is $\gamma_{eff} \simeq 13/6 \sim \mathcal{O}(1)$. It is clear then that the physics can be interpreted in terms of two fluids, one the contribution from the zero mode and the other from the fluctuations, each with an equation of state that is neither that of dust nor of radiation, but described in terms of an effective polytropic index.

We can now use our approximations to obtain an estimate for the number of particles produced during the preheating stage. In terms of dimensionless quantities, the particle number, defined with respect to the initial Fock vacuum state is given by eq.(3.11).

This particle number will only obtain a significant contribution from the unstable modes in the forbidden band where to leading order in \hat{q} we can approximate $\varphi_q(\tau)$ and $\dot{\varphi}_q(\tau)$ by its exponentially growing pieces [see eq.(4.17)], as follows:

$$|\varphi_q(\tau)|^2 \simeq \frac{1}{4\Omega_q} \left[1 + \frac{4\Omega_q^2}{\mathcal{W}_q^2} \right] |U_q(-\tau)|^2$$

$$|\dot{\varphi}_q(\tau)|^2 \simeq (1 + \eta_0^2) \cot^2 \left[\pi \left(v - \frac{\tau}{2\omega} \right) \right] |\varphi_q(\tau)|^2 + \mathcal{O}(\hat{q}).$$

The total number of produced particles $N(\tau)$ per volume $|M_R|^3$ is given by:

$$\mathcal{N} = \frac{N(\tau)}{|M_R|^3} \equiv \int \frac{d^3q}{(2\pi)^3} N_q(\tau).$$

The asymptotic behaviour (3.16) ensures that this integral converges.

Following the same steps as in eq.(4.18) and (4.28), we find

$$N(\tau)_{unst} = \frac{1}{8\pi^2} \Sigma_{est-env}(\tau) \left[\frac{1 + \eta_0^2}{\Omega_{q_1}} + \Omega_{q_1} \right] = \frac{1}{\lambda_R} \frac{4 + \frac{9}{2} \eta_0^2}{\sqrt{4 + 5 \eta_0^2}} (g \Sigma_{est-env}(\tau)) .$$

where we used eq.(4.19) and $\Sigma_{est-env}(\tau)$ is given by the simple formula (4.20). Notice that by the end of the preheating stage, when $g\Sigma(\tau) \approx 1 + \eta_0^2/2$ the total number of particles produced is non-perturbatively large, both in the amplitude as well as in the coupling

$$\mathcal{N}_{tot} \approx \frac{1}{\lambda_R} \frac{(4 + \frac{9}{2} \eta_0^2)(1 + \eta_0^2/2)}{\sqrt{4 + 5 \eta_0^2}} \quad (4.29)$$

The total number of *adiabatic* particles can also be computed in a similar manner with a very similar result insofar as the non-perturbative form in terms of coupling and initial amplitude.

B. Analytic Results in the Hartree and resummed one-loop approximations

We give in this section the analytic treatment of the Hartree and one-loop equations during preheating. The full Hartree equations (2.10)-(2.14) in dimensionless variables take the form,

$$\ddot{\eta} + \eta + \eta^3 + 3g \eta(\tau) \Sigma(\tau) = 0 \quad (4.30)$$

$$\left[\frac{d^2}{d\tau^2} + q^2 + 1 + 3\eta(\tau)^2 + 3g \Sigma(\tau) \right] \varphi_q(\tau) = 0 , \quad (4.31)$$

$$\varphi_q(0) = \frac{1}{\sqrt{\Omega_q}} \quad , \quad \dot{\varphi}_q(0) = -i \sqrt{\Omega_q} \quad (4.32)$$

$$\eta(0) = \eta_0 \quad , \quad \dot{\eta}(0) = 0 \quad (4.33)$$

where $g \Sigma(\tau)$ is given by eq.(3.6).

Eqs.(4.30)-(4.33) only differ from the large N eqs. (3.1)-(3.4) on factors of 3 in some coefficients.

As in sec. IVA, in the weak coupling regime and for times small enough so that the quantum fluctuations are not large compared to the ‘tree level’ quantities, we can neglect $g\Sigma(\tau)$. Since $\Sigma(0) = 0$, such approximation is expected to hold for an interval $0 \leq \tau < \tau_1$, where τ_1 will be called the preheating time.

During this interval of time we can then approximate $\eta(\tau)$ by the classical solution (4.1). Inserting this elliptic function for $\eta(\tau)$ in eq.(4.31) and neglecting $g\Sigma(\tau)$ yields

$$\left[\frac{d^2}{d\tau^2} + q^2 + 1 + 3\eta_0^2 \text{cn}^2 \left(\tau \sqrt{1 + \eta_0^2}, k \right) \right] \varphi_q(\tau) = 0 . \quad (4.34)$$

This is the Lamé equation for a particular value of the coefficients that make it solvable in terms of Jacobi functions [27]. We summarize here the results for the mode functions. The derivations are analogous to those given in ref. [15]. As for the large N limit, we can choose the mode functions here to be quasi-periodic on τ (Floquet type).

Eq.(4.34) corresponds to a Schrödinger-like equation with a two-zone potential [28]. We find *three* allowed bands and *three* forbidden bands. The allowed bands correspond to

$$-\sqrt{3\eta_0^4 + 6\eta_0^2 + 4} + 1 \leq q^2 \leq -\frac{3\eta_0^2}{2} \quad , \quad 0 \leq q^2 \leq \frac{3\eta_0^2}{2} + 3$$

and

$$\sqrt{3\eta_0^4 + 6\eta_0^2 + 4} + 1 \leq q^2 \leq +\infty \quad ,$$

and the forbidden bands to

$$-\infty \leq q^2 \leq -\sqrt{3\eta_0^4 + 6\eta_0^2 + 4} + 1 \quad , \quad -\frac{3\eta_0^2}{2} \leq q^2 \leq 0$$

and

$$\frac{3\eta_0^2}{2} + 3 \leq q^2 \leq \sqrt{3\eta_0^4 + 6\eta_0^2 + 4} + 1 \quad .$$

The last forbidden band is for *positive* q^2 and hence will contribute to the exponential growth of the fluctuation function $\Sigma(\tau)$.

The mode functions can be written explicitly in terms of Jacobi ϑ -functions for each band. We find,

$$\begin{aligned} U_q(\tau) &= \frac{d}{d\tau} V_q(\tau) \quad \text{where,} \\ V_q(\tau) &= e^{\tau \sqrt{1+\eta_0^2} \beta(v)} \frac{\vartheta_4(v + \frac{\tau}{2\omega})}{\vartheta_4(\frac{\tau}{2\omega})} \quad , \end{aligned} \quad (4.35)$$

where $0 \leq v \leq \frac{1}{2}$ is a function of q in the forbidden band $\frac{3\eta_0^2}{2} + 3 \leq q^2 \leq \sqrt{3\eta_0^4 + 6\eta_0^2 + 4} + 1$ defined by

$$9 \left[\frac{2(\eta_0^2 + 1)}{\text{sn}^2(2K(k)v, k)} - \eta_0^2 \right] = \frac{2q^2 (q^2 - 3)^2}{3(\eta_0^2 + 1)^2 - q^2(q^2 - 2)} \quad . \quad (4.36)$$

and

$$\beta(v) = \frac{2(\eta_0^2 + 1)}{2(\eta_0^2 + 1) + \left(\frac{1}{3}q^2 - 1 - \eta_0^2\right) \text{sn}^2(2K(k)v, k)} \frac{\text{cn dn}}{\text{sn}}(2K(k)v, k) - \frac{1}{2K(k)} \frac{\vartheta_1'}{\vartheta_1}(v) \quad .$$

Eq.(4.36) is a third order equation in q^2 defining q^2 as a function of v . We can express its solution in compact form as follows

$$q^2 = 1 - w(v) [1 + 2 \cos(\alpha + 2\pi/3)] \quad ,$$

where

$$w(v) = 3(\eta_0^2 + 1) \left[\frac{1}{2} + \frac{\text{cn}^2(2K(k)v, k)}{\text{sn}^2(2K(k)v, k)} \right] + \frac{1}{2}$$

and

$$\cos 3\alpha = 1 - \frac{9(\eta_0^2 + 1)^2 + 3}{2w(v)^2} - \frac{9(\eta_0^2 + 1)^2 - 1}{2w(v)^3} \quad ,$$

with $0 \leq \alpha \leq \pi/3$. At the upper border of the band, $q^2 = \sqrt{3\eta_0^4 + 6\eta_0^2 + 4} + 1$, we have $v = \alpha = 0$. The lower border of the band, $q^2 = \frac{3\eta_0^2}{2} + 3$, corresponds to $v = \frac{1}{2}$, $\alpha = \pi/3$.

The Floquet index defined by eq.(4.3) takes here the form

$$F(q) = -2i K(k) \beta(v) .$$

The mode functions in the other bands follow from eq.(4.35) by analytic continuation in v . In addition, explicit and accurate expressions for the Floquet indices as well as the for the mode functions can be obtained by expanding in powers of \hat{q} as in sec. IV A.

In this approximation valid for times early than the preheating time, the Hartree and the resummed one-loop approximation are indeed identical.

C. Numerical Results

We now evolve our equations for the zero and non-zero modes numerically, including the effects of back-reaction. We will see that up to the preheating time, our analytic results agree extremely well with the full numerical evolution.

The procedure used was to solve equations (3.1, 3.2) with the initial conditions (3.3, 3.4,3.5) and (3.6) using a fourth order Runge-Kutta algorithm for the differential equation and an 11-point Newton-Cotes integrator to compute the fluctuation integrals. We tested the cutoff sensitivity by running our code for cutoffs $\Lambda/|M_R| = 100, 70, 50, 20$ and for very small couplings (which is the case of interest). We found no appreciable cutoff dependence. The typical numerical error both in the differential equations and the integrals are less than one part in 10^9 .

Figure 2.a shows $\eta(\tau)$ vs. τ for $\eta_0 = 4.0$, $g = 10^{-12}$. For this weak coupling, the effect of back-reaction is negligible for a long time, allowing several undamped oscillations of the zero mode. Figure 2.b shows $g\Sigma(\tau)$ vs. τ . It can be seen that the back-reaction becomes important when $g\Sigma(\tau) \approx 1 + \eta_0^2/2$ as the evolution of $\eta(\tau)$ begins to damp out. This happens for $\tau \approx 25$ in excellent agreement with the analytic prediction given by eq.(4.24) $\tau_1 = 26.2 \dots$, the difference between the analytic estimate for $\Sigma(\tau)$ given by eq.(4.20) and the numerical result is less than 1% in the range $0 < \tau < 30$. Figure 2.c shows $g\mathcal{N}(\tau)$ vs. τ and we see that the analytic expression (4.29) gives an approximate estimation $\lambda_R \mathcal{N}_{tot} \approx 74.6 \dots$ for the final number of produced particles.

Figures 2.d-2.f, show $gN_q(\tau)$ for $\tau = 40, 120, 200$, we see that the prediction of the width of the unstable band $0 < q < \eta_0/\sqrt{2}$ is excellent and is valid even for very long times beyond the regime of validity of the small time, weak coupling approximation. However, we see that the peak becomes higher, narrower and moves towards $q \approx 0.5$ as time evolves beyond τ_1 . This feature persists in all numerical studies of the unbroken phase that we have carried out, this changes in the peak width, height and position are clearly a result of back-reaction effects. We have searched for unstable bands for $0 < q < 20$ and we only found one band precisely in the region predicted by the analytic estimate. All throughout the evolution *there is only one unstable band*. The band develops some structure with the height, position and width of the peak varying at long times but no other unstable bands develop and the width of the band remains constant. For values of q outside the unstable band we find typically $gN_q < 10^{-13}$ at all times. This is a remarkable and unexpected feature.

Obviously this is very different from the band structure of a Mathieu equation. The Mathieu equation gives rise to an infinite number of narrowing bands, so that quantitative estimates of particle production, etc. using the Mathieu equation approximation would be gross misrepresentations of the actual dynamics, with discrepancies that are non-perturbatively large when the back-reaction becomes important [38]. Since particle production essentially happens in the forbidden bands, the quantitative predictions obtained from a single forbidden band and an infinite number, as predicted by WKB or Mathieu equation analysis, will yield different physics.

We have carried the numerical evolution including only the wave-vectors in the unstable region and we find that this region of q -wavevectors is the most relevant for the numerics. Even using a cutoff as low as $q_c = 4$ in this case gives results that are numerically indistinguishable from those obtained with much larger cutoffs $q_c = 70 - 100$. The occupation number of modes outside the unstable bands very quickly becomes negligible small and for $q \approx 4$ it is already of the same order of magnitude as the numerical error $\leq 10^{-10}$. Clearly this is a feature of the weak coupling case under consideration. Keeping only the contribution of the modes in the unstable band, the energy and pressure can be written as

$$\varepsilon = \frac{2|M_R|^4}{\lambda_R} \left\{ \frac{\dot{\eta}^2}{2} + \frac{\eta^2}{2} + \frac{\eta^4}{4} + 2g \int_0^{q_c} q^2 dq \Omega_q N_q(\tau) + \frac{g}{2} \Sigma(\tau) \left[\eta^2(\tau) - \eta_0^2 + \frac{g}{2} \Sigma(\tau) \right] + \mathcal{O}(g) \right\} \quad (4.37)$$

$$p = \frac{2|M_R|^4}{\lambda_R} \left\{ g \int_0^{q_c} q^2 dq \left[\frac{q^2}{3} |\varphi_q(\tau)|^2 + |\dot{\varphi}(\tau)|^2 \right] + \dot{\eta}^2 + \mathcal{O}(g) \right\} - \varepsilon \quad (4.38)$$

$$q_c = \frac{\eta_0}{\sqrt{2}}$$

where we have made explicit that we have neglected terms of order g in eqs.(4.37-4.38). The terms multiplied by g in eqs.(4.37, 4.38) become of order 1 during the preheating stage. For the parameters used in figures 2, we have checked numerically that the energy (4.37) is conserved to order g within our numerical error. Figure 2.g shows the pressure $2|M_R|^4 p(\tau)/\lambda_R$ versus τ . Initially $p(0) = -\varepsilon$ (vacuum dominated) but at the end of preheating the equation of state becomes almost that of radiation $p_\infty = \varepsilon/3$.

For very small coupling ($g \sim 10^{-12}$), the backreaction shuts-off suddenly the particle production at the end of the preheating (see fig. 2c). Later on, (τ larger than 100 for $g \sim 10^{-12}$) the time evolution is periodic in a very good approximation. That is, this non-linear system exhibits a limiting cycle behaviour. The modulus of the k -modes do not grow in time and no particle production takes place. This tells us that no forbidden bands are present for $q^2 > 0$ in the late time regime.

We have numerically studied several different values of η_0 , g finding the same qualitative behavior for the evolution of the zero mode, particle production and pressure. In all cases we have found remarkable agreement (at most 5% difference) with the analytical predictions in the time regime for which $0 < g\Sigma(\tau) \leq 1$. The asymptotic value of the pressure, however, only becomes consistent with a radiation dominated case for large initial amplitudes. For smaller amplitudes $\eta_0 = 1$ we find that asymptotically the polytropic index is smaller than $4/3$. This asymptotic behavior is beyond the regime of validity of the approximations in the analytic treatment and must be studied numerically. This polytropic index depends

crucially on the band structure because most of the contribution comes from the unstable modes.

In ref. [18] results of ref. [8] are rederived with a different renormalization scheme.

V. THE BROKEN SYMMETRY CASE

A. Analytic Results

As in the unbroken case, for $g \ll 1$ we can neglect $g\Sigma(\tau)$ in eq. (3.7) until a time τ_2 at which point the fluctuations have grown to be comparable to the ‘tree level’ terms. The zero mode equation then becomes,

$$\ddot{\eta} - \eta + \eta^3 = 0 .$$

which correspond to the evolution on the classical potential

$$V = \frac{1}{4}(\eta^2 - 1)^2 , \tag{5.1}$$

with the initial conditions (3.4). We then find for $0 \leq \eta_0 \leq 1$,

$$\eta(\tau) = \frac{\eta_0}{\text{dn}\left(\tau\sqrt{1 - \frac{\eta_0^2}{2}}, k\right)}$$

$$k = \sqrt{\frac{1 - \eta_0^2}{1 - \frac{\eta_0^2}{2}}} , \tag{5.2}$$

Notice that $\eta(\tau)$ has period $2\omega \equiv \frac{2K(k)}{\sqrt{1 - \frac{\eta_0^2}{2}}}$. The elliptic modulus k is given by eq.(5.2).

For $1 \leq \eta_0 \leq \sqrt{2}$ we find

$$\eta(\tau) = \eta_0 \text{dn}\left(\tau\eta_0/\sqrt{2}, k\right)$$

$$k = \sqrt{2(1 - \eta_0^{-2})} . \tag{5.3}$$

This solution follows by shifting eq.(5.2) by a half-period and changing $\eta_0^2 \rightarrow 2 - \eta_0^2$. It has a period $2\omega \equiv \frac{2\sqrt{2}}{\eta_0} K(k)$. For $\eta_0 \rightarrow 1$, $2\omega \rightarrow \pi\sqrt{2}$ and the oscillation amplitude vanishes, since $\eta = 1$ is a minimum of the classical potential.

For $\eta_0 > \sqrt{2}$ we obtain

$$\eta(\tau) = \eta_0 \text{cn}\left(\sqrt{\eta_0^2 - 1}\tau, k\right)$$

$$k = \frac{\eta_0}{\sqrt{2(\eta_0^2 - 1)}} . \tag{5.4}$$

This solution has $4\omega \equiv \frac{4K(k)}{\sqrt{\eta_0^2 - 1}}$ as period.

The solutions for $\eta_0 < \sqrt{2}$ and $\eta_0 > \sqrt{2}$ are qualitatively different since in the second case $\eta(\tau)$ oscillates over the two minima $\eta = \pm 1$. In the limiting case $\eta_0 = \sqrt{2}$ these solutions degenerate into the instanton solution

$$\eta(\tau) = \frac{\sqrt{2}}{\cosh \tau},$$

and the period becomes infinite.

Inserting this form for $\eta(\tau)$ in eq.(3.8) and neglecting $g\Sigma(\tau)$ yields for $0 \leq \eta_0 \leq 1$,

$$\left[\frac{d^2}{d\tau^2} + q^2 - 1 + \frac{\eta_0^2}{\operatorname{dn}^2\left(\tau\sqrt{1 - \frac{\eta_0^2}{2}}, k\right)} \right] \varphi_q(\tau) = 0. \quad (5.5)$$

This is again a Lamé equation for a one-zone potential and can also be solved in closed form in terms of Jacobi functions. We summarize here the results for the mode functions, with the derivations again given in ref. [15].

As for unbroken symmetry case, there are *two* allowed bands and *two* forbidden bands. The allowed bands for $0 \leq \eta_0 \leq 1$ correspond to

$$0 \leq q^2 \leq \frac{\eta_0^2}{2} \quad \text{and} \quad 1 - \frac{\eta_0^2}{2} \leq q^2 \leq +\infty,$$

and the forbidden bands to

$$-\infty \leq q^2 \leq 0 \quad \text{and} \quad \frac{\eta_0^2}{2} \leq q^2 \leq 1 - \frac{\eta_0^2}{2}. \quad (5.6)$$

The last forbidden band exists for positive q^2 and hence contributes to the growth of $\Sigma(\tau)$.

The Floquet solutions obey eqs. (4.3) and the modes $\varphi_q(\tau)$ can be expressed in terms of $U_q(\tau)$ and $U_q(-\tau)$ following eq.(4.4).

It is useful to write the solution $U_q(\tau)$ in terms of Jacobi ϑ -functions. For the forbidden band $\frac{\eta_0^2}{2} \leq q^2 \leq 1 - \frac{\eta_0^2}{2}$ after some calculation (see ref. [15]),

$$U_q(\tau) = e^{-\tau} \sqrt{1 - \frac{\eta_0^2}{2}} Z(2K(k)v) \frac{\vartheta_3(0) \vartheta_2(v + \frac{\tau}{2\omega})}{\vartheta_2(v) \vartheta_3(\frac{\tau}{2\omega})}, \quad (5.7)$$

where $0 \leq v \leq \frac{1}{2}$ is related with q through

$$q^2 = 1 - \frac{\eta_0^2}{2} - (1 - \eta_0^2) \operatorname{sn}^2(2K(k)v, k),$$

and k is a function of η_0 as defined by eq.(5.2).

We see explicitly here that $U_q(\tau)$ factorizes into a real exponential with an exponent linear in τ and an antiperiodic function of τ with period 2ω .

The Floquet indices for this forbidden band are given by

$$F(q) = 2iK(k)Z(2K(k)v) \pm \pi.$$

For the allowed band $1 - \frac{\eta_0^2}{2} \leq q^2 \leq +\infty$, we find for the modes,

$$U_q(\tau) = e^{-\frac{\tau}{2\omega} \frac{\vartheta_1'}{\vartheta_1}(\frac{i\alpha}{2\omega})} \frac{\vartheta_3(0) \vartheta_3(\frac{i\alpha+\tau}{2\omega})}{\vartheta_3(\frac{i\alpha}{2\omega}) \vartheta_3(\frac{\tau}{2\omega})},$$

where q and α are related by:

$$q = \frac{\sqrt{1 - \frac{\eta_0^2}{2}}}{\text{sn}\left(\alpha\sqrt{1 - \frac{\eta_0^2}{2}}, k'\right)}$$

with $\frac{K'(k)}{\sqrt{1-\eta_0^2}} \geq \alpha \geq 0$. The Floquet indices for this first allowed band are given by

$$F(q) = i \frac{\vartheta_1'}{\vartheta_1}\left(\frac{i\alpha}{2\omega}\right).$$

Analogous expressions hold in the other allowed band, $0 \leq q^2 \leq \frac{\eta_0^2}{2}$:

$$U_q(\tau) = e^{-\frac{\tau}{2\omega} \frac{\vartheta_2'}{\vartheta_2}(\frac{i\alpha}{2\omega})} \frac{\vartheta_3(0) \vartheta_4(\frac{i\alpha+\tau}{2\omega})}{\vartheta_4(\frac{i\alpha}{2\omega}) \vartheta_3(\frac{\tau}{2\omega})}.$$

Here, $q = \frac{\eta_0}{\sqrt{2}} \text{sn}\left(\alpha\sqrt{1 - \frac{\eta_0^2}{2}}, k'\right)$ and $\frac{K'(k)}{\sqrt{1-\eta_0^2}} \geq \alpha \geq 0$, and the Floquet indices for this band are given by

$$F(q) = i \frac{\vartheta_2'}{\vartheta_2}\left(\frac{i\alpha}{2\omega}\right).$$

For $\eta_0 \approx 1$ the situation is very similar to the unbroken symmetry case; the zero mode oscillates quasi-periodically around the minimum of the tree level potential. There are effects from the curvature of the potential, but the dynamics can be analyzed in the same manner as in the unbroken case, with similar conclusions and will not be repeated here.

The case $\eta_0 \ll 1$ is especially interesting [8,15] for broken symmetry because of new and interesting phenomena [8,15] that has been recently associated with symmetry restoration [7,20,34,35].

In this limit, the elliptic modulus k [see eq. (5.2)] approaches unity and the (real) period 2ω grows as

$$2\omega \simeq 2K(k) + O(\eta_0^2) \simeq 2 \ln\left(\frac{\sqrt{32}}{\eta_0}\right) + O(\eta_0^2)$$

In this limit, both the potential in eq.(5.5) and the mode functions (5.7) can be approximated by hyperbolic functions [29]:

$$\frac{1}{\text{dn}\left(\tau\sqrt{1 - \frac{\eta_0^2}{2}}, k\right)} = \cosh \tau + O(\eta_0^2)$$

$$Z(u) = \tanh u - \frac{u}{\Lambda} + O(\eta_0^2)$$

where

$$\begin{aligned}\cosh u &= \frac{4}{\eta_0^2} \left(q - \sqrt{q^2 - \frac{\eta_0^2}{2}} \right) \left[1 + O(\eta_0^2) \right] , \\ \Lambda &\equiv \log \left(\frac{\sqrt{32}}{\eta_0} \right) , \quad 0 \leq u \leq \Lambda\end{aligned}\tag{5.8}$$

Using the imaginary Jacobi transformation [29],

$$\vartheta_{2,3}(v|\hat{q}) = \sqrt{\frac{K(k)}{K(k')}} e^{-\frac{\pi K(k)}{K(k')} v^2} \vartheta_{4,3}\left(-i \frac{K(k)}{K(k')} v|\hat{q}\right) ,$$

where $\hat{q} = e^{-\frac{\pi K(k')}{K(k)}}$, $\hat{q} = e^{-\frac{\pi K(k)}{K(k'')}}$ and the series expansions [29]

$$\begin{aligned}\vartheta_3(v|\hat{q}) &= 1 + 2 \sum_{n=1}^{\infty} \hat{q}^{n^2} \cos(2\pi n v) \\ \vartheta_4(v|\hat{q}) &= \vartheta_3\left(v + \frac{1}{2}|\hat{q}\right) ,\end{aligned}$$

we can derive expressions for the mode functions $U_q(\tau)$ valid for small η_0 :

$$U_q(\tau) = e^{-\tau \tanh u \left(1 + \frac{\eta_0^2}{8}\right)} \frac{1 - \frac{\eta_0^2}{8} \cosh u \cosh(u + 2\tau)}{1 - \frac{\eta_0^2}{8} \cosh u} \left[1 + O(\eta_0^2) \right] .\tag{5.9}$$

Here u is related with q through eq.(5.8). We see that the function $U_q(-\tau)$ grows with τ almost as e^τ for q near the lower border of the forbidden band $u \simeq \Lambda$. This fast growth can be interpreted as the joint effect of the non-periodic exponential factor in eq.(5.7) and the growth of the periodic ϑ -functions. Since the real period is here of the order Λ , the two effects cannot be separated. The unstable growth for $\tau \leq \omega$ also reflects the spinodal instabilities associated with phase separation [3].

In this case, there is a range of parameters for which the quantum fluctuations grow to become comparable to the tree level contribution within just one or very few periods. The expression (5.9) determines that $\Sigma(\tau) \approx e^{2\tau}$ from the contributions of modes near the lower edge of the band. The condition for the quantum fluctuations to become of order 1 within just one period of the elliptic function is $ge^{4\omega} \approx 1$ which leads to the conclusion that for $\eta(0) < g^{1/4}$ the quantum fluctuations grow very large before the zero mode can actually execute a single oscillation. In such a situation an analysis in terms of Floquet (quasi-periodic) solutions is not correct because the back reaction prevents the zero mode from oscillating enough times for periodicity to be a reasonable approximation.

We now analyze the behavior of the pressure for the zero mode to compare to the previous case. In the approximation where eqs.(5.2), (5.3) and (5.4) hold and adjusting the constant \mathcal{C} in the definition of the energy, we have

$$\begin{aligned}\epsilon_0 &= \frac{1}{4} \left(\eta_0^2 - 1 \right)^2 , \\ p_0(\tau) &= -\epsilon_0 + \dot{\eta}(\tau)^2\end{aligned}\tag{5.10}$$

Inserting eqs.(5.2), (5.3) and (5.4) in eq.(5.10) yields

$$\begin{aligned}
0 \leq \eta_0 \leq 1 & : & p_0(\tau) &= -\epsilon_0 \left[1 - 8 \operatorname{sn}^2 \operatorname{cn}^2 \left((\tau + K) \sqrt{1 - \frac{\eta_0^2}{2}}, k \right) \right], \\
1 \leq \eta_0 \leq \sqrt{2} & : & p_0(\tau) &= -\epsilon_0 \left[1 - 8 \operatorname{sn}^2 \operatorname{cn}^2 \left(\tau \eta_0 / \sqrt{2}, k \right) \right], \\
\eta_0 \geq \sqrt{2} & : & p_0(\tau) &= -\epsilon_0 \left[1 - 8 k^2 \operatorname{sn}^2 \operatorname{dn}^2 \left(\tau \sqrt{\eta_0^2 - 1}, k \right) \right].
\end{aligned} \tag{5.11}$$

Notice that the functional form of the elliptic modulus k as a function of η_0 is different in each interval [see eqs.(5.2), (5.3) and (5.4)].

Let us now average the pressure over a period as in eq.(4.26). We find

$$\begin{aligned}
\langle p_0 \rangle &= \epsilon_0 \left\{ \frac{8}{3} \left[\frac{k^2 - 2}{k^4} \left(1 - \frac{E(k)}{K(k)} \right) + \frac{1}{k^2} \right] - 1 \right\} \\
&\quad \text{for } 0 \leq \eta_0 \leq \sqrt{2}, \\
\langle p_0 \rangle &= \epsilon_0 \left\{ \frac{8}{3} \left[(1 - 2k^2) \left(1 - \frac{E(k)}{K(k)} \right) + k^2 \right] - 1 \right\} \\
&\quad \text{for } \eta_0 \geq \sqrt{2}.
\end{aligned} \tag{5.12}$$

The dimensionless energy ϵ_0 tends to 1/4 both as $\eta_0 \rightarrow 0$ and $\eta_0 \rightarrow \sqrt{2}$ in both cases we find using eq.(5.12)

$$\frac{\langle p_0 \rangle}{\epsilon_0} \rightarrow -1 - \frac{16}{3 \log |\frac{1}{4} - \epsilon_0|} + O(\epsilon_0 - \frac{1}{4}).$$

This result is recognized as vacuum behaviour in this limit.

For $\eta_0 \rightarrow 1$, eq. (5.12) yields,

$$\frac{\langle p_0 \rangle}{\epsilon_0} \stackrel{\eta_0 \rightarrow 1}{\cong} O(\eta_0 - 1)^2.$$

That is a dust type behaviour, which is consistent with the small amplitude limit of the unbroken symmetry case studied before.

Finally, for $\eta_0 \rightarrow \infty$, when the zero mode is released from high up the potential hill, we find that the pressure approaches radiation behaviour (from above)

$$\begin{aligned}
\frac{\langle p_0 \rangle}{\epsilon_0} &\stackrel{\eta_0 \rightarrow \infty}{\cong} \frac{1}{3} + \frac{4}{3} \left[\frac{1}{\sqrt{2}} - 1 + \left(2 - \frac{1}{\sqrt{2}} \right) \frac{E(\frac{1}{\sqrt{2}})}{K(\frac{1}{\sqrt{2}})} \right] \frac{1}{\eta_0^2} + O\left(\frac{1}{\eta_0^4}\right) \\
&= \frac{1}{3} + \frac{0.86526\dots}{\eta_0^2} + O\left(\frac{1}{\eta_0^4}\right).
\end{aligned}$$

Figure 3 shows $\langle p_0 \rangle / \epsilon_0$ vs. ϵ_0 .

As mentioned before, we expect that for $\eta_0 \ll 1$ the conclusion will be modified dramatically by the quantum corrections.

B. Numerical Results

In the region $\eta_0 \approx 1$ the analytic estimates are a good approximation for large times and weak couplings. We have studied numerically many different cases with $\eta_0 \geq 0.5$ and weak coupling and confirmed the validity of the analytic estimates. These cases are qualitatively similar to the unbroken symmetry case with almost undamped oscillations for a long time compatible with the weak coupling approximation and when $g\Sigma(\tau)$ grows by parametric amplification to be of order one with a consequently large number of produced particles and the evolution of the zero mode damps out.

However as argued above, for $\eta_0 \ll 1$ the analytic approximation will not be very reliable because the quantum fluctuations grow on a time scale of a period or so (depending on the coupling) and the back-reaction term cannot be neglected. Thus this region needs to be studied numerically.

We numerically solved equations (3.7)-(3.8) with the initial conditions (3.9), (3.10) and (3.10). The numerical routines are the same as in the unbroken symmetry case. Again we tested cutoffs $\Lambda/|M_R| = 100, 70, 50, 20$ and for very small couplings (which is the case of interest, $g = 10^{-6} \dots g = 10^{-12}$) we found no appreciable cutoff dependence, with results that are numerically indistinguishable even for cutoffs as small as $q_c \approx 2$. The typical numerical error both in the differential equations and the integrals are the same as in the unbroken case, less than one part in 10^9 .

We begin the numerical study by considering first the case of very small coupling and $\eta_0 \ll 1$; later we will deal with the case of larger couplings and initial values of the zero mode. Figure 4.a shows $\eta(\tau)$ vs. τ for $\eta_0 = 10^{-5}$, $g = 10^{-12}$. In this case we see that within one period of the classical evolution of the zero mode, $g\Sigma(\tau)$ becomes of order one, the quantum fluctuations become non-perturbatively large and the approximation valid for early times and weak couplings breaks down. Fig. 4.b shows $g\Sigma(\tau)$ and fig. 4.c shows $g\mathcal{N}(\tau)$ vs. τ for these parameters. We find that only the wave vectors in the region $0 < q < 1$ are important i.e. there is only one unstable band whose width remains constant in time. This is seen in figs. 4.d-f, which show the particle number (defined with respect to the initial state) as a function of wave vector for different times, $gN_q(\tau = 30)$, $gN_q(\tau = 90)$, $gN_q(\tau = 150)$ respectively. Although the analytic approximation breaks down, the prediction eq.(5.6) for the band width agrees remarkably well with the numerical result. As in the unbroken case, the band develops structure but its width is constant throughout the evolution. As can be seen in these figures the peak of the distribution becomes higher, narrower and moves towards smaller values of q . The concentration of particles at very low momentum is a consequence of the excitations being effectively massless in the broken symmetry case. The features are very distinct from the unbroken symmetry case, in which the peak approaches $q \approx 0.5$.

We found in all cases that the asymptotic behavior corresponds to

$$\mathcal{M}^2(\tau) = -1 + \eta^2(\tau) + g\Sigma(\tau) \xrightarrow{\lim \tau \rightarrow \infty} 0$$

This is a consistent asymptotic solution that describes massless ‘‘pions’’ and broken symmetry in the case $\eta(\infty) \neq 0$.

For times $\tau \approx 100 - 150$ the value of the zero mode is somewhat larger than the initial value: $\eta(\tau = 150) \approx 2 \times 10^{-5}$. This result, when combined with the result that the average

of the effective mass approaches zero is clearly an indication that the symmetry is *broken*. We found numerically that the final value of the zero mode depends on the initial value and the coupling and we will provide numerical evidence for this behavior below.

Figure 4.a, presents a puzzle. Since the zero mode begins very close to the origin with zero derivative and *ends up* very close to the origin with zero derivative, the classical energy of the zero mode is conserved. At the same time, however, the dynamical evolution results in copious particle production as can be seen from fig. 4.c. We have shown in a previous section that the total energy is conserved and this was numerically checked within the numerical error. Thus the puzzle: how is it possible to conserve the *total* energy, conserve the classical zero mode energy and at the same time create $\mathcal{O}(1/g)$ particles? The answer is that there is a new term in the total energy that acts as a ‘zero point energy’ that diminishes during the evolution and thus maintains total energy conservation with particle production. The most important contribution to the energy arises from the zero mode and the unstable modes $0 < q < q_u$. The energy and pressure are given by (adjusting the constant \mathcal{C} such that the energy coincides with the classical value):

$$\varepsilon = \frac{2|M_R|^4}{\lambda_R} \{ \varepsilon_{cl} + \varepsilon_N + \varepsilon_C + \mathcal{O}(g) \}$$

$$\varepsilon_{cl}(\tau) = \frac{\dot{\eta}^2}{2} + \frac{1}{4} (\eta^2 - 1)^2 \quad (5.13)$$

$$\varepsilon_N(\tau) = 2g \int_0^{q_u} q^2 dq \Omega_q N_q(\tau)$$

$$\varepsilon_C(\tau) = \frac{g}{2} \Sigma(\tau) \left[-1 - \eta_0^2 + \mathcal{M}^2(\tau) - \frac{g}{2} \Sigma(\tau) \right] \quad (5.14)$$

$$p(\tau) = \frac{2|M_R|^4}{\lambda_R} \left\{ g \int_0^{q_u} q^2 dq \left[\frac{q^2}{3} |\varphi_q(\tau)|^2 + |\dot{\varphi}(\tau)|^2 \right] + \dot{\eta}^2 + \mathcal{O}(g) \right\} - \varepsilon \quad (5.15)$$

$$\mathcal{M}^2(\tau) = -1 + \eta^2(\tau) + g\Sigma(\tau)$$

where $\mathcal{M}(\tau)^2$ is the effective squared mass of the $N - 1$ ‘pions’ and again $\mathcal{O}(g)$ stand for perturbatively small terms of order g . The terms displayed in (5.13- 5.15) are all of $\mathcal{O}(1)$ during the preheating stage.

We find that whereas $\varepsilon_N(\tau)$ grows with time, the term $\varepsilon_C(\tau)$ becomes negative and decreases. In all the cases that we studied, the effective mass $\mathcal{M}(\tau)$ approaches zero asymptotically; this is seen in figure 4.g for the same values of the parameters as in figs. 4.a-c. This behavior and an asymptotic value $\eta_\infty \neq 0$ is consistent with broken symmetry and massless pions by Goldstone’s theorem. The term $\varepsilon_C(\tau)$ in eq.(5.14) can be identified with the ‘zero’ of energy. It contributes to the equation of state as a vacuum contribution, that is $p_C = -\varepsilon_C$ and becomes negative in the broken symmetry state. It is **this** term that compensates for the contribution to the energy from particle production.

This situation is generic for the cases of interest for which $\eta_0 \ll 1$, such is the case for the slow roll scenario in inflationary cosmology. Figs. 4.h-k show $\varepsilon_{cl}(\tau)$ vs. τ , $\varepsilon_N(\tau)$ vs. τ , $\varepsilon_C(\tau)$ vs. τ and $\frac{\lambda_R}{2|M_R|^4} p(\tau)$ vs τ for the same values of parameters as fig. 4.a. The pressure has a remarkable behavior. It begins with $p = -\varepsilon$ corresponding to vacuum domination and ends asymptotically with a radiation-like equation of state $p = \varepsilon/3$. A simple explanation for radiation-like behavior would be that the equation of state is dominated by

the quantum fluctuations which as argued above correspond to massless pions and therefore ultrarelativistic. It must be noticed that we obtain a radiation-like equation of state in spite of the fact that the distribution is out of equilibrium and far from thermal as can be seen from figs. 4.d-f.

An important question to address at this point is: why does the zero mode reach an asymptotic value *different* from the minimum of the effective potential? The answer to this question is that once there is profuse particle production, the zero mode evolves in a non-equilibrium bath of these excitations.

Through the time evolution, more of these particles are produced and the zero mode evolves in a highly excited, out of thermal equilibrium state. Furthermore we have seen in detail that this mechanism of particle production modifies dramatically the zero point origin of energy through the large and negative term $\varepsilon_C(\tau)$ and therefore the minimum of the effective action, which is the appropriate concept to use for a **time dependent** evolution as the present one. The final value reached by the zero mode in the evolution will be determined by all of these *non-perturbative* processes, and only a full non-linear study (including the back-reaction of modes on themselves) captures the relevant aspects. As we have argued above, approximations based on Mathieu-type equations or the WKB approximation are bound to miss such important non-linear processes and will lead to an incomplete picture of the evolution.

These time dependent processes cannot be studied using the effective potential. For example, the profuse particle production taking place here is a feature completely missed by the effective potential. We find that the effective potential is an irrelevant quantity to study the dynamics [8,15,3].

VI. BROKEN SYMMETRY AND ITS QUANTUM RESTORATION AT PREHEATING

The numerical result depicted by figures 4.a-c, [8,15], has motivated the suggestion that the growth of quantum fluctuations is so strong that the non-equilibrium fluctuations restore the symmetry [7,20]. The argument is that the non-equilibrium fluctuations given by the term $g \eta(\tau) \Sigma(\tau)$ in eq.(3.8) for the mode functions grow exponentially and eventually this term overcomes the term $-|m^2|$ leading to an effective potential with a *positive* mass squared for the zero mode [see eq. (3.7)].

Although this is a very interesting suggestion, it is *not* borne out by our numerical investigation for $\eta_0 < 1$. The signal for broken or restored symmetry is the final value of the zero mode when the system reaches an equilibrium situation. Any argument about symmetry restoration based solely on the dynamics of the fluctuation term $g \eta(\tau) \Sigma(\tau)$ is incomplete if it does not address the dynamics of the zero mode. In particular for the case of figures 4.a-c, the initial value of the zero mode $\eta_0 \neq 0$ and the final value is very close to the initial value but still *different from zero*.

At the same time, the asymptotic effective mass of the ‘pions’ is on average zero. Clearly this is a signal for symmetry breaking. Because the initial and final values of the order parameter are so small on the scale depicted in the figures, one could be tempted to conclude that the symmetry originally broken by a very small value of the order parameter is restored asymptotically by the growth of non-equilibrium fluctuations. To settle this issue we show a

different set of parameters in figures 5.a,b that clearly show that the final value of the order parameter $\eta_\infty \neq 0$, while the effective mass of the pions $\mathcal{M}(\tau) \rightarrow 0$. Here $\eta_0 = 0.01$ and $g = 10^{-5}$, and asymptotically we find $\eta(\tau = 150) \approx 0.06$, the average of the effective mass squared $\mathcal{M}^2(\tau) = 0$ and the symmetry is broken, despite the fact that the fluctuations have grown exponentially and a number of particles $\mathcal{O}(1/g)$ has been produced.

The reason that the symmetry is **not** restored is that when the effective mass becomes positive, the instabilities shut off and the quantum fluctuations become small. When this happens $g\Sigma$ is no longer of order one and the instabilities appear again, producing the oscillatory behavior that is seen in the figures for $g\Sigma(\tau)$ at long times, such that the contributions of the oscillatory terms average to zero. It is rather straightforward to see that there is a self-consistent solution of the equations of motion for the zero mode and the fluctuations with constant η_∞ and $\mathcal{M}^2(\infty) = 0$. Eq.(3.7) takes the asymptotic form [8]

$$\eta_\infty \left[-1 + \eta_\infty^2 + g \Sigma(\infty) \right] = 0 .$$

In addition, eq.(3.8) yields when $\mathcal{M}(\infty)^2 = 0$,

$$\varphi_q(\tau) \xrightarrow{\tau \rightarrow \infty} A_q e^{-iq\tau} + B_q e^{iq\tau} ,$$

where A_q and B_q depend on the initial conditions and g . We get from eqs.(3.6) and (3.11),

$$\eta_\infty^2 = 1 - 4g \int_0^\infty \frac{q^2 \Omega_q}{q^2 + \Omega_q^2} N_q(\infty) dq - g S(\eta_0) , \quad (6.1)$$

where $S(\eta_0) \equiv \frac{1}{4}(1 - \eta_0^2) \left[\log \frac{1 - \eta_0^2}{4} - \frac{\pi}{2} \right] + \frac{1}{2}(1 + \eta_0^2) \left[\text{ArgTh} \sqrt{\frac{1 - \eta_0^2}{2}} - \text{arctg} \sqrt{\frac{1 - \eta_0^2}{2}} \right]$.

We see that the value of η_∞ depends on the initial conditions. Whereas the last term in eq. (6.1) is perturbatively small, the contribution from the produced particles is non-perturbatively large, as $N_q(\infty) \approx 1/g$ for the unstable wavevectors. Thus the asymptotic value of the zero mode is drastically modified from the tree level v.e.v (in terms of renormalized parameters) because of the profuse particle production due to the non-equilibrium growth of fluctuations.

Another way to argue that the symmetry is indeed broken in the final state is to realize that the distribution of ‘‘pions’’ at late times will be different than the distribution of the quanta generated by the fluctuations in the σ field, if for no other reason than that the pions are asymptotically massless while the σ quanta are massive, as long as η_∞ is different from zero. If the symmetry were restored during preheating, these distributions would have to be identical.

In the situation of ‘chaotic initial conditions’ but with a broken symmetry tree level potential, the issue of symmetry breaking is more subtle. In this case the zero mode is initially displaced with a large amplitude and very high in the potential hill. The total energy *density* is non-perturbatively large. Classically the zero mode will undergo oscillatory behavior between the two classical turning points, of very large amplitude and the dynamics will probe both broken symmetry states. Even at the classical level the symmetry is respected by the dynamics in the sense that the time evolution of the zero mode samples equally both vacua. This is not the situation that is envisaged in usual symmetry breaking scenarios. For broken symmetry situations there are no finite energy field configurations that can sample

both vacua. In the case under consideration with the zero mode of the scalar field with very large amplitude and with an energy density much larger than the top of the potential hill, there is enough energy in the system to sample both vacua. (The energy is proportional to the spatial volume). Parametric amplification transfers energy from the zero mode to the quantum fluctuations. Even when only a fraction of the energy of the zero mode is transferred thus creating a non-perturbatively large number of particles, the energy in the fluctuations is very large, and the equal time two-point correlation function is non-perturbatively large and the field fluctuations are large enough to sample both vacua. The evolution of the zero mode is damped because of this transfer of energy, but in most generic situations it does not reach an asymptotic time-independent value, but oscillates around zero, sampling the tree level minima with equal probability. This situation is reminiscent of finite temperature in which case the energy density is finite and above a critical temperature the ensemble averages sample both tree level vacua with equal probability thus restoring the symmetry. In the dynamical case, the “symmetry restoration” is just a consequence of the fact that there is a very large energy density in the initial state, much larger than the top of the tree level potential, thus under the dynamical evolution the system samples both vacua equally. This statement is simply the dynamical equivalent of the equilibrium finite temperature statement that the energy in the quantum fluctuations is large enough that the fluctuations can actually sample both vacua with equal probability.

Thus the criterion for symmetry restoration when the tree level potential allows for broken symmetry states is that the energy density in the initial state be larger than the top of the tree level potential. That is when the amplitude of the zero mode is such that $V(\eta_0) > V(0)$. In this case the dynamics will be very similar to the unbroken symmetry case, the amplitude of the zero mode will damp out, transferring energy to the quantum fluctuations via parametric amplification, but asymptotically oscillating around zero with a fairly large amplitude.

To illustrate this point clearly, we plot in figs. 6 and 7, $\eta(t)$ and $\Sigma(t)$ for $\eta_0 = 1.6 > \sqrt{2}$ [and hence $V(\eta_0) > V(0)$, see eq.(5.1)] and $g = 10^{-3}$. We find the typical behaviour of unbroken symmetry. Notice again that the effective or tree level potential is an irrelevant quantity for the dynamics, the asymptotic amplitude of oscillation of the zero mode is $\eta \approx 0.5$, which is smaller than the minimum of the tree level potential $\eta = 1$ but the oscillations are symmetric around $\eta = 0$.

Since the dynamical evolution sampled both vacua symmetrically from the beginning, there never was a symmetry breaking in the first place, and “symmetry restoration” is just the statement that the initial state has enough energy density such that the *dynamics* probes both vacua symmetrically despite the fact that the tree level potential allows for broken symmetry ground states.

VII. LINEAR VS. NONLINEAR DISSIPATION (THROUGH PARTICLE CREATION)

As already stressed, the field theory dynamics is unavoidable nonlinear for processes like preheating and reheating. It is however interesting to study such processes in the amplitude expansion. This is done in detail in refs. [8–10]. To dominant order, the amplitude expansion means to linearize the zero mode evolution equations. This approach permits an

analytic resolution of the evolution in closed form by Laplace transform. Explicit integral representations for $\eta(t)$ follow as functions of the initial data [8–10]. Moreover, the results can be clearly described in terms of S-matrix concepts (particle poles, production thresholds, resonances, etc.).

Let us consider the simplest model where the inflaton Φ couples to a another scalar σ and to a fermion field ψ , and potential [10]

$$V = \frac{1}{2} [m_\Phi^2 \Phi^2 + m_\sigma^2 \sigma^2 + g \sigma^2 \Phi^2] \\ + \frac{\lambda_\Phi}{4!} \Phi^4 + \frac{\lambda_\sigma}{4!} \sigma^4 + \bar{\psi}(m_\psi + y\Phi)\psi .$$

In the unbroken symmetry case ($m_\Phi^2 > 0$) the inflaton is always stable and we found for the order parameter (expectation value of Φ) evolution in the amplitude expansion [10],

$$\eta(t) = \frac{\eta_i}{1 - \frac{\partial \Sigma(i m_\Phi)}{\partial m_\Phi^2}} \cos[m_\Phi t] \\ + \frac{2 \eta_i}{\pi} \int_{m_\Phi + 2m_\sigma}^{\infty} \frac{\omega \Sigma_I(\omega) \cos \omega t d\omega}{[\omega^2 - m_\Phi^2 - \Sigma_R(\omega)]^2 + \Sigma_I(\omega)^2} . \quad (7.1)$$

where $\Sigma_{\text{physical}}(i\omega \pm 0^+) = \Sigma_R(\omega) \pm i\Sigma_I(\omega)$ is the inflaton self-energy in the physical sheet, $\eta_i = \eta(0)$ and $\dot{\eta}(0) = 0$. The first term is the contribution of the one-particle pole (at the physical inflaton mass). This terms oscillates forever with constant amplitude corresponding to the asymptotic single particle state. The second term is the cut contribution $\eta(t)_{\text{cut}}$ corresponding to the process $\Phi \rightarrow \Phi + 2\sigma$ above the three particle threshold.

In general, when

$$\Sigma_I(\omega \rightarrow \omega_{\text{th}}) \stackrel{\omega \rightarrow \omega_{\text{th}}}{\cong} B (\omega - \omega_{\text{th}})^\alpha ,$$

the the cut contribution behaves for late times as

$$\eta(t)_{\text{cut}} \simeq \frac{2 \eta_i}{\pi} \frac{B \omega_{\text{th}} \Gamma(1 + \alpha)}{[\omega^2 - m_\Phi^2 - \Sigma_R(\omega_{\text{th}})]^2} \\ t^{-1-\alpha} \cos \left[\omega_{\text{th}} t + \frac{\pi}{2}(1 + \alpha) \right] .$$

Here, $\omega_{\text{th}} = m_\Phi + 2M_\sigma$ is the threshold energy and $\alpha = 2$ since to two-loops, [10]

$$\Sigma_I(\omega) \stackrel{\omega \rightarrow m_\Phi + 2M_\sigma}{\cong} \frac{2g^2 \pi^2}{(4\pi)^4} \frac{M_\sigma \sqrt{m_\Phi}}{(m_\Phi + 2M_\sigma)^{7/2}} [\omega^2 - (m_\Phi + 2M_\sigma)^2] .$$

In the broken symmetry case ($m_\Phi^2 < 0$) we may have either $M < 2m_\sigma$ or $M > m_\sigma$, where M is the physical inflaton mass. ($M = |m_\Phi| \sqrt{2}$ at the tree level). In the first case the inflaton is stable and eq.(7.1) holds. However, the self-energy starts now at one-loop and vanishes at threshold with a power $\alpha = 1/2$. For $M > m_\sigma$ the ‘‘inflaton’’ becomes a resonance (an unstable particle) with width (inverse lifetime)

$$\Gamma = \frac{g^2 \Phi_0^2}{8\pi M} \sqrt{1 - \frac{4m_\sigma^2}{M^2}} .$$

This pole dominates $\eta(t)$ for non asymptotic times

$$\delta(t) \simeq \delta_i A e^{-\Gamma t/2} \cos(Mt + \gamma), \quad (7.2)$$

where

$$A = 1 + \frac{\partial \Sigma_R(M)}{\partial M^2}, \quad \gamma = -\frac{\partial \Sigma_I(M)}{\partial M^2}.$$

In summary, eq.(7.2) holds provided: a) the inflaton is a resonance and b) $t \leq \Gamma^{-1} \ln(\Gamma/M_\sigma)$. For later times the fall off is with a power law $t^{-3/2}$ determined by the spectral density at threshold as before [10]. The full study of ‘‘inflaton’’ decaying into lighter scalars in DeSitter space-time has been recently presented in reference [39].

In ref. [10] the selfconsistent nonlinear evolution is computed to one-loop level for the model (7.1). In fig. 8 $\eta(t)$ is plotted as a function of time for $\lambda = g = 1.6\pi^2$, $y = 0$, $m_\sigma = 0.2m_\Phi$, $\eta(0) = 1$ and $\dot{\eta}(0) = 0$.

Figure 8 shows a very rapid, non-exponential damping within few oscillations of the expectation value and a saturation effect when the amplitude of the oscillation is rather small (about 0.1 in this case), the amplitude remains almost constant at the latest times tested. Figures 8 and 9 clearly show that the time scale for dissipation (from fig. 8) is that for which the particle production mechanism is more efficient (fig. 9). Notice that the total number of particles produced rises on the same time scale as that of damping in fig. 8 and eventually when the expectation value oscillates with (almost) constant amplitude the average number of particles produced remains constant. This behaviour is a close analog to the selfcoupled inflaton for unbroken symmetry (fig.1). The amplitude expansion predictions are in qualitative agreement with both results.

These figures clearly show that damping is a consequence of particle production. At times larger than about $40 m_\Phi^{-1}$ (for the initial values and couplings chosen) there is no appreciable damping. The amplitude is rather small and particle production has practically shut off. If we had used the *classical* evolution of the expectation value in the mode equations, particle production would not shut off (parametric resonant amplification), and thus we clearly see the dramatic effects of the inclusion of the back reaction.

In ref. [10] the broken symmetry case $m_\Phi^2 < 0$ is then studied. Figures 11-13 show $\eta(\tau)$ vs τ , $\mathcal{N}_\sigma(\tau)$ vs τ and $\mathcal{N}_{q,\sigma}(\tau = 200)$ vs q respectively, for $\lambda/8\pi^2 = 0.2$; $g/\lambda = 0.05$; $m_\sigma = 0.2|m_\Phi|$; $\eta(0) = 0.6$; $\dot{\eta}(0) = 0$. Notice that the mass for the linearized perturbations of the Φ field at the broken symmetry ground state is $\sqrt{2}|m_\Phi| > 2m_\sigma$. Therefore, for the values used in the numerical analysis, the two-particle decay channel is open. For these values of the parameters, linear relaxation predicts exponential decay with a time scale $\tau_{rel} \approx 300$ (in the units used). Figure 11 shows very rapid non-exponential damping on time scales about *six times shorter* than that predicted by linear relaxation. The expectation value reaches very rapidly a small amplitude regime, once this happens its amplitude relaxes very slowly. In the non-linear regime relaxation is clearly *not* exponential but extremely fast. The amplitude at long times seems to relax to the expected value, shifted slightly from the minimum of the tree level potential at $\eta = 1$. This is as expected from the fact that there are quantum corrections. Figure 12 shows that particle production occurs during the time scale for which dissipation is most effective, giving direct proof that dissipation is a consequence of particle production. Asymptotically, when the amplitude of the expectation value is small, particle production shuts off. We point out again that this is a consequence of the back-reaction in

the evolution equations. Without this back-reaction, as argued above, particle production would continue without indefinitely. Figure 13 shows that the distribution of produced particles is very far from thermal and concentrated at low momentum modes $k \leq |m_\Phi|$. This distribution is qualitatively similar to that in the unbroken symmetry case, and points out that the excited state obtained asymptotically is far from thermal.

In ref. [10] the case where the inflaton is only coupled to fermions is studied ($g = 0$, $y \neq 0$). The damping of the zero mode is very inefficient in such case due to Pauli blocking. Namely, the Pauli exclusion principle forbids the creation of more than 2 fermions per momentum state. Pauli blocking shuts off particle production and dissipation very early on.

VIII. THE REHEATING TEMPERATURE

The arena in which these results become important is that of inflationary cosmology. In particular, the process of preheating is of vital importance in understanding how the big-bang cosmology is regained at the end of inflation, i.e. the reheating mechanism.

While our analysis has been entirely a Minkowski space one, we can make some comments concerning the reheating temperature. However, a more detailed analysis incorporating the expanding universe must eventually be done along the lines suggested in this work, to get more accurate results.

Since the particles created during the preheating stage are far from equilibrium, thermalization and equilibration will be achieved via collisional relaxation. In the approximation that we are studying, however, collisions are absent and the corresponding contributions are of $\mathcal{O}(1/N)$. The difficulty with the next order calculation and incorporation of scattering terms is that these are non-local in time and very difficult to implement numerically.

However we can obtain an estimate for the reheating temperature under some reasonable assumptions: in the cosmological scenario, *if* the equilibration time is shorter than the inverse of the expansion rate H , then there will not be appreciable redshifting of the temperature because of the expansion and we can use our Minkowski space results.

The second assumption is that the time scales between particle production and thermalization and equilibration are well separated. Within the large N approximation this is clearly correct because at large N , scattering processes are suppressed by $1/N$. If these two time scales are widely separated then we can provide a fairly reliable estimate of the reheating temperature as follows.

Equilibration occurs via the *redistribution* of energy and momentum via elastic collisional processes. Assuming that thermalization occurs on time scales larger than that of particle production and parametric amplification, then we can assume energy conservation in the scattering processes. Although a reliable and quantitative estimate of the reheating temperature can only be obtained after a detailed study of the collisional processes which depend on the interactions, we can provide estimates in two important cases. If the scattering processes do not change chemical equilibrium, that is conserve particle number, the energy per particle is conserved. Since the energy (density) stored in the non-equilibrium bath and the total number of particles per unit volume are, as shown in the previous sections:

$$\varepsilon \approx \frac{|M_R|^4}{\lambda_R}$$

$$N \approx \frac{|M_R|^3}{\lambda_R}$$

with proportionality constants of order one, we can estimate the reheating temperature to be:

$$\frac{\varepsilon}{N} \approx T \approx |M_R| \tag{8.1}$$

Here $|M_R|$ is the inflaton mass. This is consistent with previous results [8].

This result seems puzzling, since naively one would expect $\varepsilon \approx T_R^4$; $N \approx T_R^3$ but the powers of λ do not match. This puzzle arises from intuition based on an ultrarelativistic free particle gas. However the “medium” is highly excited with a large density of particles and the “in medium” properties of the equilibrated particles may drastically modify this naive result as is known to happen in most theories at high temperature, where the medium effects are strong and perturbation theory breaks down requiring hard thermal loop resummation.

In the case in which the collisional processes do not conserve particle number and therefore change chemical equilibrium, the only conserved quantity is the energy. Such is the case for massless particles interacting with a quartic couplings for example or higher order processes in a quartic theory with massive particles. Processes in which $3 \rightarrow 1$ conserving energy and momentum can occur. The inverse process $1 \rightarrow 3$ occurs with far less probability since the high momentum modes are much less populated than the low momentum modes in the unstable bands. In this case only energy is conserved whereas the total number of particles is *not conserved* and in this case an estimate of the reheating temperature compares the energy density in the bath of produced particles to that of an ultrarelativistic gas in equilibrium at temperature T_R ,

$$\varepsilon \approx \frac{|M_R|^4}{\lambda_R} \approx T_R^4$$

leading to the estimate

$$T_R \approx \frac{|M_R|}{\lambda_R^{\frac{1}{4}}}$$

Thus we can at least provide a bound for the reheating temperature

$$|M_R| \leq T_R \leq \frac{|M_R|}{\lambda}$$

and a more quantitative estimate requires a deeper understanding of the collisional processes involved.

Within the large N approximation, scattering terms will appear at order $1/N$ and beyond. The leading contribution $\mathcal{O}(1/N)$ to collisional relaxation conserves particle number in the unbroken symmetry state because the product particles are massive. This can be seen from the fact that the self-energy to this order is given by the same chain of bubbles that gives the scattering amplitude but with two external legs contracted. All cut diagrams (that give the imaginary part) correspond to $2 \rightarrow 2$ processes that conserve particle number because of kinematic reasons. Certainly at higher order in $1/N$ there will be processes that change chemical equilibrium, but for large N these are suppressed formally. This argument

based on the leading collisional contribution in the $1/N$ expansion allows us to provide a further consistent estimate in the unbroken symmetry case (when the produced particles are massive). In this approximation and consistently with energy and particle number conservation we can assume that the final equilibrium temperature is of the order of the typical particle energy before thermalization. Recalling that the unstable band remains stable during the evolution with the peak shifting slightly in position we can estimate the typical energy per particle by the position of the peak in the distribution at q_1 , and use the analytical estimate for the peak given in section 2. Restoring the units we then obtain the estimate

$$T_R \approx |M_R| q_1 \approx |M_R| \frac{\eta_0}{2} \approx \sqrt{\frac{\lambda_R}{8}} \Phi_0 \quad (8.2)$$

which displays the dependence on η_0 explicitly. Eq. (8.2) is an improvement of the simple estimate (8.1).

It must be noticed that the peak in the momentum distribution decreases with time for $t > t_{reh}$ (see fig. 2f-2h). This drift follows from the non-linear interaction between the modes. For the case of fig. 2, one sees that T_R reduces by approximately a factor 3 with respect to the value (8.2).

The large N model studied in this article is not a typical model used in inflationary cosmology, and since we want to make a quantitative statement for inflationary scenarios (within the approximation of only considering Minkowski space) we now study a model that incorporates other scalar fields coupled to the inflaton.

The simplest model [2] contains in addition to the inflaton a lighter scalar field σ with a $g\sigma\Phi^2$ coupling. That is, we consider the Lagrangian [8],

$$\mathcal{L} = -\frac{1}{2}\Phi(\partial^2 + m^2 + g\sigma)\Phi - \frac{\lambda}{4!}\Phi^4 - \frac{1}{2}\sigma(\partial^2 + m_\sigma^2)\sigma - \frac{\lambda_\sigma}{4!}\sigma^4.$$

We will consider again the preheating regime of weak couplings and early times such that we can neglect the back-reaction of the quantum fluctuations of the σ field as well as the back-reaction of the quantum fluctuations of the inflation itself, focussing only on the parametric growth of the σ fluctuations in the unbroken symmetry case. The mode equations for the σ field take the form

$$\left[\frac{d^2}{dt^2} + k^2 + m_\sigma^2 + g\phi^2(t) \right] f_k(t) = 0.$$

In dimensionless variables this equation becomes

$$\left[\frac{d^2}{d\tau^2} + q^2 + \left(\frac{m_\sigma}{m}\right)^2 + \frac{6g}{\lambda}\eta^2(\tau) \right] f_k(\tau) = 0.$$

In the short time approximation we can replace $\eta(\tau)$ by the classical form (4.1). We then find a Lamé equation which admits closed form solutions for [28]

$$\frac{12g}{\lambda} = n(n+1) \quad , \quad n = 1, 2, 3, \dots$$

Although these are not generic values of the couplings, the solubility of the model and the possibility of analytic solution for these cases makes this study worthwhile. In the simplest case, ($n = 1$, $6g = \lambda$), there is only one forbidden band for $q^2 > 0$. It goes from $q^2 = 1 - \left(\frac{m_\sigma}{m}\right)^2$ to $q^2 = 1 - \left(\frac{m_\sigma}{m}\right)^2 + \eta_0^2/2$. That is,

$$\text{forbidden band} : m^2 - m_\sigma^2 < k^2 < m^2 - m_\sigma^2 + \frac{\lambda}{4} \Phi_0^2 .$$

The Floquet index in this forbidden band takes the form

$$F(q) = 2i K(k) Z(2K(k)v) \pm \pi ,$$

where now v and q are related by the following equation

$$q^2 = 1 - \left(\frac{m_\sigma}{m}\right)^2 + \frac{\eta_0^2}{2} \text{cn}^2(2K(k)v, k) .$$

and $0 \leq v \leq 1/2$.

The imaginary part of the Floquet index is now maximal at $q_1^2 = 1 - \left(\frac{m_\sigma}{m}\right)^2 + \frac{\eta_0^2}{4}$ and we can use this value to provide an estimate for the reheating temperature in this model in the same manner as for eq.(8.2), yielding the following estimate for the reheating temperature

$$T_{reh} \simeq \sqrt{m^2 - m_\sigma^2 + \frac{\lambda}{8} \Phi_0^2} . \quad (8.3)$$

In the special case $m_\sigma = m = |M_R|$, we recover eq.(8.2), as expected.

Again, the non-linear field evolution for $t > t_{reh}$ decreases T_{reh} . In the third reference under [8], we found for late times a T_{reh} ten times smaller than the value (8.3) for $g = 1.6\pi^2$.

The estimates on the reheating temperature provided above should not be taken rigorously, but as an approximate guide. A consistent estimate of the reheating temperature and the thermalization time scales would in principle involve setting up a Boltzmann equation [2]. Under the assumption of a separation between the preheating and thermalization time scales one could try to use the distribution functions N_q at the end of the preheating stage as input in the kinetic Boltzmann equation. However, we now argue that such a kinetic description is *not valid* to study thermalization. A kinetic approach based on the Boltzmann equation, with binary collisions, for example, would begin by writing the rate equation for the distribution of particles

$$\begin{aligned} \dot{N}_k \propto \lambda^2 \int d^3k_1 d^3k_2 d^3k_3 \delta^4(k_1 + k_2 + k_3 + k) [(1 + n_k)(1 + n_{k_1})n_{k_2}n_{k_3} - \\ n_k n_{k_1} (1 + n_{k_2})(1 + n_{k_3})] . \end{aligned}$$

However this equation is only valid in the *low density* regime. In particular for the case under study, the occupation numbers for wavevectors in the unstable bands are non-perturbatively large $\propto 1/\lambda$ and one would be erroneously led to conclude that thermalization occurs on the same time scale or *faster than* preheating.

Clearly such a statement would be too premature. Without a separation of time scales the kinetic approach is unwarranted. The solution of the Boltzmann equation provides a

partial resummation of the perturbative series which is valid whenever the time scales for relaxation is much longer than the microscopic time scales [36], in this case that of particle production.

In the case under study there is an expansion parameter, $1/N$ and clearly these scattering terms are subleading in this formal limit, so that the separation of time scales is controlled. In the absence of such an expansion parameter, some resummation scheme must be invoked to correctly incorporate scattering. In particular when the symmetry is broken, the asymptotic excitations are Goldstone bosons, the medium is highly excited but with very long-wavelength Goldstones and these have very small scattering cross sections. Such a resummation is also necessary in the large temperature limit of field theories in equilibrium. In this case the perturbative expansion of the scattering cross section involves powers of $\lambda T/m$ with m being the mass. A correct resummation of the (infrared) divergent terms leads to $\lambda(T) \rightarrow m/T$ in the large T/m limit [37]. In particular the $1/N$ corrections in the formal large N limit involve such a resummation, but in the non-equilibrium situation, the numerical implementation of this resummation remains a formidable problem.

IX. CONCLUSIONS

It is clear that preheating is both an extremely important process in a variety of settings, as well as one involving very delicate analysis. In particular, its non-perturbative nature renders any treatment that does not take into account effects such as the quantum back-reaction due to the produced particles, consistent conservation (or covariant conservation) of the relevant quantities and Ward identities, incapable of correctly describing the important physical phenomena during the preheating stage.

In this work, we dealt with these issues by using the $O(N)$ vector model in the large N limit. This allows for a controlled non-perturbative approximation scheme that conserves energy and the proper Ward identities, to study the non-equilibrium dynamics of scalar fields. Using this model we were able to perform a full analysis of the evolution of the zero mode as well as of the particle production during this evolution.

Our results are rather striking. We were able to provide analytic results for the field evolution as well as the particle production and the equation of state for all these components in the weak coupling regime and for times for which the quantum fluctuations, which account for back-reaction effects, are small. What we found is that, in the unbroken symmetry situation, the field modes satisfy a Lamé equation that corresponds to a Schrödinger equation with a two-zone potential. There are two allowed and two forbidden bands, which is *decidedly* unlike the Mathieu equation used in previous analysis [6,7,19]. The difference between an equation with two forbidden bands and one with an infinite number is profound. We were also able to estimate analytically the time scale at which preheating would occur by asking when the quantum fluctuations as calculated in the absence of back-reaction would become comparable to the tree level terms in the equations of motion. The equations of state of both the zero mode and “pions” were calculated and were found to be describable as polytropes. These results were then confirmed by numerical integration of the equations, and we found that the analytic results were in great agreement with the numerical ones in their common domain of validity.

When the $O(N)$ symmetry is spontaneously broken, more subtle effects can arise, again in the weak coupling regime. If the zero mode starts off very near the origin, then the quantum back-reaction grows to be comparable to the tree level terms within one or at most a few oscillations even for very weak coupling. In this case the periodic approximation for the dynamics of the zero mode breaks down very early on and the full dynamics must be studied numerically.

When numerical tools are brought to bear on this case we find some extremely interesting behavior. In particular, there are situations in which the zero mode starts near the origin (the initial value depends on the coupling) and then in one oscillation, comes back to almost the same location. However, during the evolution it has produced $1/g$ particles. Given that the total energy is conserved, the puzzle is to find where the energy came from to produce the particles. We found the answer in a term in the energy density that has the interpretation of a “vacuum energy” that becomes *negative* during the evolution of the zero mode and whose contribution to the equation of state is that of “vacuum”. The energy given up by this term is the energy used to produce the particles.

This example also allows us to study the possibility of symmetry restoration during preheating [7,20,34]. While there have been arguments to the effect that the produced particles will contribute to the quantum fluctuations in such a way as to make the effective mass squared of the modes positive and thus restore the symmetry, we argued that they were unfounded. Whereas the effective squared mass oscillates, taking positive values during the early stages of the evolution, its asymptotic value is zero, compatible with Goldstone bosons as the asymptotic states.

Furthermore, this says nothing about whether the symmetry is restored or not. This is signaled by the final value of the zero mode. In all the situations examined here, the zero mode is driven to a *non-zero* final value. At this late time, the “pions” become massless, i.e. they truly are the Goldstone modes required by Goldstone’s theorem.

The arguments presented in favor of symmetry restoration rely heavily on the effective potential. We have made the point of showing explicitly why such a concept is completely irrelevant for the non-equilibrium dynamics when profuse particle production occurs and the evolution occurs in a highly excited, out of equilibrium state.

Finally, we dealt with the issue of how to use our results to calculate the reheating temperature due to preheating in an inflationary universe scenario. Since our results are particular to Minkowski space, we need to assume that preheating and thermalization occur on time scales shorter than the expansion time, i.e. H^{-1} . We also need to assume that there is a separation of time scale between preheating and thermalization. Under these assumptions we can estimate the reheating temperature as $T_{reh} \propto |M_R|$ in the case where the produced particles are massive and $T_{reh} \propto |M_R|/\lambda^{1/4}$ in the massless case.

We have made the important observation that due to the large number of long-wavelength particles in the forbidden bands, a kinetic or Boltzmann equation approach to thermalization is *inconsistent* here. A resummation akin to that of hard thermal loops, that consistently arises in the next order in $1/N$ must be employed. In equilibrium such a resummation shows that the scattering cross section for soft modes is perturbatively small despite their large occupation numbers.

There is a great deal left to explore. Recently we reported on our study of the non-linear quantum field evolution in de Sitter and FRW backgrounds in refs. [16] and [17],

respectively. The next important step is to consider the background dynamics as a full backreaction problem, including the inflaton dynamics and the dynamics of the scale factor self-consistently.

Such a detailed study will lead to a consistent and thorough understanding of the inflationary period, the post-inflationary and reheating periods. Further steps should certainly include trying to incorporate thermalization effects systematically within the $1/N$ expansion.

The preheating and reheating theory in inflationary cosmology is currently a very active area of research in fast development, with the potential for dramatically modifying the picture of the late stages of inflationary phase transitions.

As remarked before, reliable and consistent estimates and field theory calculations have been done mostly assuming Minkowski spacetime. The matter state equations obtained in Minkowski [15] and recently in de Sitter backgrounds [16] give an indication, through the Einstein-Friedmann equation, of the dynamics of scale factor and give a glimpse of the important physics to be unraveled by a deeper study.

The formulation described in detail in these lectures are uniquely suited to provide complete description of the full dynamics of inflationary cosmology, from times prior to the phase transitions or the beginning of the chaotic era, through the inflationary regime, to the post-inflationary and reheating stage.

Such a program provides the ultimate tool to test physical predictions of particle physics models. Thus this new consistent formulation provides the practical means to input a particle physics model and extract from it reliable *dynamical* predictions which will have to ultimately be tested against the next generation of cosmological experiments.

REFERENCES

- * Laboratoire Associé au CNRS, UA280.
- [1] A. H. Guth, *Phys. Rev.* **D23**, 347 (1981).
- [2] See for reviews,
E. W. Kolb and M. S. Turner, “The Early Universe”, Addison Wesley (Frontiers in Physics) (1990),
A. Linde, *Particle Physics and Inflationary Cosmology*, Harwood Academic Publishers (1990), and references therein.
- [3] D. Boyanovsky and H. J. de Vega, *Phys. Rev.* **D47**, 2343 (1993).
D. Boyanovsky, D.-S. Lee, and A. Singh, *Phys. Rev.* **D48**, 800 (1993).
- [4] D. Boyanovsky, H. J. de Vega and R. Holman, *Phys. Rev.* **D49**, 2769 (1994).
- [5] D. Boyanovsky, H. J. de Vega and R. Holman, *Phys. Rev.* **D51**, 734 (1995).
- [6] J. Traschen, and R. Brandenberger, *Phys. Rev. D* **42**, 2491 (1990).
Y. Shtanov, J. Traschen and R. Brandenberger, *Phys. Rev.* **D51**, 5438 (1995).
- [7] L. Kofman, A. Linde and A. Starobinsky, *Phys. Rev. Lett.* **73**, 3195 (1994); *Phys. Rev. Lett.* **76**, 1011 (1996). A. Linde, *Lectures on Inflationary Cosmology*, in *Current Topics in Astrofundamental Physics*, ‘The Early Universe’, Proceedings of the Chalonge Erice School, N. Sánchez and A. Zichichi Editors, Nato ASI series C, vol. 467, 1995, Kluwer Acad. Publ. L. Kofman, astro-ph/9605155.
- [8] D. Boyanovsky, H. J. de Vega, R. Holman, D.-S. Lee and A. Singh, *Phys. Rev.* **D51**, 4419 (1995);
- [9] See for reviews,
D. Boyanovsky, H. J. de Vega and R. Holman, ‘Non-equilibrium dynamics of phase transitions in the early universe’, in ‘Advances in Astrofundamental Physics’ 1995, N. Sánchez and A. Zichichi Editors, p. 343, World Scientific, 1995.
D. Boyanovsky, M. D’Attanasio, H. J. de Vega, R. Holman and D.-S. Lee, ‘New aspects of reheating’, in the Proceedings of the Erice Chalonge School, ‘String Gravity and Physics at the Planck Energy Scale’, NATO Advanced Study Institute, N. Sánchez and A. Zichichi Editors, Kluwer 1996, p. 451-492.
D. Boyanovsky, H. J. de Vega and R. Holman, in the Proceedings of the Second Paris Cosmology Colloquium, Observatoire de Paris, June 1994, p. 127-215,
H. J. de Vega and N. Sánchez Editors, World Scientific, 1995;
- [10] D. Boyanovsky, M. D’Attanasio, H. J. de Vega, R. Holman and D. S. Lee, *Phys. Rev.* **D52**, 6805 (1995);
- [11] D. Boyanovsky, M. D’Attanasio, H. J. de Vega and R. Holman, *Phys. Rev.* **D54**, 1748 (1996), and references therein.
- [12] A. D. Dolgov and A. D. Linde, *Phys. Lett.* **B116**, 329 (1982);
L. F. Abbott, E. Farhi and M. Wise, *Phys. Lett.* **B117**, 29 (1982).
- [13] S. Mrowczynski and B. Muller, *Phys. Lett.* **B363**,1, (1995).
- [14] F. Cooper, J. M. Eisenberg, Y. Kluger, E. Mottola, B. Svetitsky, *Phys. Rev. Lett.* **67**, 2427 (1991);
F. Cooper, J. M. Eisenberg, Y. Kluger, E. Mottola, B. Svetitsky, *Phys. Rev.* **D48**, 190 (1993);
F. Cooper and E. Mottola, *Mod. Phys. Lett. A* **2**, 635 (1987);
F. Cooper, S. Habib, Y. Kluger, E. Mottola, J. P. Paz, P. R. Anderson,

- Phys. Rev. D50, 2848 (1994);
 F. Cooper, S.-Y. Pi and P. N. Stancioff, Phys. Rev. D34, 3831 (1986);
 F. Cooper, Y. Kluger, E. Mottola, J. P. Paz, Phys. Rev. D51, 2377 (1995).
 S. Habib, Y. Kluger, E. Mottola and J.P. Paz, Phys. Rev. Lett. 76, 4660 (1996).
- [15] D. Boyanovsky, H. J. de Vega, R. Holman and J. Salgado, ‘Analytic and Numerical Study of Reheating Dynamics’, hep-ph/9608205, to appear in Phys. Rev. **D**, December 15, 1996.
- [16] D. Boyanovsky, D. Cormier, H. J. de Vega and R. Holman, ‘Out of equilibrium dynamics of an inflationary phase transition’, hep-ph/9610396.
- [17] D. Boyanovsky, D. Cormier, H. J. de Vega, R. Holman, A. Singh and M. Srednicki, ‘Preheating the FRW universe’, hep-ph/9609527.
- [18] J. Baacke, K. Heitmann and C. Paetzold, hep-th/9608006, to appear in Phys. Rev. **D**.
- [19] M. Yoshimura, Prog. Theor. Phys. **94**, 873 (1995); hep-th/9506176; H. Fujisaki, K. Kumekawa, M. Yamaguchi, M. Yoshimura, Phys. Rev. D **53**, 6805 (1996), hep-ph/9508378. H. Fujisaki, K. Kumekawa, M. Yamaguchi, and M. Yoshimura, TU/95/493, hep-ph/9511381; M. Yoshimura, TU-96-500 preprint, hep-ph/9605246. S. Kasuya and M. Kawasaki, preprint ICRR-Report-360-96-11, hep-ph/9603317.
- [20] I. I. Tkachev, hep-th/9510146, OSU-TA-21/95 (1996); A. Riotto and I. I. Tkachev, hep-ph/9604444, OSU-TA-12/96 (1996). S. Klebnikov and I. Tkachev, Phys. Rev. Lett. 77, 219 (1996); hep-ph/9603378.
- [21] J. Schwinger, J. Math. Phys. 2, 407 (1961) P. M. Bakshi and K. T. Mahanthappa, J. of Math. Phys. 4, 1 (1963); *ibid.* 12. ; L. V. Keldysh, Sov. Phys. JETP 20, 1018 (1965); A. Niemi and G. Semenoff, Ann. of Phys. (N.Y.) 152, 105 (1984); Nucl. Phys. B [FS10], 181, (1984); E. Calzetta, Ann. of Phys. (N.Y.) 190, 32 (1989); R. D. Jordan, Phys. Rev. D33, 444 (1986); N. P. Landsman and C. G. van Weert, Phys. Rep. 145, 141 (1987); R. L. Kobes and K. L. Kowalski, Phys. Rev. D34, 513 (1986); R. L. Kobes, G. W. Semenoff and N. Weiss, Z. Phys. C 29, 371 (1985).
- [22] see for example: E. Calzetta and B. L. Hu, Phys. Rev. D35, 495 (1988); *ibid* D37, 2878 (1988); J. P. Paz, Phys. Rev. D41, 1054 (1990); *ibid* D42, 529 (1990); B. L. Hu, Lectures given at the Canadian Summer School For Theoretical Physics and the Third International Workshop on Thermal Field Theories (Banff, Canada, 1993) (to appear in the proceedings) and in the Proceedings of the Second Paris Cosmology Colloquium, Observatoire de Paris, June 1994, p.111, H. J. de Vega and N. Sánchez Editors, World Scientific, 1995, and references therein.
- [23] A. Vilenkin, Nucl. Phys. B226, 504 (1983); Nucl. Phys. B226, 527 (1986).
 O. Eboli, R. Jackiw and S-Y. Pi, Phys. Rev. D37, 3557 (1988); M.Samiullah, O. Eboli and S-Y. Pi, Phys. Rev. D44, 2335 (1991).
- [24] G. Semenoff and N. Weiss, Phys. Rev. D31, 699 (1985).
 H. Leutwyler and S. Mallik, Ann. of Phys. (N.Y.) 205, 1 (1991).
- [25] See for example,
 N. D. Birrell and P.C.W. Davies, ‘Quantum fields in curved space’,
 Cambridge Univ. Press, (Cambridge, 1986).
- [26] See for example, J. Zinn-Justin, Quantum Field Theory and Critical Phenomena,
 Oxford Univ. Press, 1989.

- [27] C. Hermite, Notes de Cours à l'École Polytechnique, 1872 (unpublished).
Whittaker and Watson, A Course on Modern Analysis. (AMS, Press 1979).
- [28] E.L.Ince, Ordinary Differential Equations, Dover 1944.
- [29] Bateman Manuscript Project, chapter XIII, vol. II,
A. Erdély Editor, McGraw-Hill, 1953.
- [30] I. S. Gradshteyn and I. M. Ryshik, Table of Integrals, Series and Products, Academic Press.
- [31] D.T. Son, hep-ph/9604340, UW/PT-96-05 (1996).
- [32] Handbook of Mathematical functions,
Edited by M. Abramowitz and I. A. Stegun, NBS, 1965.
- [33] A. P. Prudnikov, Yu. A. Brichkov and O. I. Marichev, Integrals and series, vol II, Nauka, Moscow, 1981.
- [34] E. W. Kolb and A. Riotto, astro-ph/9602095 , FERMILAB-Pub-96/036-A (1996).
- [35] E. W. Kolb, A. Linde, and A. Riotto, hep-ph/9606260, FERMILAB-Pub-96/133-A, SU-ITP-96-22 (1996); G..W. Anderson, A. Linde, and A. Riotto, hep-ph/9606416, FERMILAB-Pub-96/078-A, SU-ITP-96-27 (1996).
- [36] D. Boyanovsky, D.S.-Lee and I. D. Lawrie, Phys.Rev. D54, 4013 (1996).
- [37] N. Tetradis, Phys. Lett. B347, 120 (1995);
N. Tetradis and C. Wetterich, Int. J. Mod. Phys. A9, 4029 (1994).
- [38] See for a critical discussion,
D. Boyanovsky, H.J. de Vega, R. Holman and J. F. J. Salgado,
'Preheating and Reheating in Inflationary Cosmology: a pedagogical survey', astro-ph/9609007.
- [39] 'Inflation decay in de Sitter spacetime', D.Boyanovsky, R.Holman and S.Prem Kumar, hep-ph-9606208

TABLES

η_0	\hat{q}	B	N
1	0.017972387...	0.1887167...	3.778...
3	0.037295557...	0.8027561...	0.623...
4	0.03966577...	1.1007794...	0.4...
$\eta_0 \rightarrow \infty$	0.043213918...	$0.28595318 \eta_0 + O(\eta_0^{-1})$	$3.147 \eta_0^{-3/2} [1 + O(\eta_0^{-2})]$

TABLE I. Quantum Fluctuations $\Sigma(\tau) \approx \frac{1}{N\sqrt{\tau}} e^{B\tau}$ during the preheating period.

FIGURES

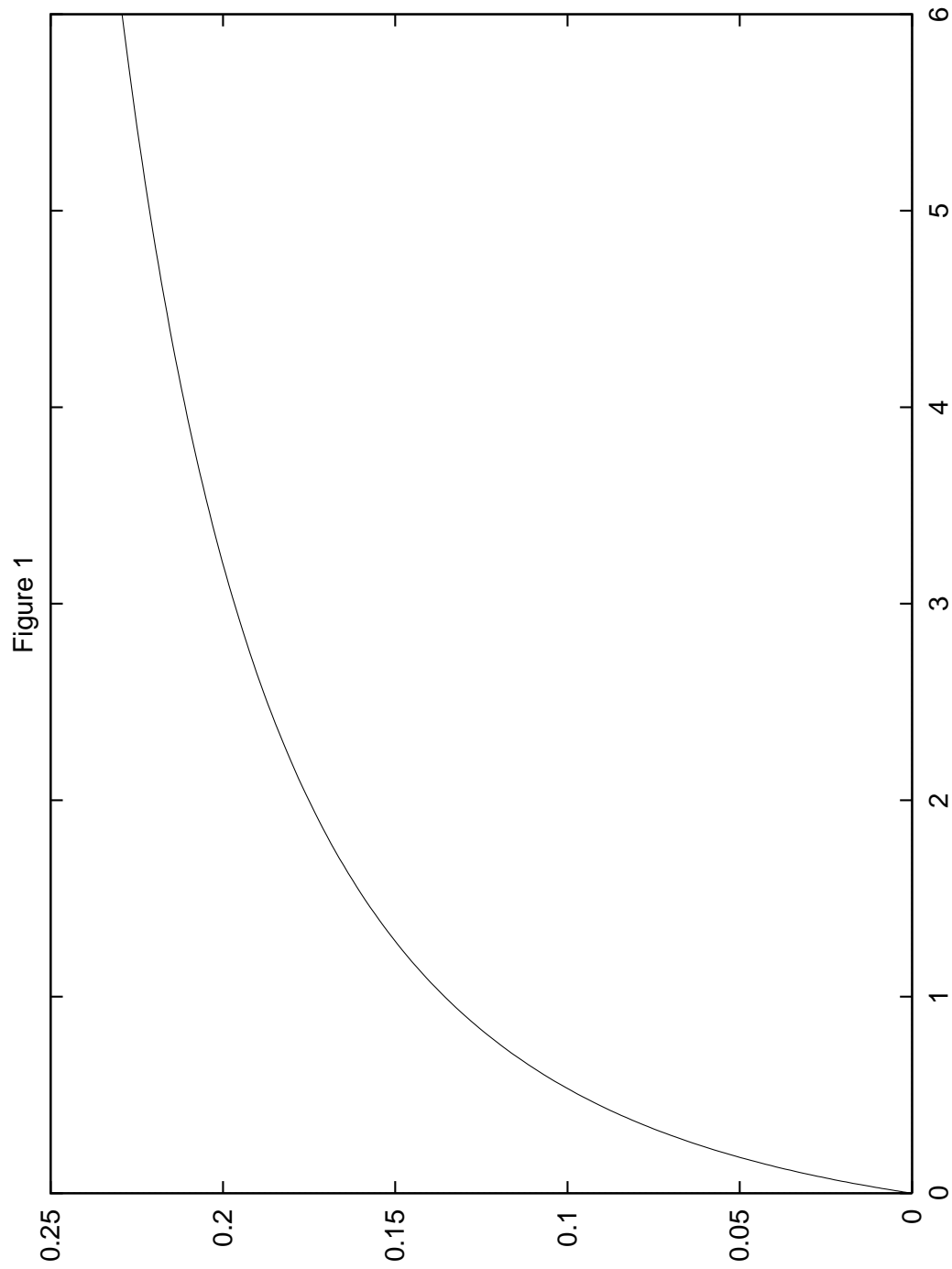
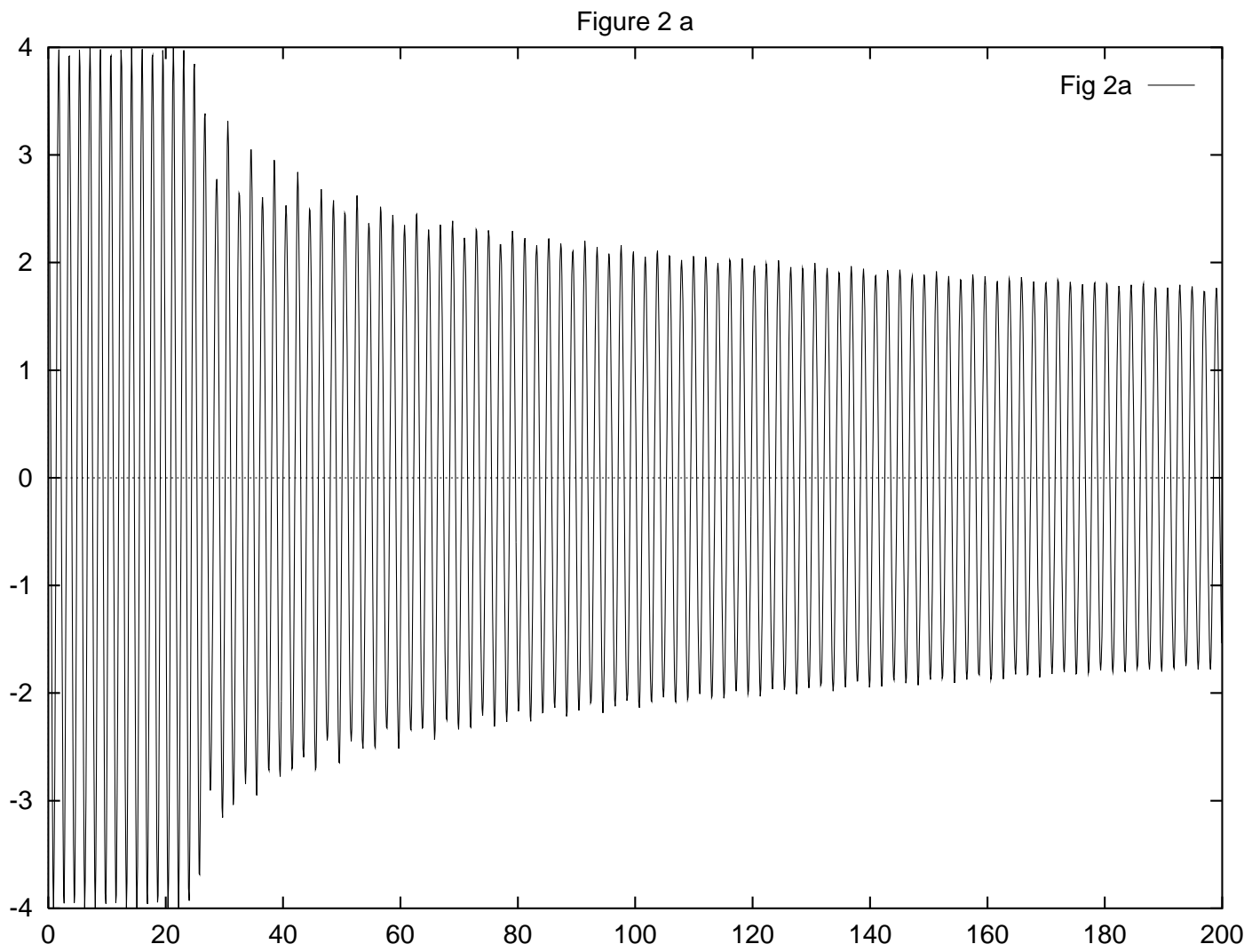


Figure 1: The ratio $\langle p_0 \rangle / \varepsilon_0$ for zero mode vs. $\lambda_R \varepsilon_0 / 2 |M_R|^4$ for the unbroken symmetry case.

Figure 2a: $\eta(\tau)$ vs. τ for the unbroken symmetry case with $\eta_0 = 4$, $g = 10^{-12}$.



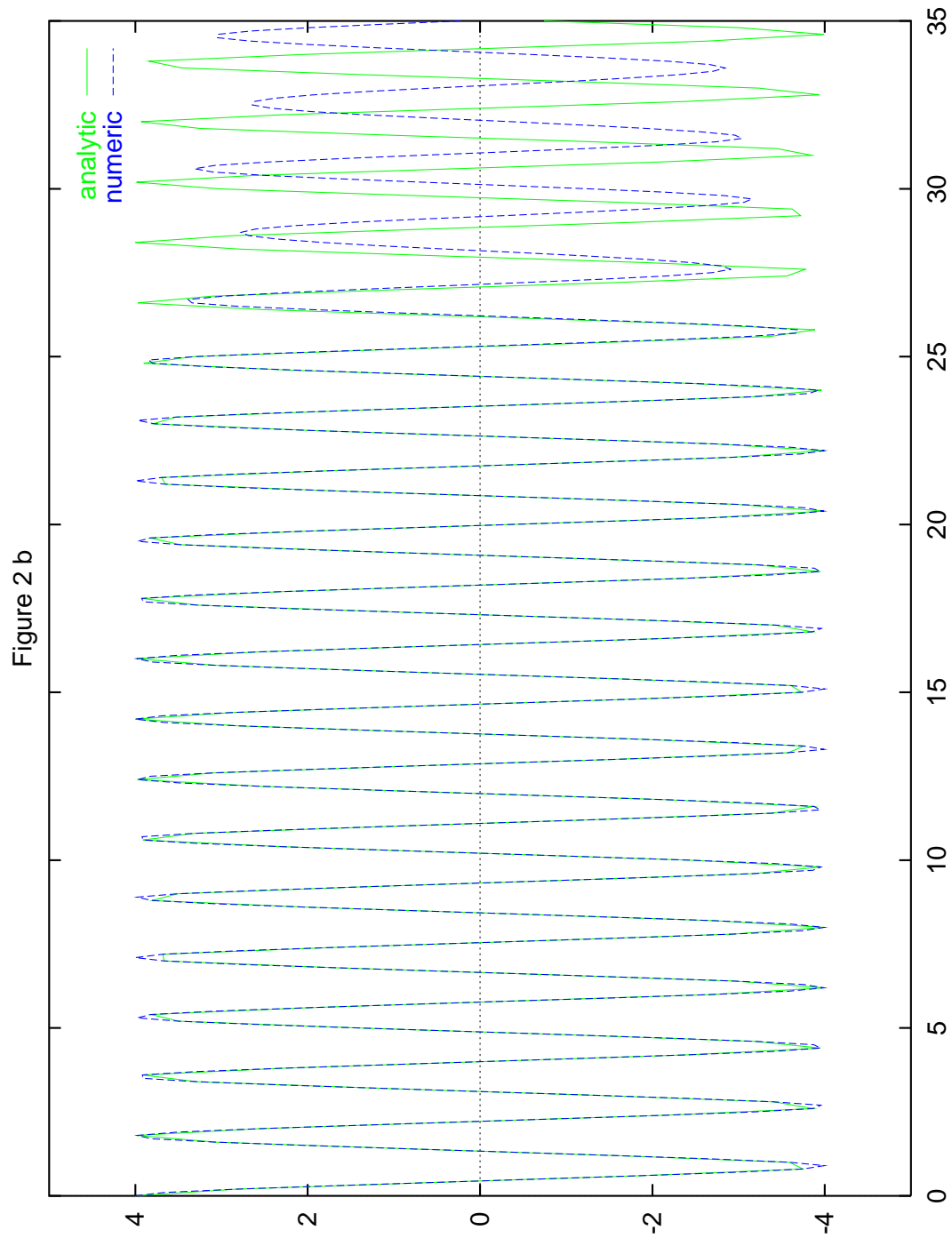
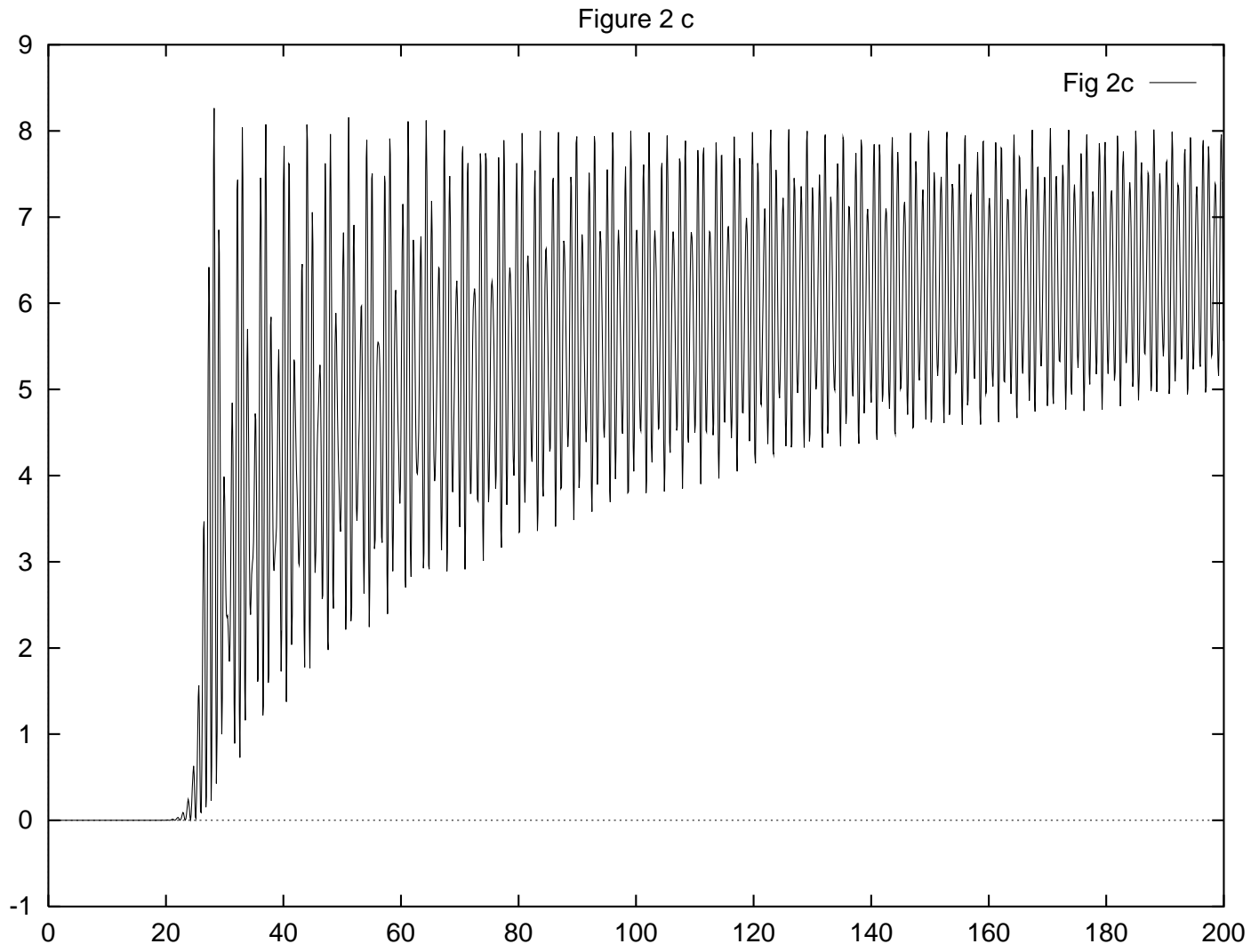


Figure 2 b

Figure 2b: $\eta(\tau)$ for the same values of the parameters as in Fig. 2(a). The agreement with the analytic prediction is to within 5% for $0 < \tau \leq 30$.

Figure 2c: $g^\Sigma(\tau)$ for the same parameters as in fig. 2a.



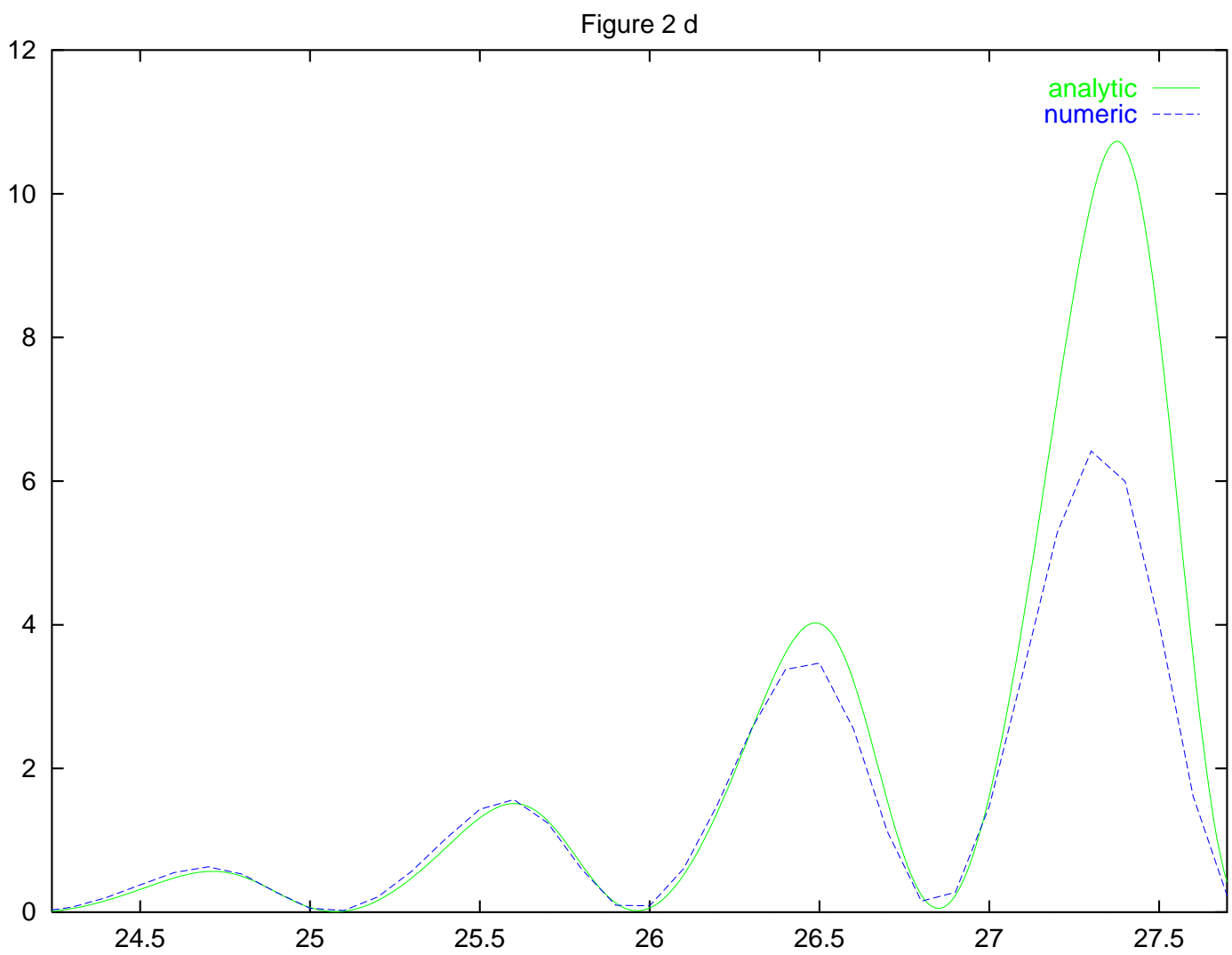


Figure 2d: $g^\Sigma(\tau)$, analytic approximation and numerical results for the same values of parameters as in fig. 2a.

Figure 2e: $g^N(\tau)$ vs. τ for the same values of parameters as fig. 2(a).

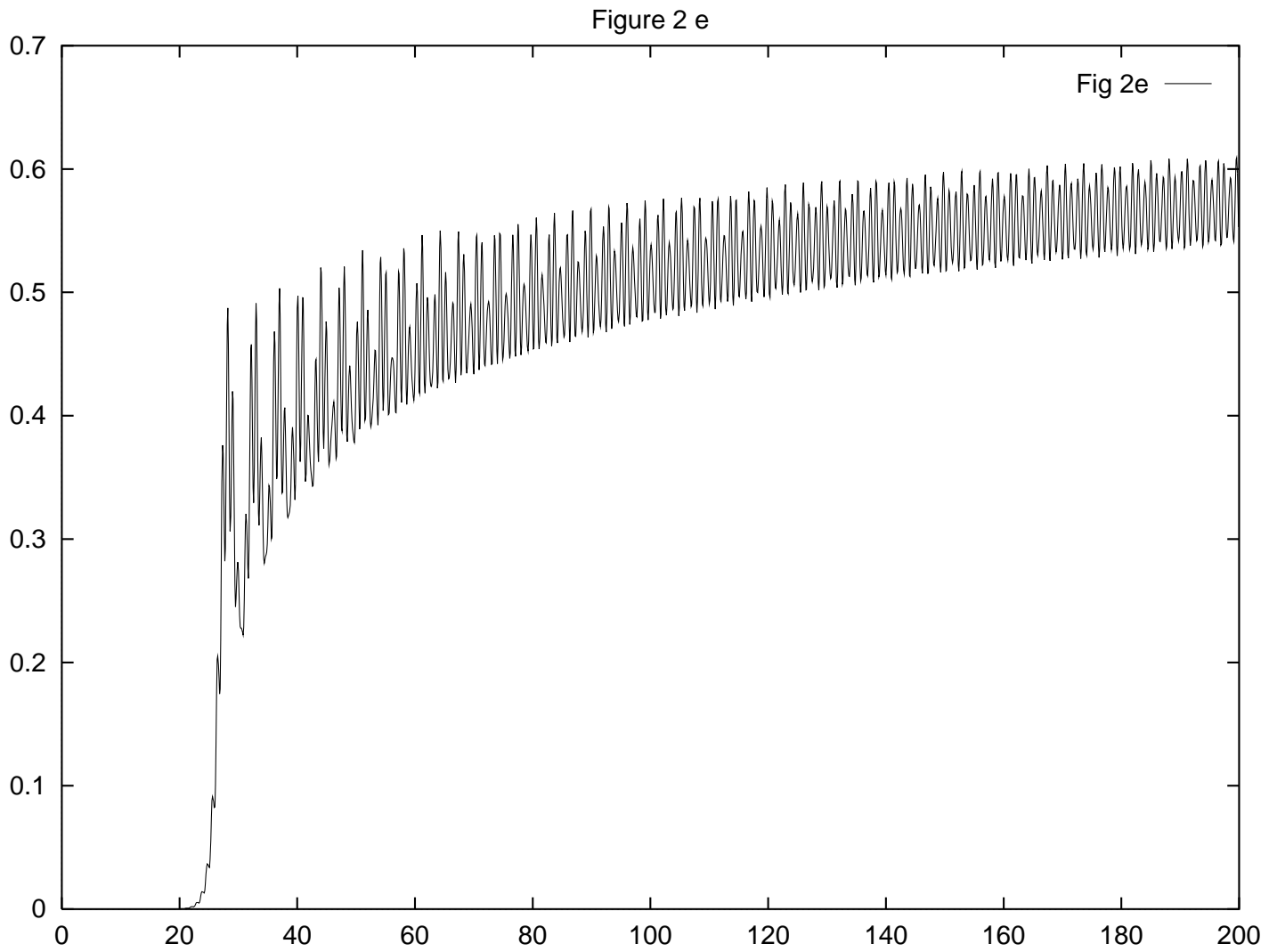
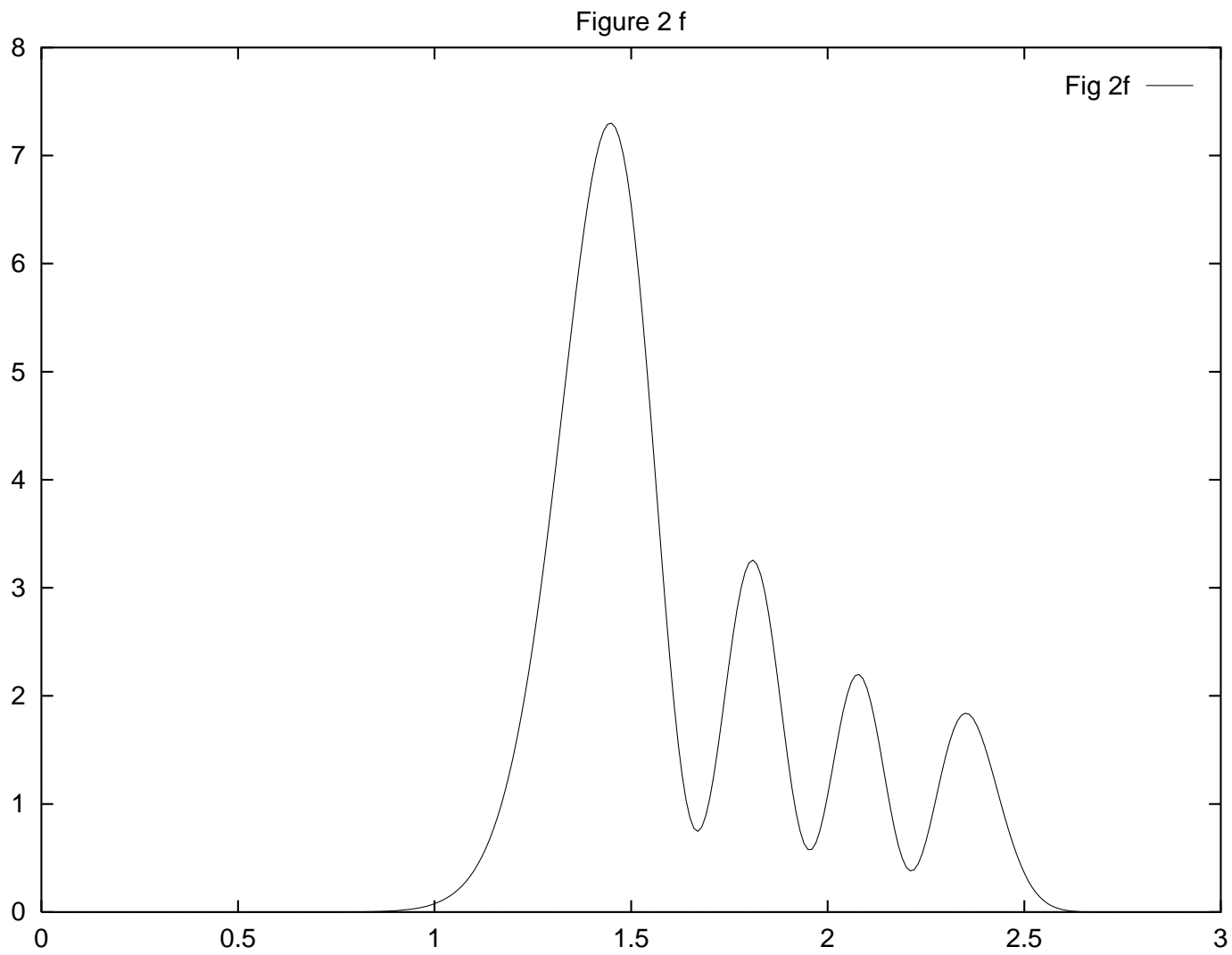


Figure 2f: $qN_q(\tau)$ vs. q for $\tau = 200$ for the same values of parameters as fig. 2(a).



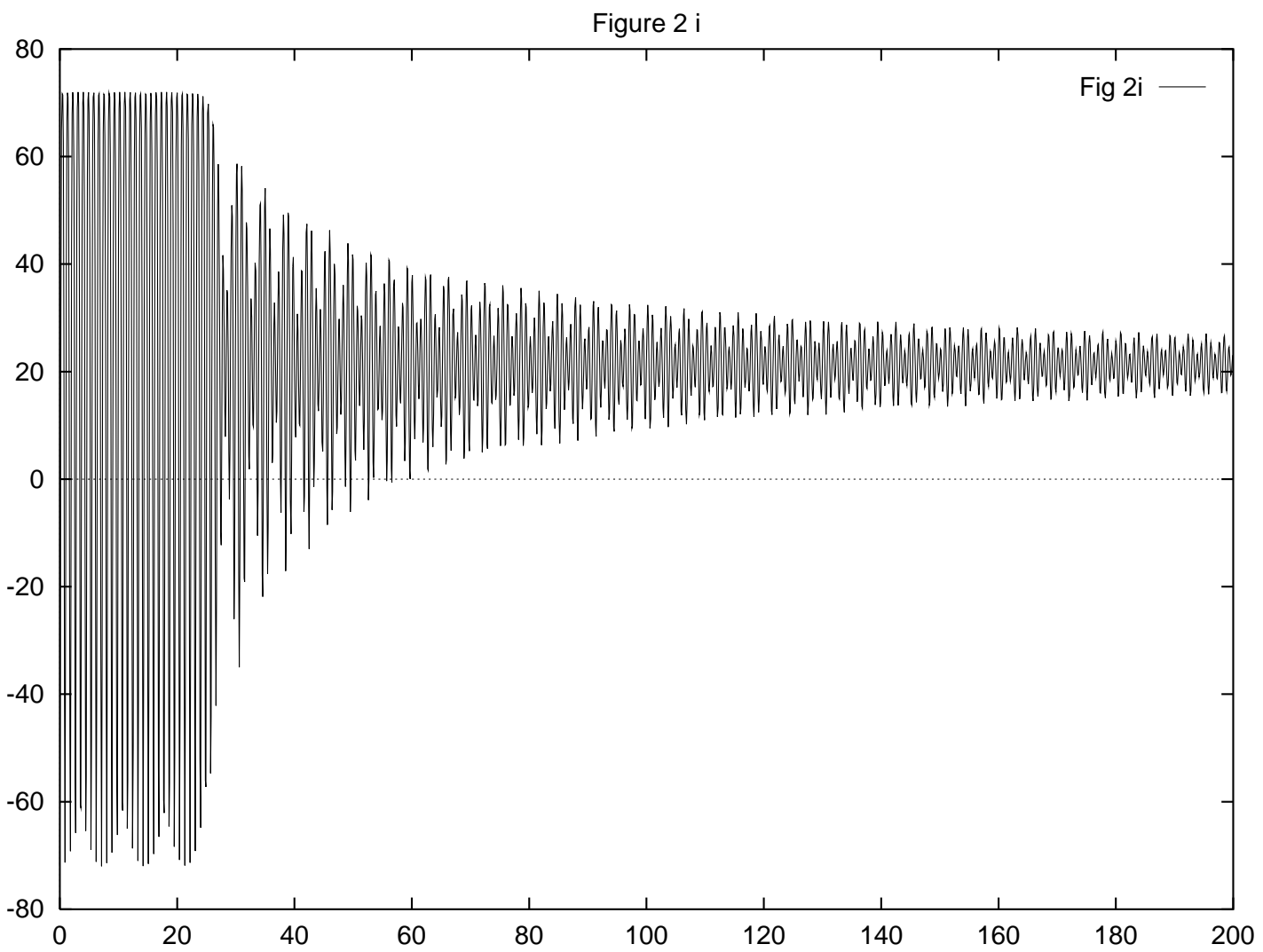


Figure 2g: $\left(\frac{\lambda R}{2|M|R_1^4}\right) p(\tau)$ for the same values of the parameters as in Fig. 2(a). Asymptotically the average over a period gives $p_\infty \approx \varepsilon/3$.

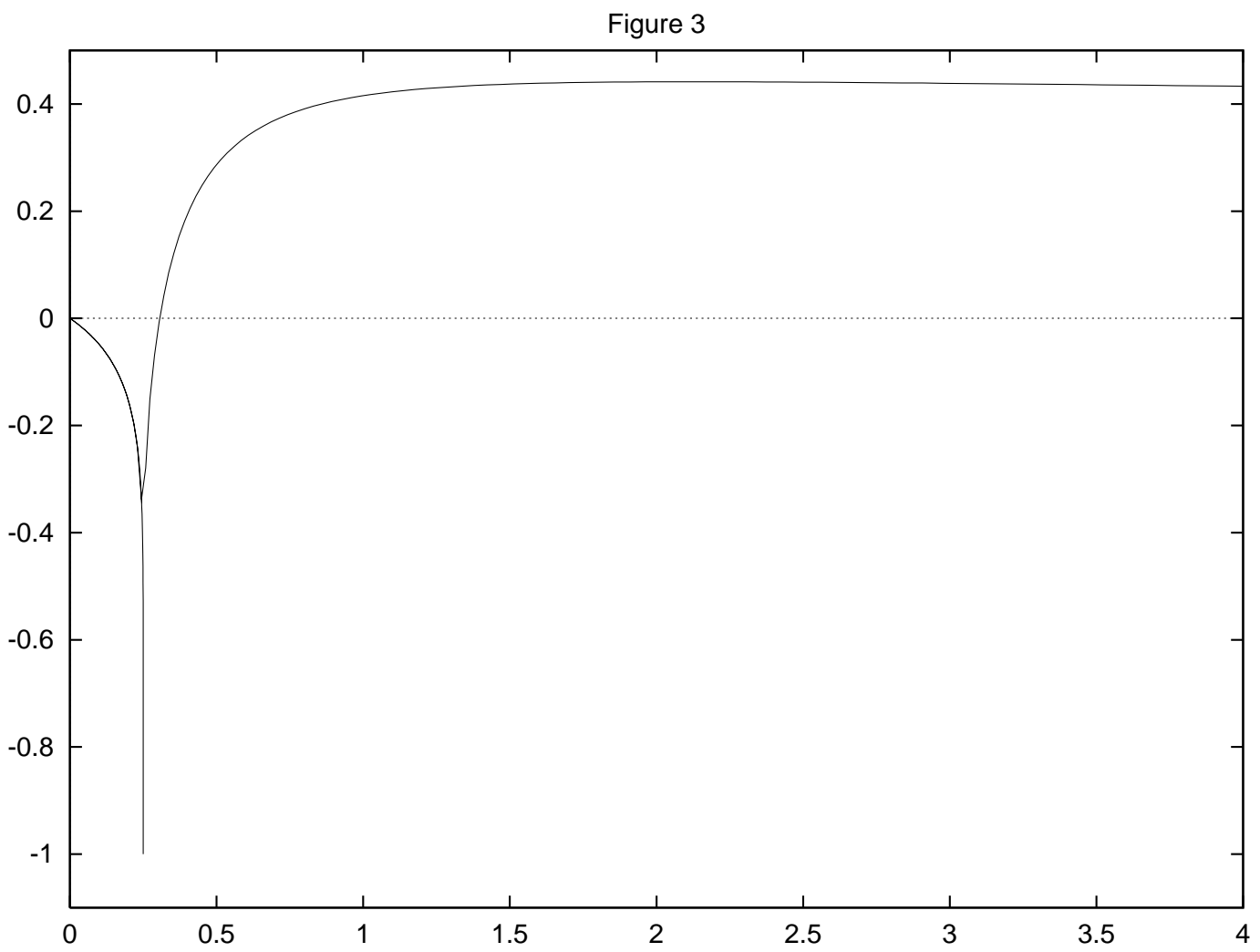


Figure 3: The ratio $\langle p_0 \rangle / \epsilon_0$ for zero mode vs. $\lambda_{R\epsilon_0}/2|M_R|^4$ for the broken symmetry case.

Figure 4 a

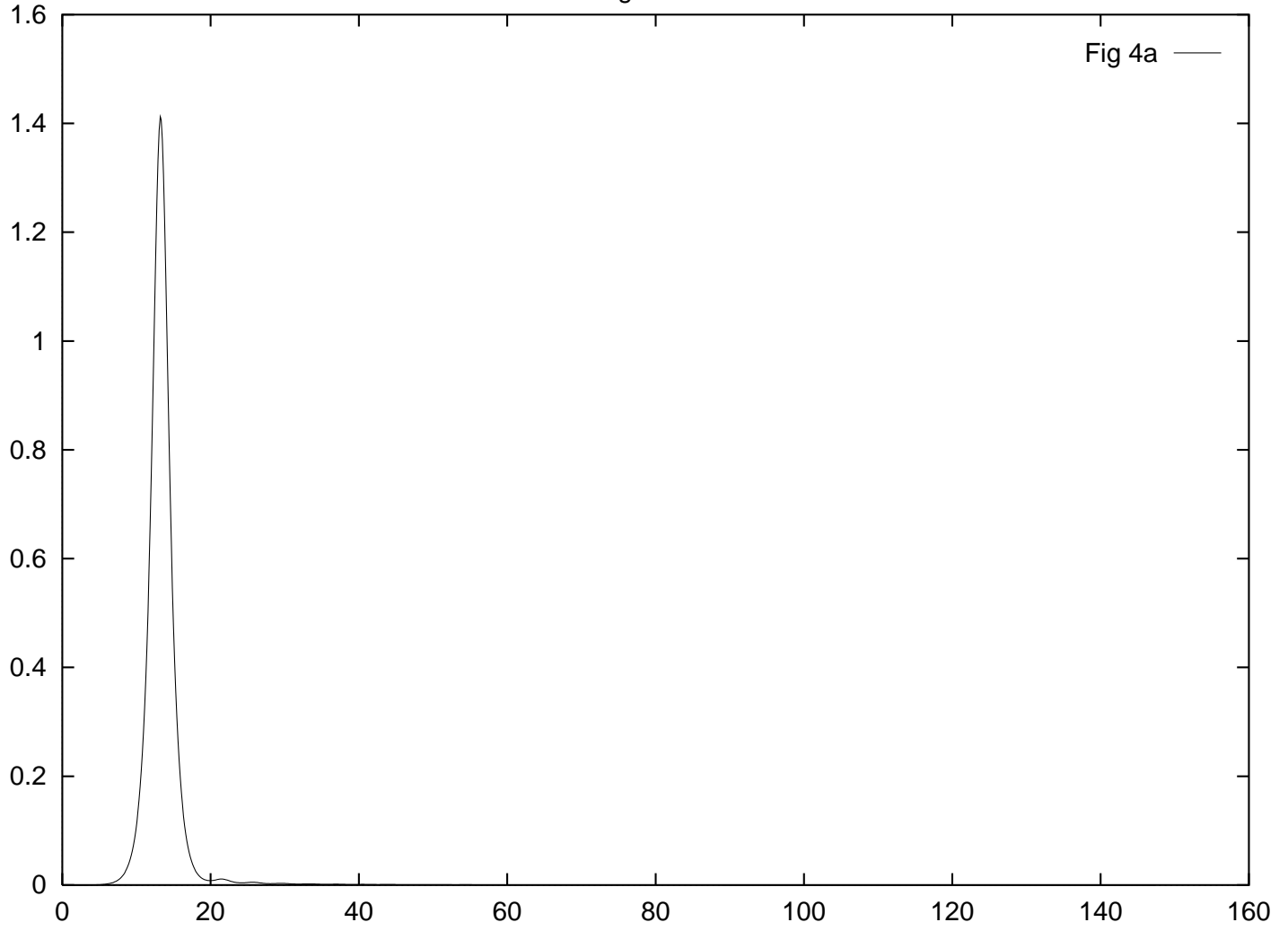


Figure 4a: $\eta(\tau)$ vs. τ for the broken symmetry case with $\eta_0 = 10^{-5}$, $g = 10^{-12}$.

Figure 4b: $g^\Sigma(\tau)$ for the same values of the parameters as in fig. 4a.

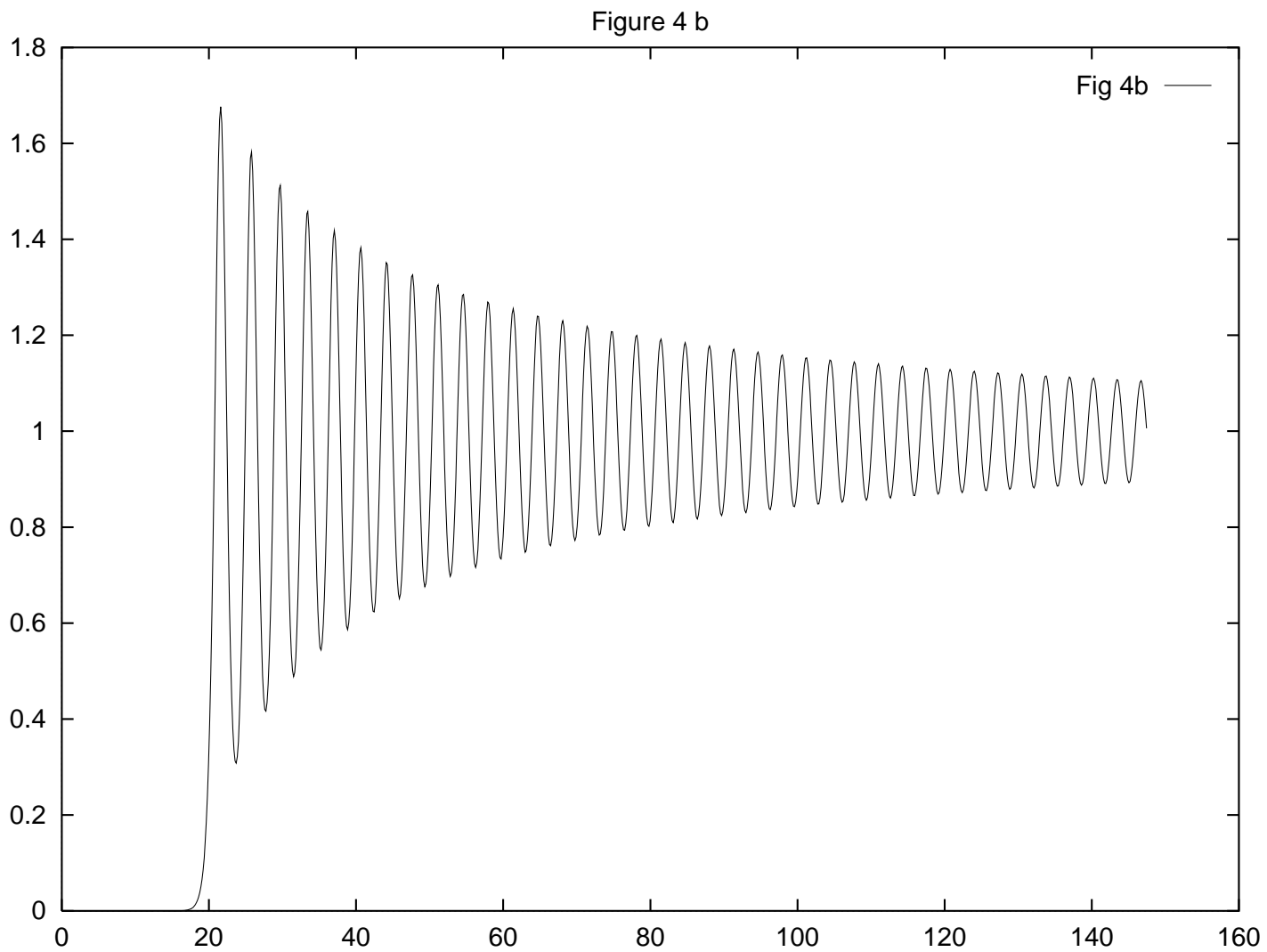


Figure 4c: $gN(\tau)$ for the same parameters as in fig. 4a.

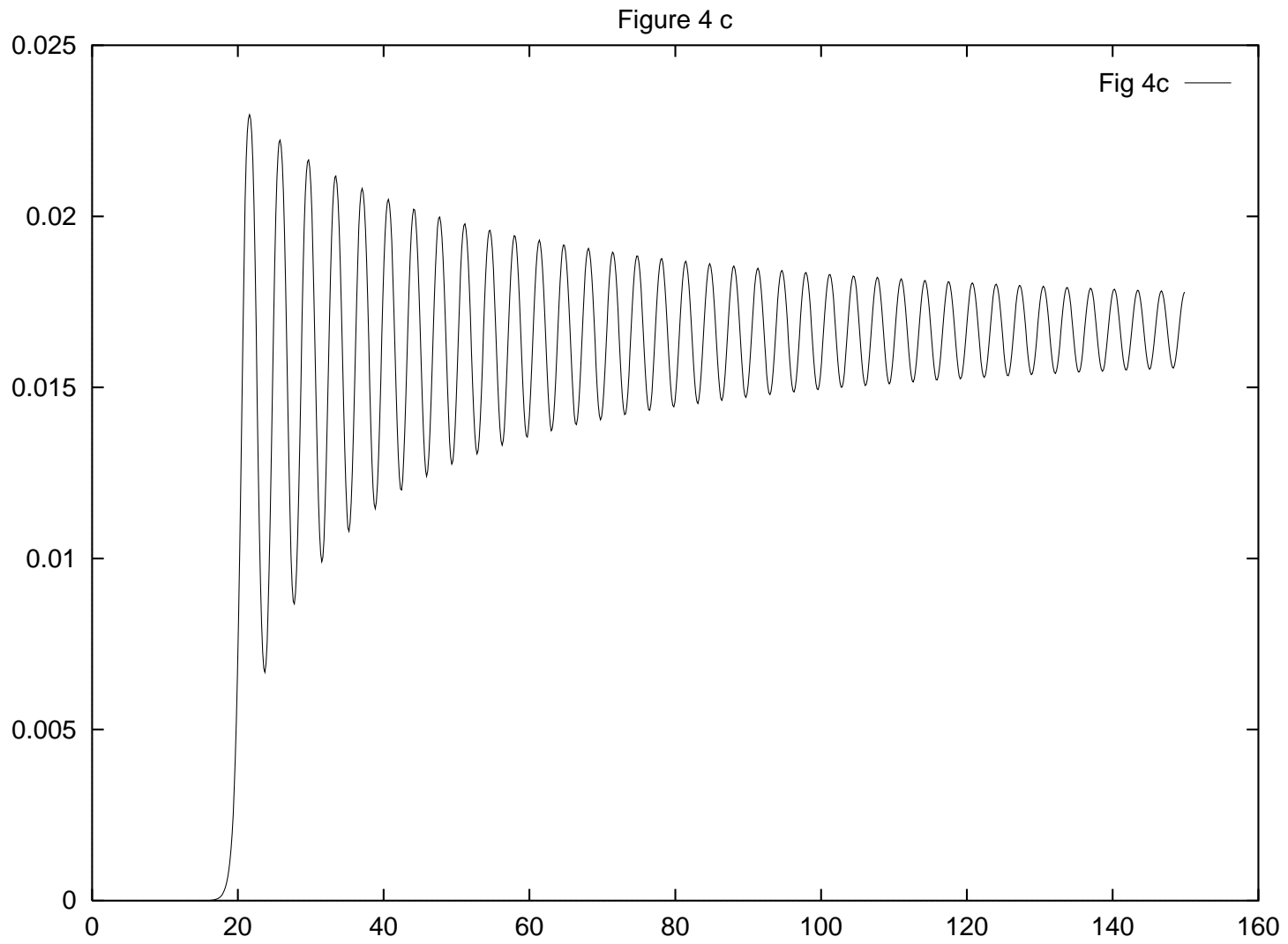


Figure 4d: $gN_q(\tau)$ vs. q for $\tau = 30$ for the same values of parameters as Fig. 4a.

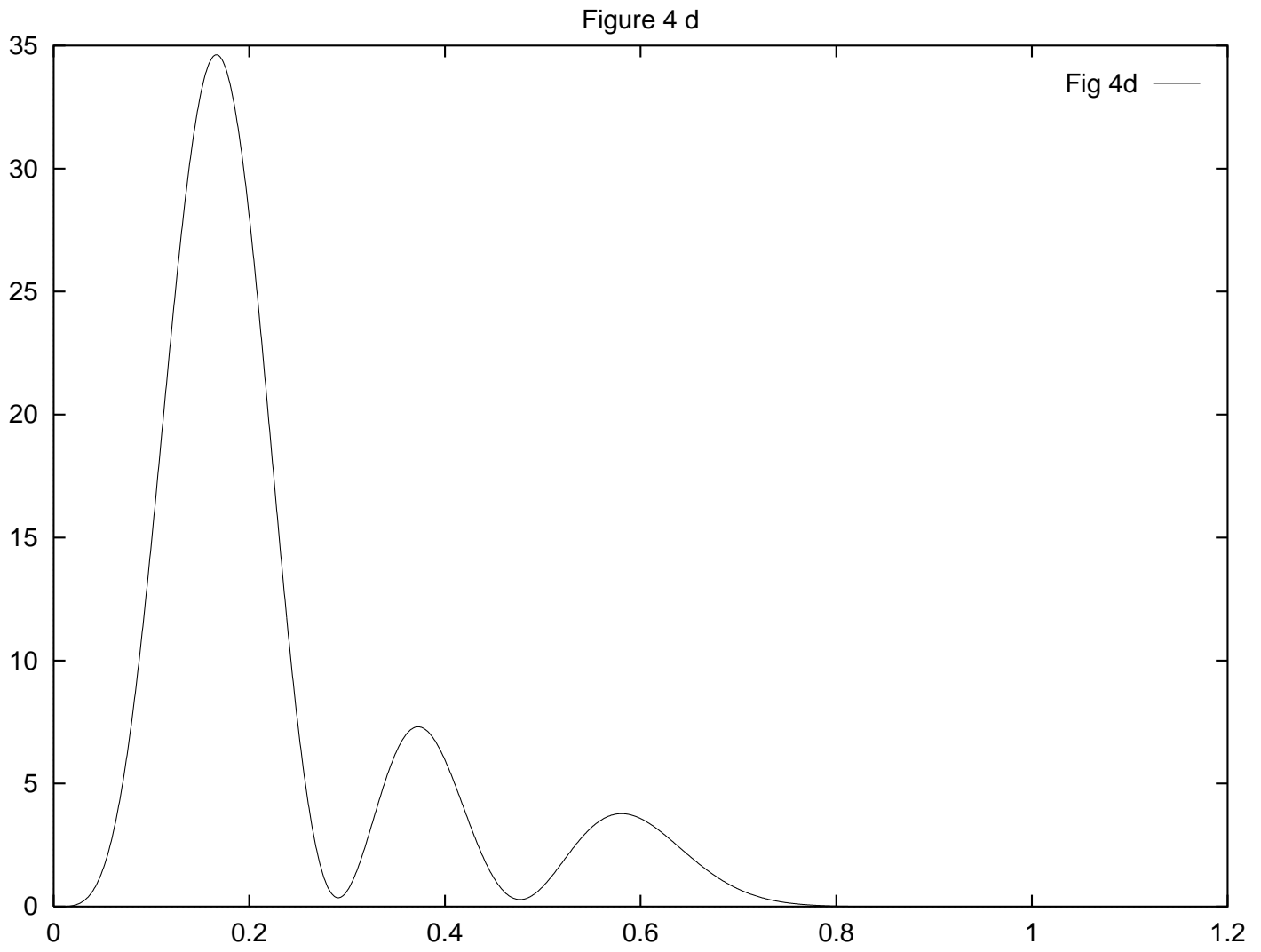


Figure 4e: $g^N N_q(\tau)$ vs. q for $\tau = 90$ for the same values of parameters as Fig. 4a.

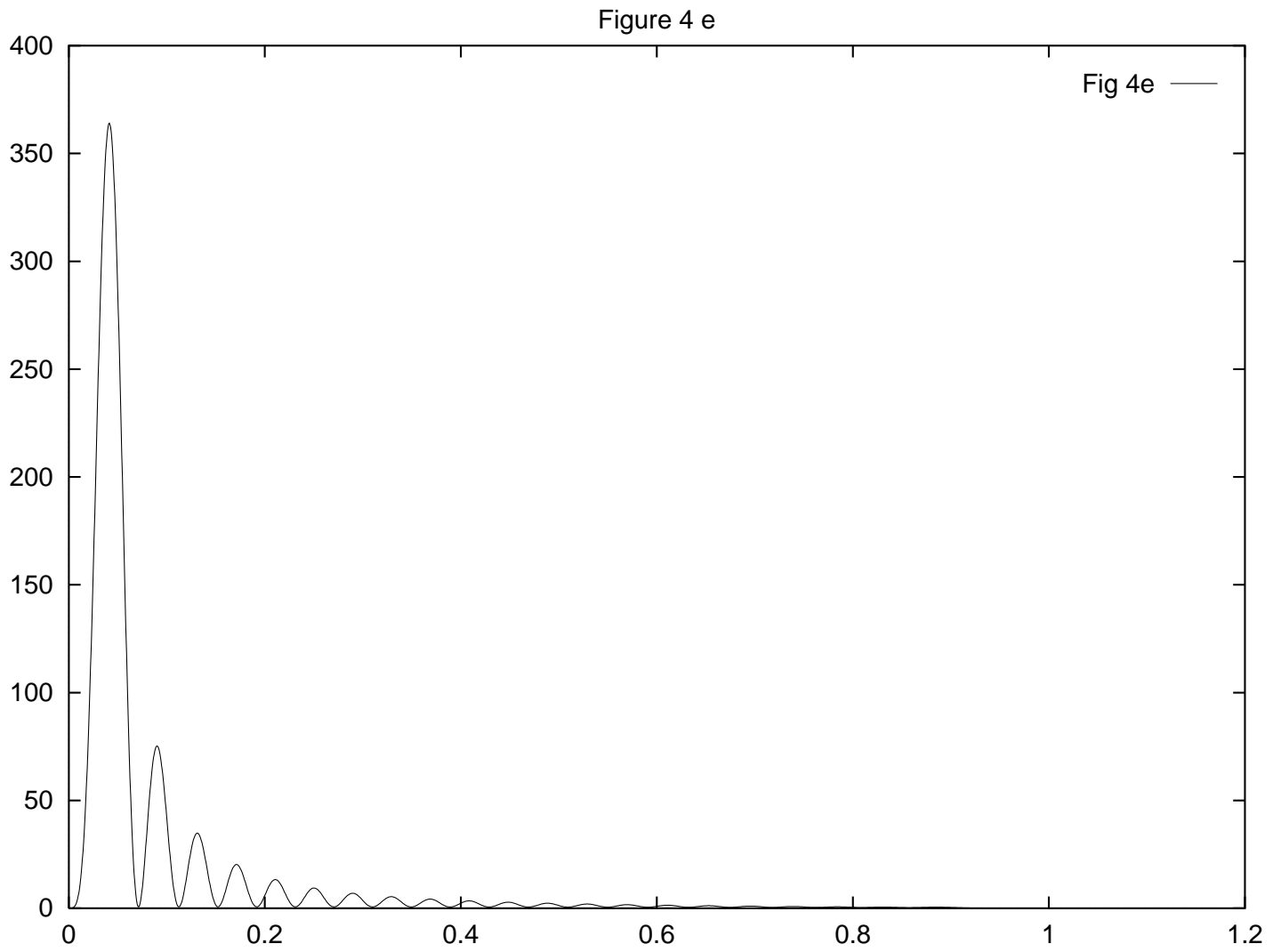


Figure 4 f

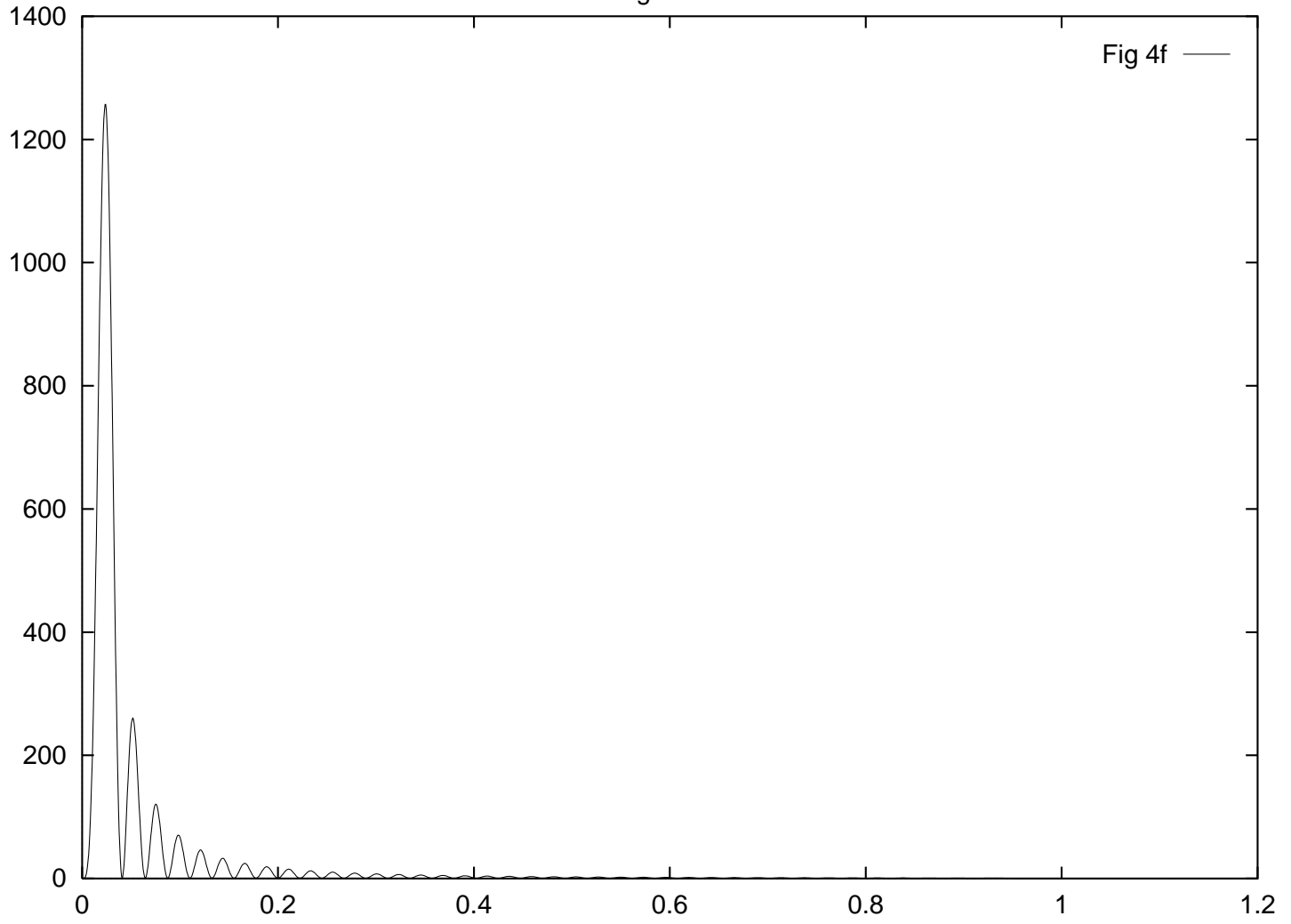


Figure 4f: $qN_q(\tau)$ vs. q for $\tau = 150$ for the same values of parameters as Fig. 4a.

Figure 4 g

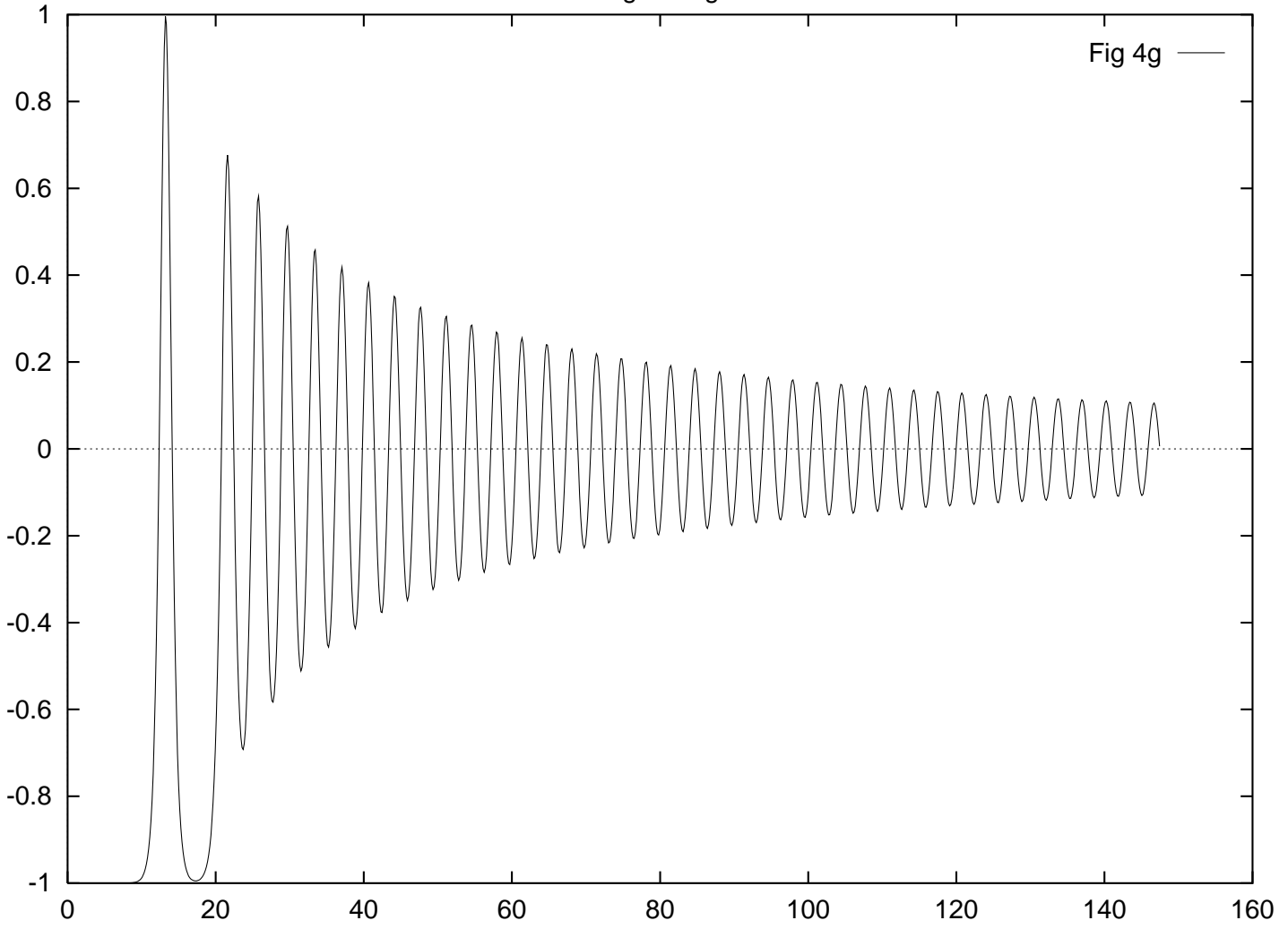


Figure 4g: $M^2(\tau)$ vs. τ for the same parameters as Fig. 4a.

Figure 4h: $\varepsilon_{el}(\tau)$ vs. τ for the same parameters as Fig. 4a.

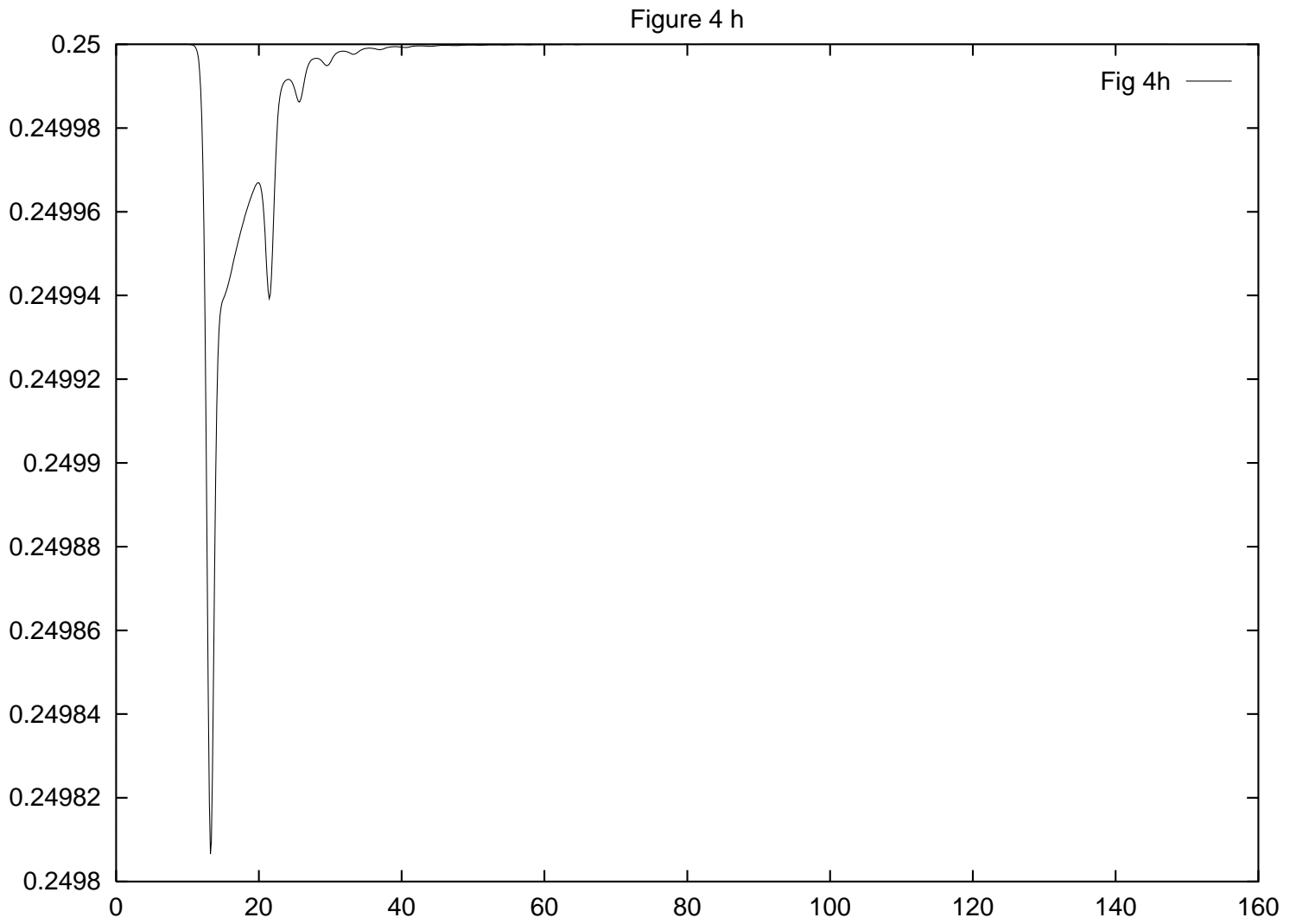
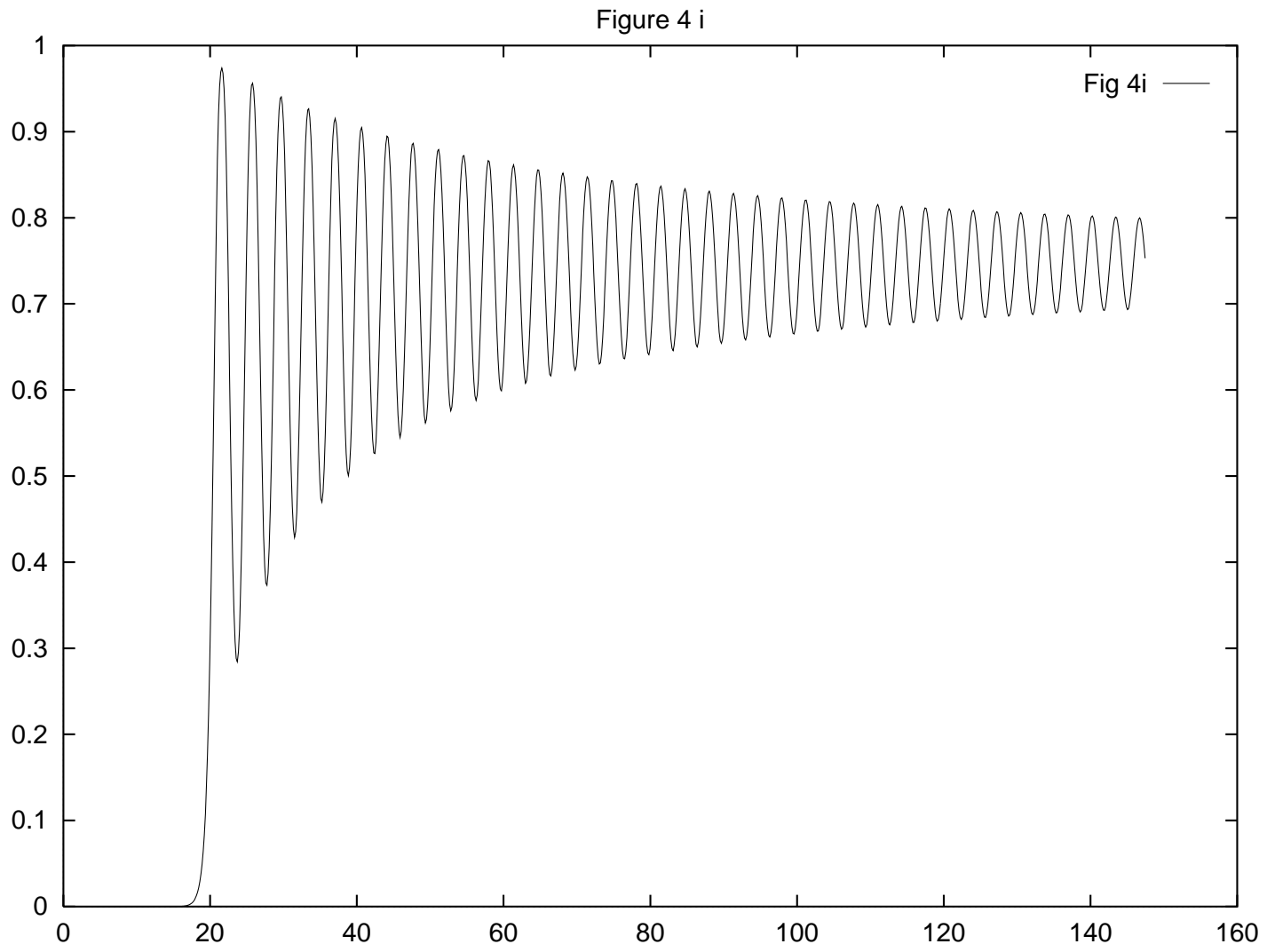


Figure 4i: $\epsilon_N(\tau)$ vs. τ for the same parameters as Fig. 4a.



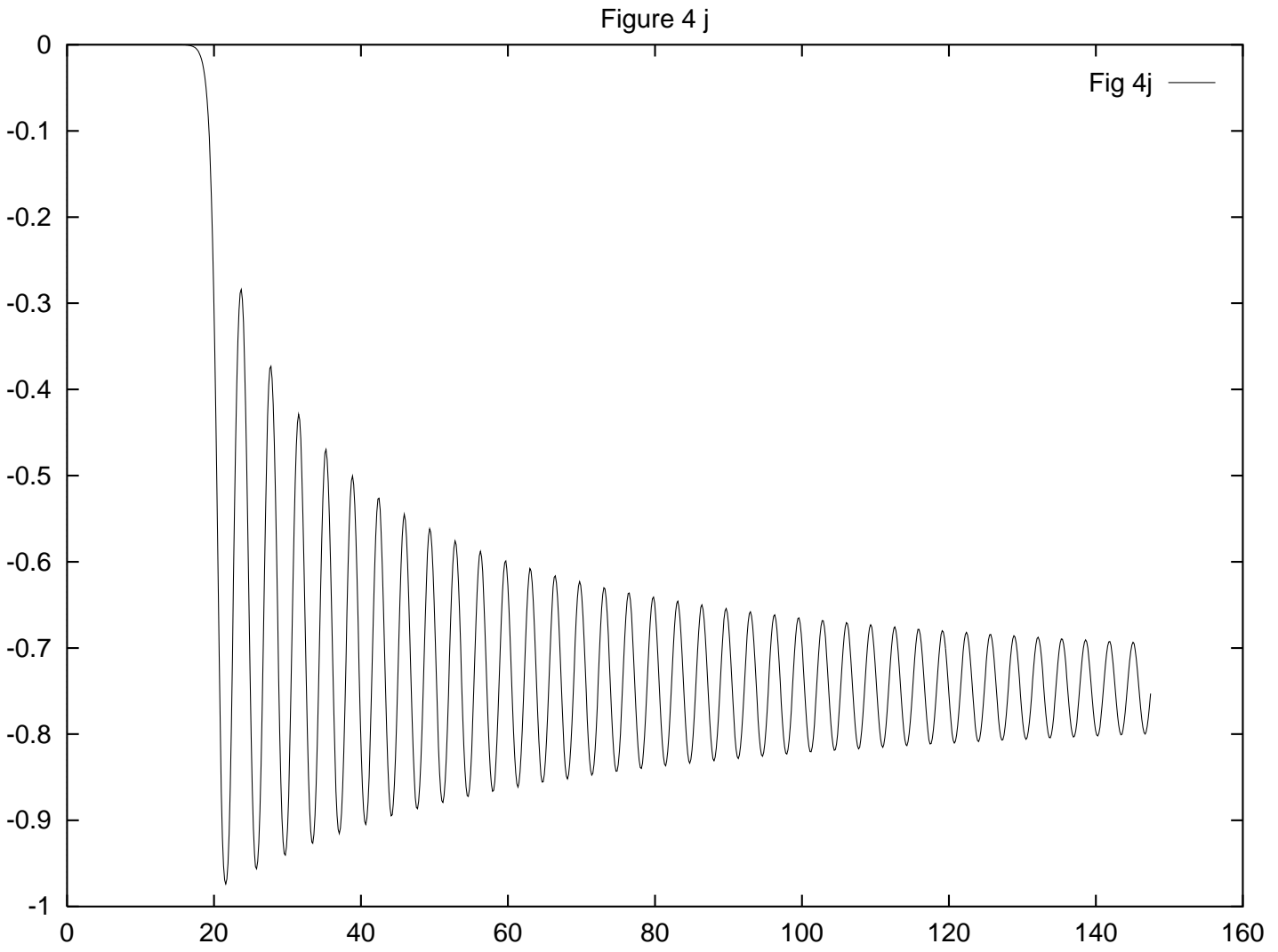


Figure 4j: $\varepsilon_C(\tau)$ vs. τ for the same parameters as Fig. 4a.

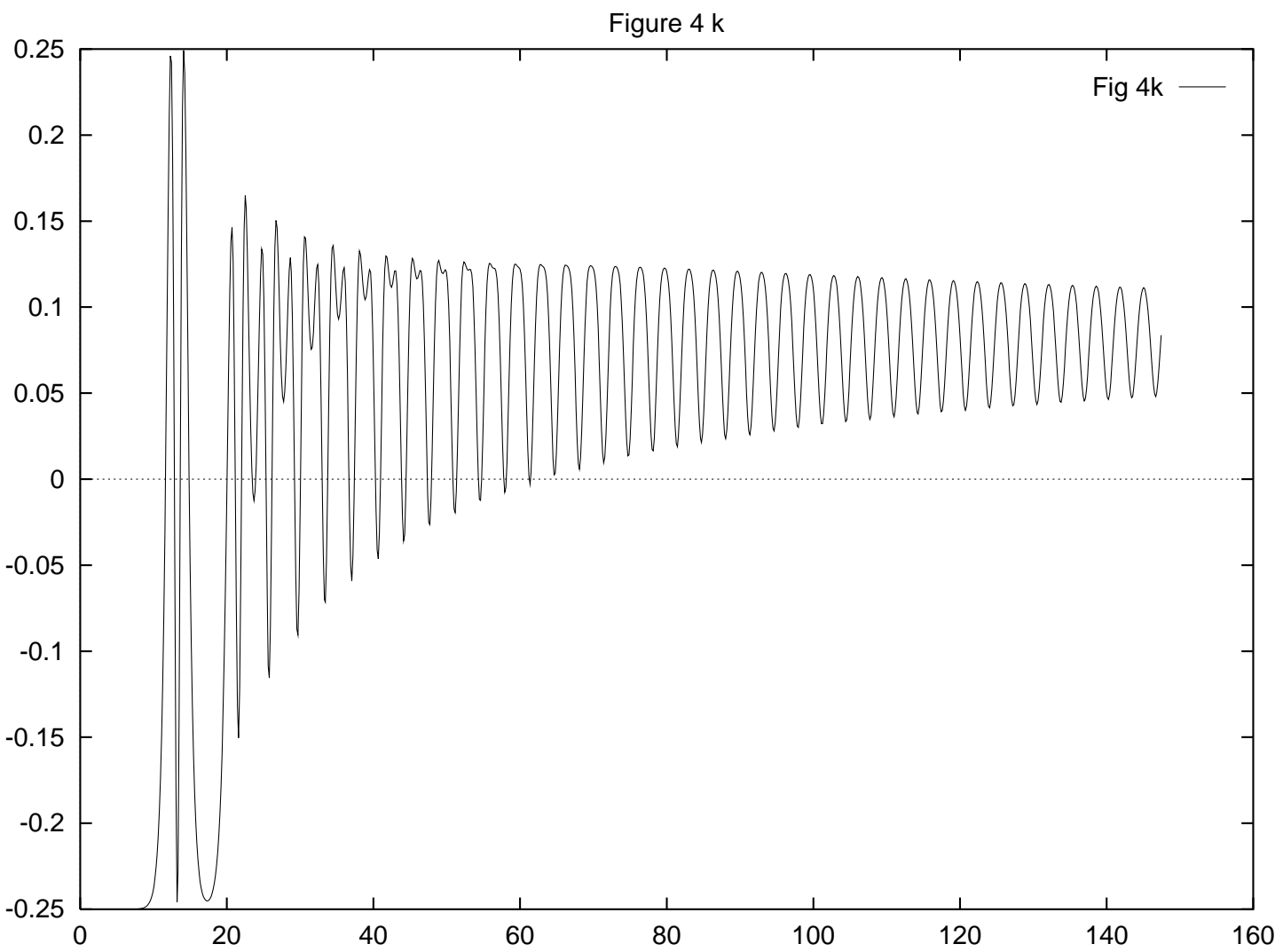


Figure 4k: $\left(\frac{\lambda R}{2|M|R^4}\right) p(\tau)$ for the same values of the parameters as in Fig. 4a. Asymptotically the average over a period gives $p_\infty = \varepsilon/3$.

Figure 5 a

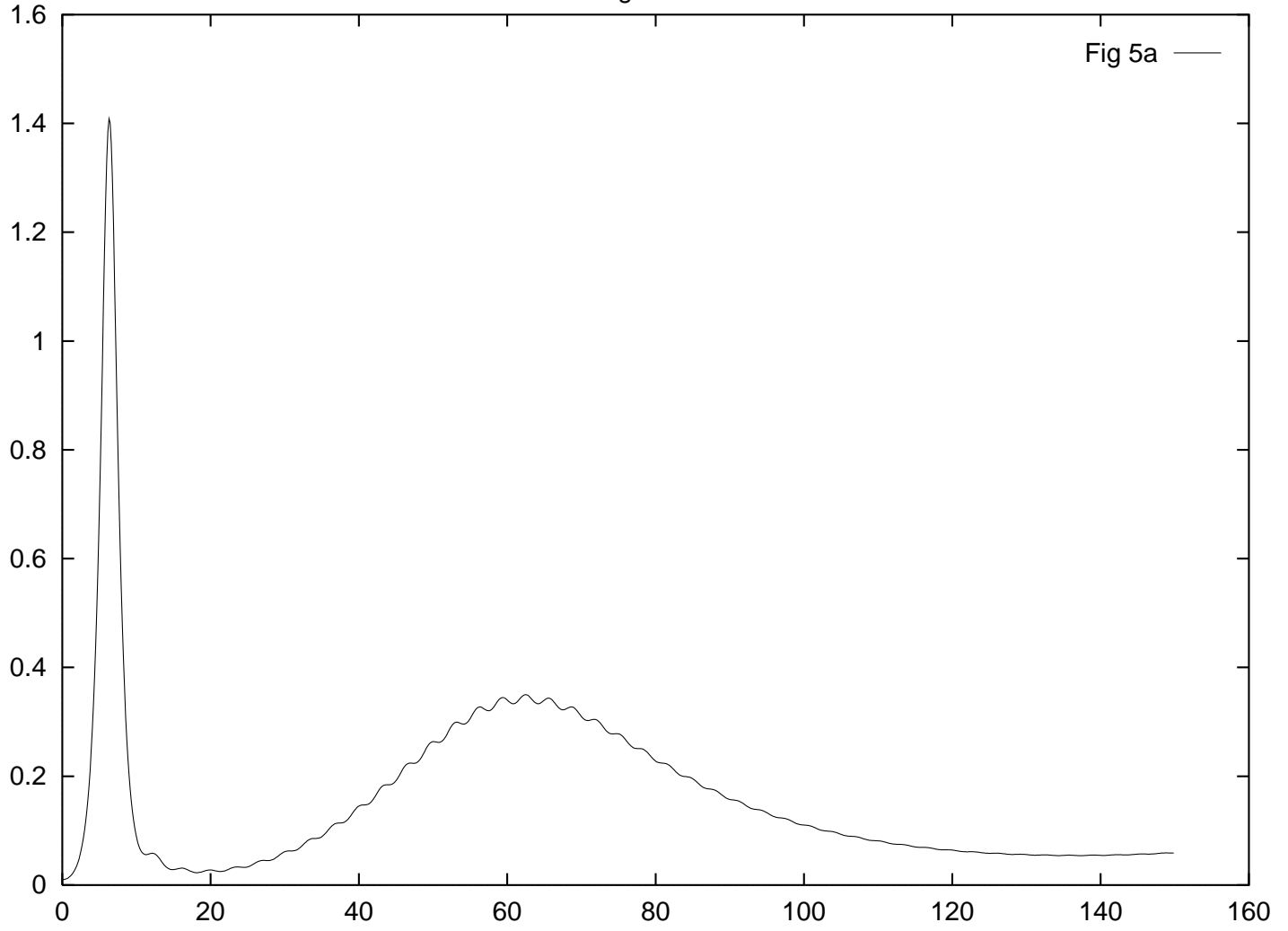


Figure 5a: $\eta(\tau)$ vs. τ for the broken symmetry case with $\eta_0 = 10^{-2}$, $g = 10^{-5}$.

Figure 5 b

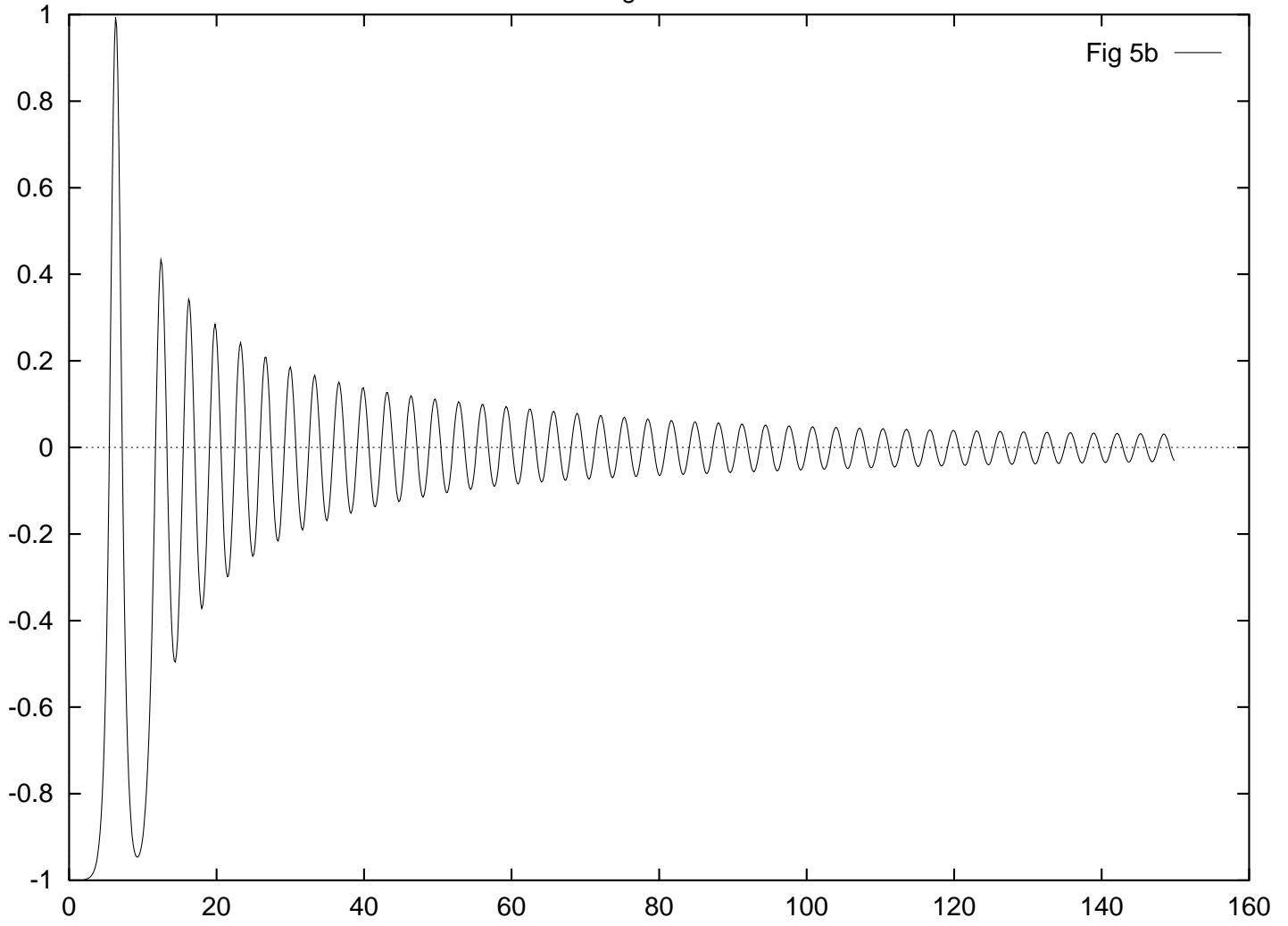


Figure 5b: $M^2(\tau)$ vs. τ for the same parameters as fig. 5(a).

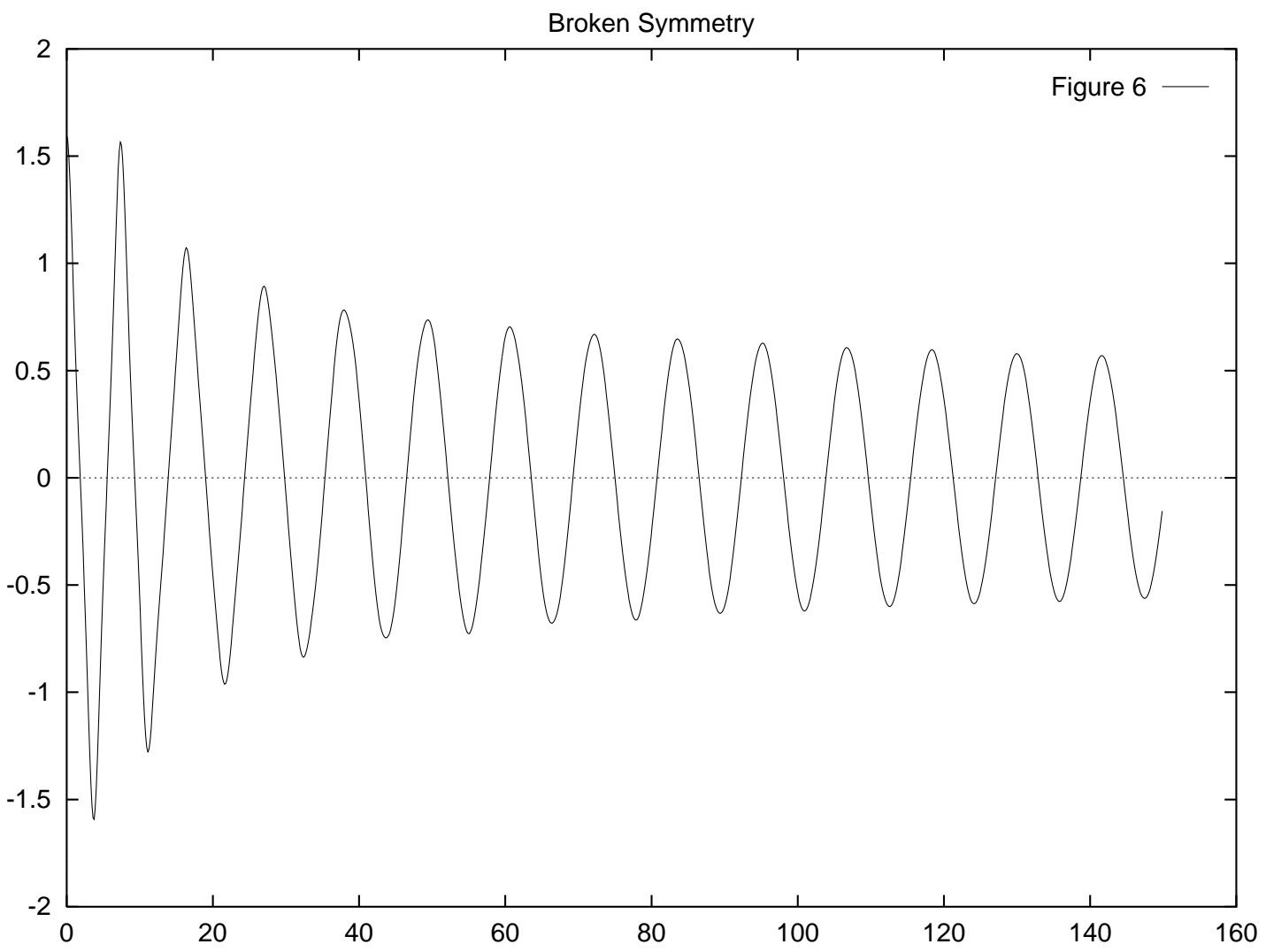


Figure 6: $\eta(\tau)$ vs. τ for the broken symmetry case with $\eta_0 = 1.6 > \sqrt{2}$, $g = 10^{-3}$.

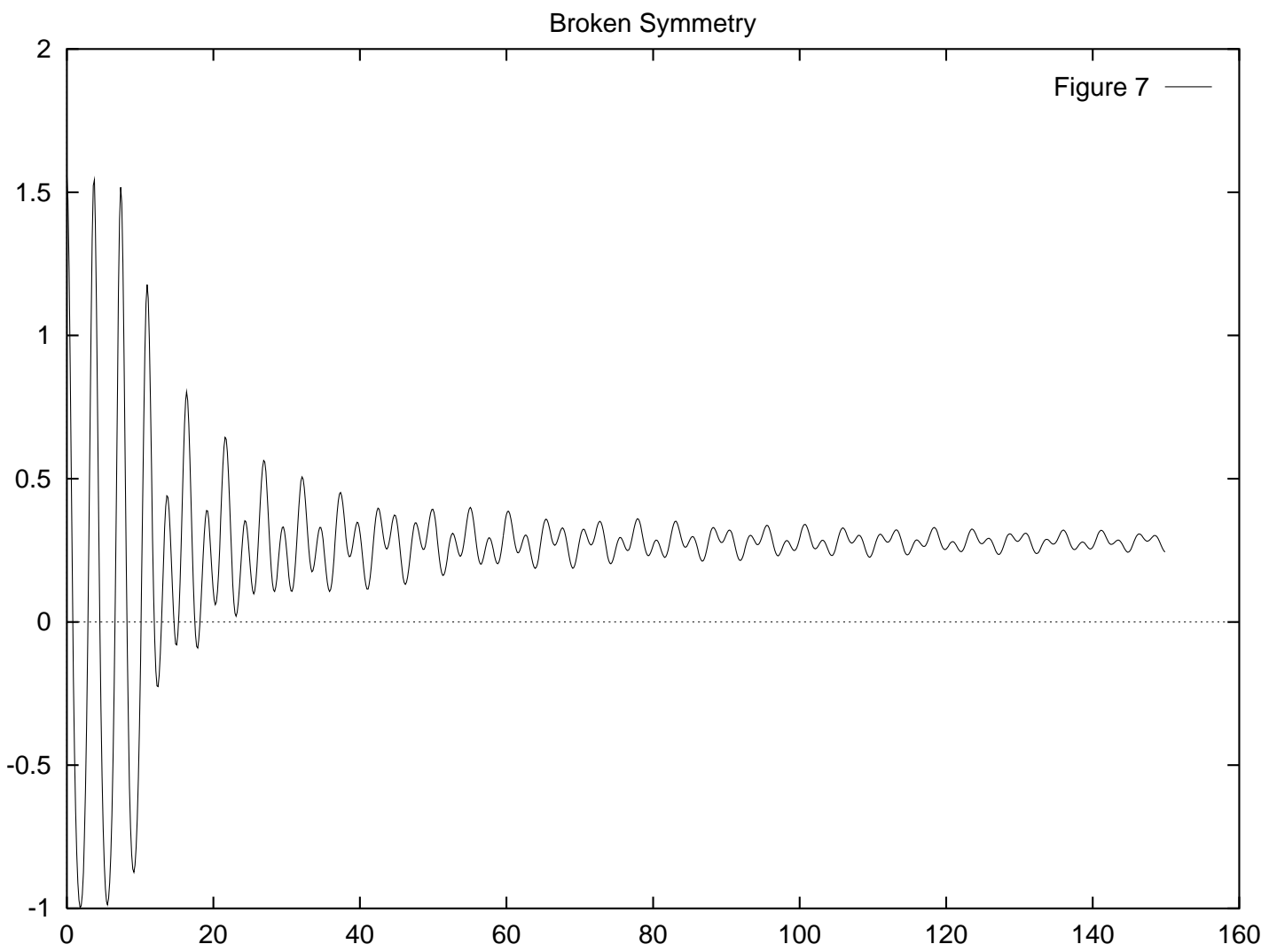


Figure 7: The effective mass squared vs. τ for the same values of the parameters as in fig. 6.

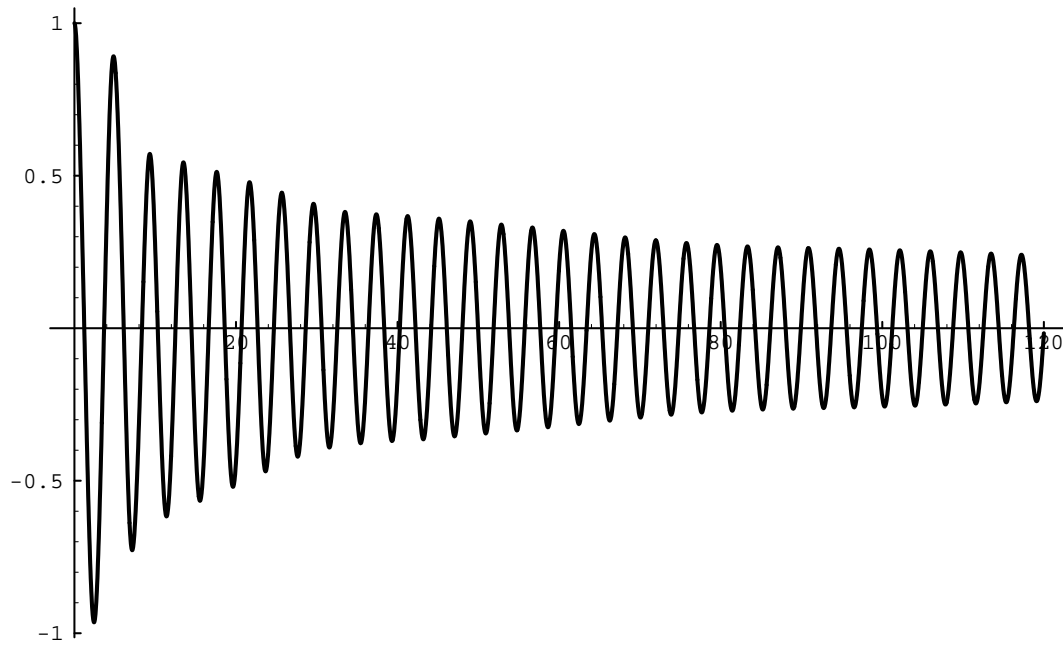


Figure 8: The inflaton coupled to a lighter scalar field σ : $\eta(\tau)$ vs τ for the values of the parameters $y = 0$; $\lambda/8\pi^2 = 0.2$; $g = \lambda$; $m_\sigma = 0.2 m_\phi$; $\eta(0) = 1.0$; $\dot{\eta}(0) = 0$.

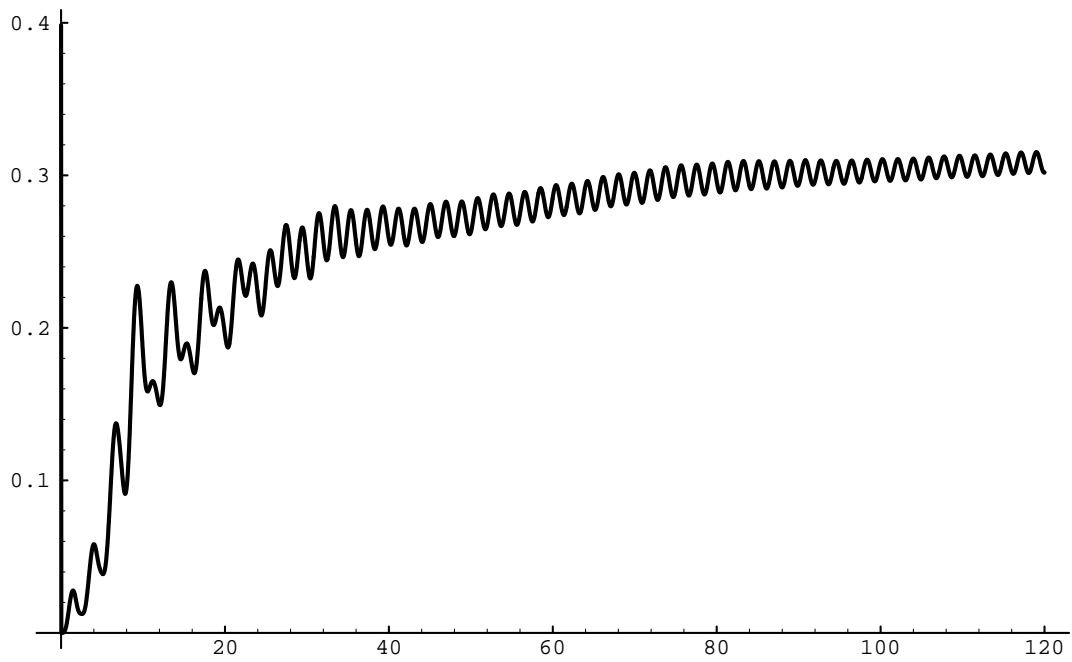


Figure 9: $\mathcal{N}_\sigma(\tau)$ vs. τ for the same value of the parameters as figure 8.

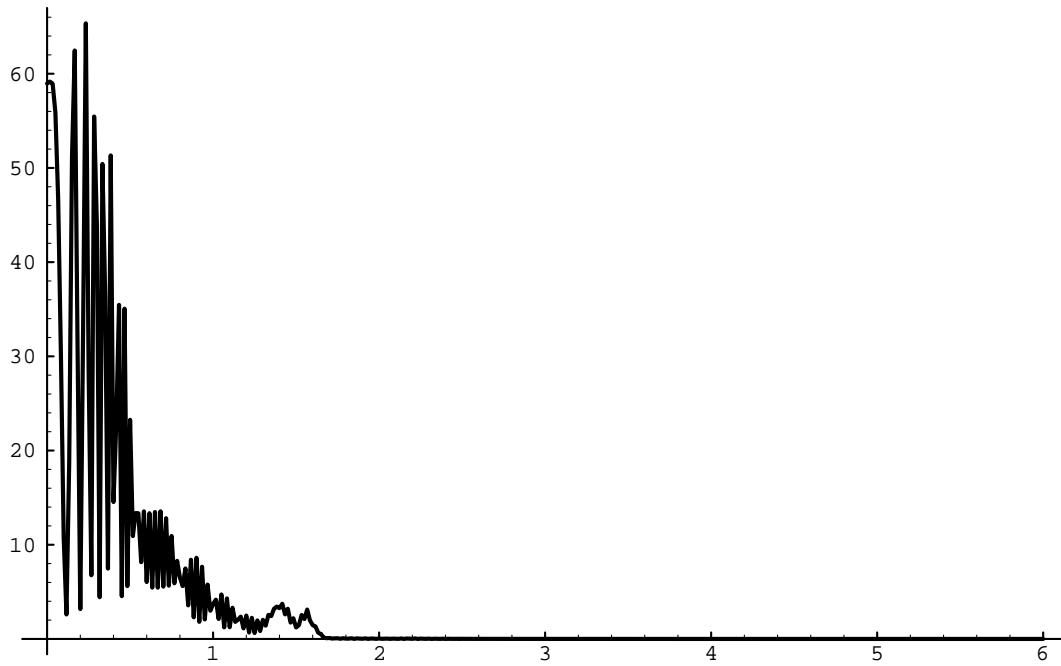


Figure 10: $\mathcal{N}_{q,\sigma}(\tau = 120)$ vs. q for the same values as in fig. 8.

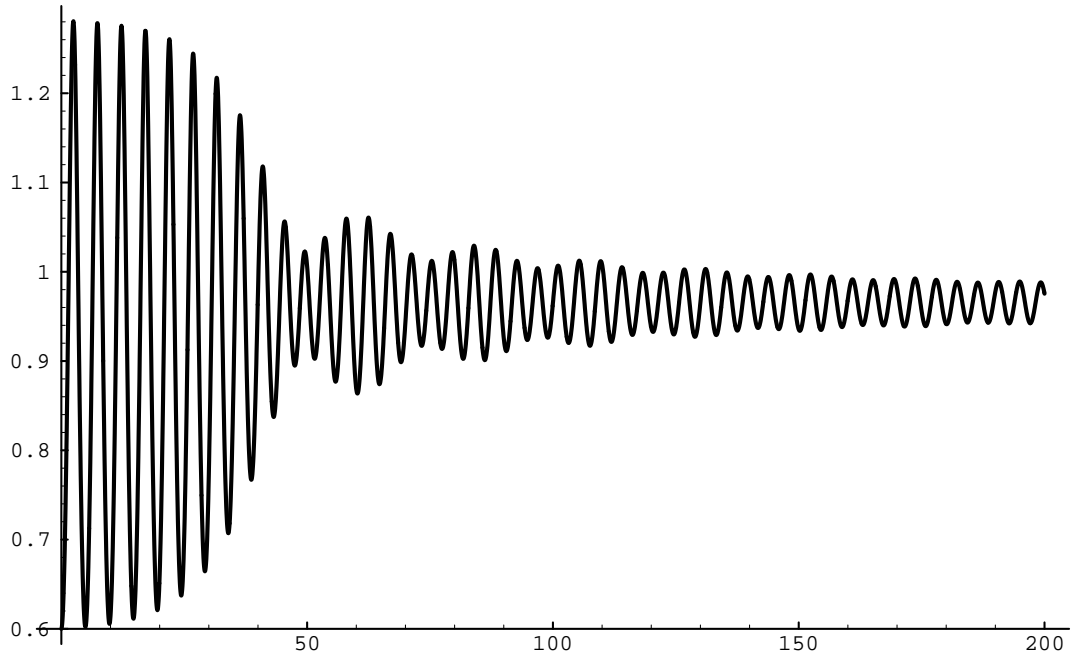


Figure 11: The inflaton in the broken symmetry case coupled to a lighter scalar σ . $\eta(\tau)$ vs τ for the values of the parameters $y = 0$; $\lambda/8\pi^2 = 0.2$; $g = \lambda$; $m_\sigma = 0.2|m_\phi|$; $\eta(0) = 0.6$; $\dot{\eta}(0) = 0$.

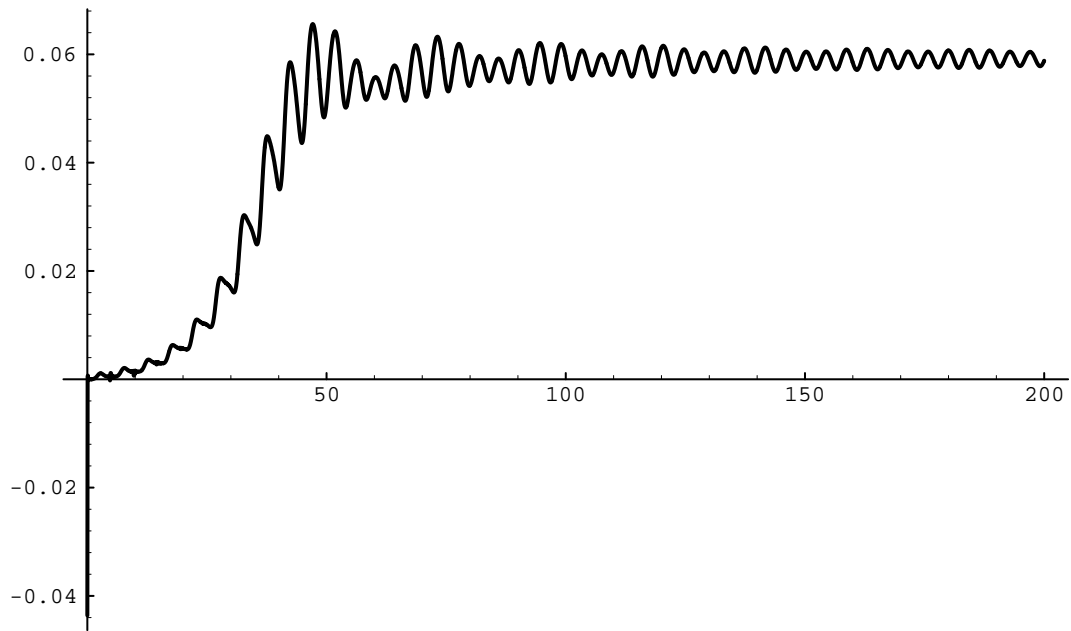


Figure 12: $\mathcal{N}_\sigma(\tau)$ vs. τ for the same value of the parameters as fig. 11.

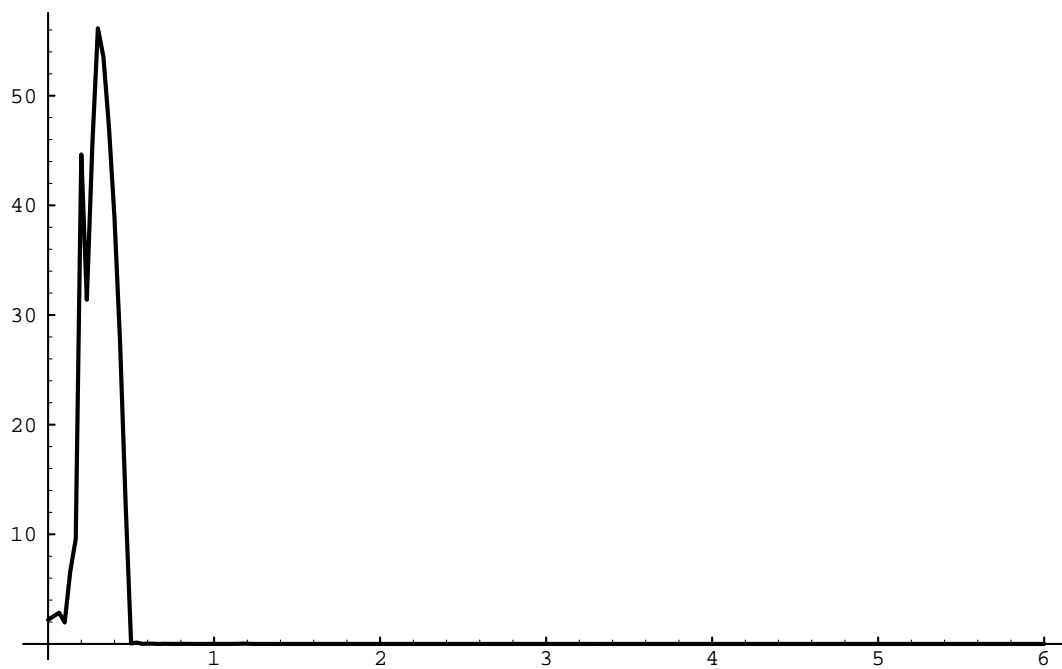


Figure 13: $\mathcal{N}_{q,\sigma}(\tau = 200)$ vs. q for the same values as in fig. 11.

Figure 2 g

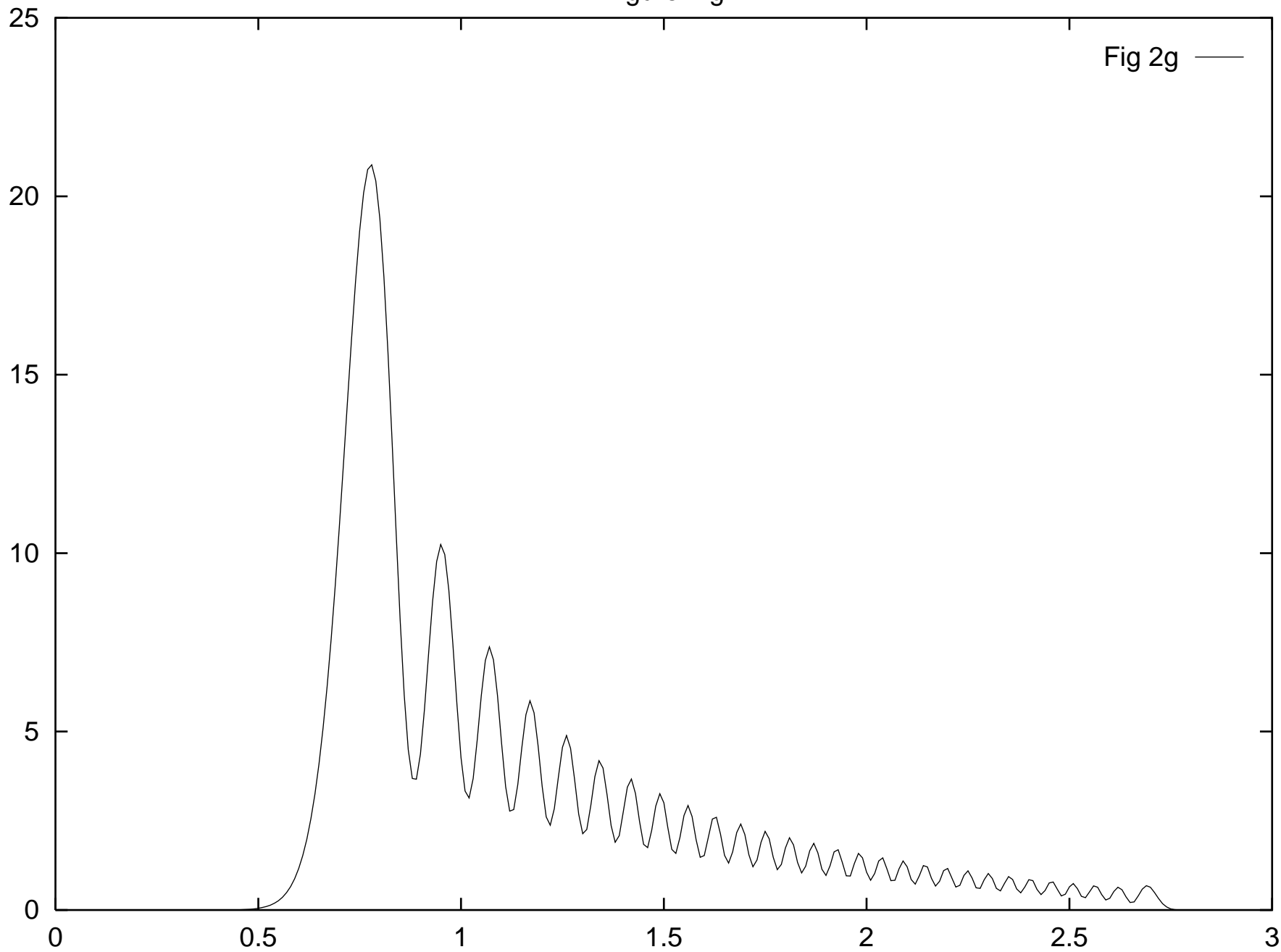


Fig 2g —

Figure 2 h

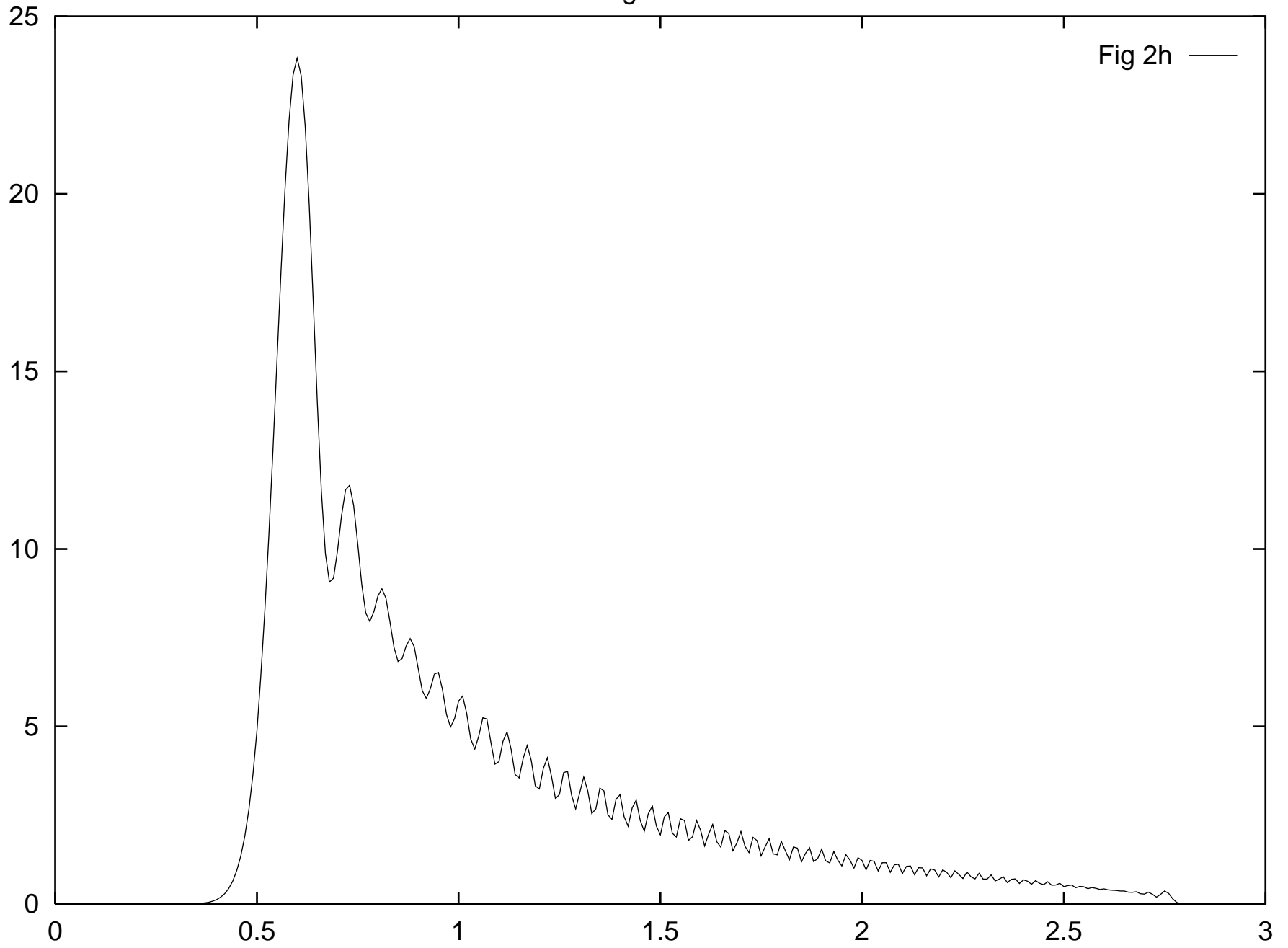


Fig 2h —